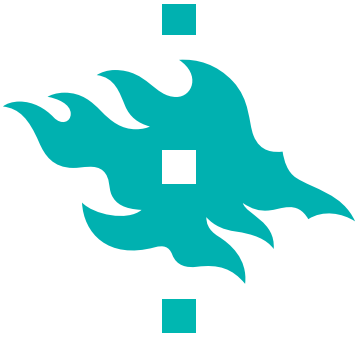

DISSERTATIONES SCHOLAE DOCTORALIS AD SANITATEM INVESTIGANDAM
UNIVERSITATIS HELSINKIENSIS

FLAVIA FONTANA

BIOHYBRID CLOAKED NANOVACCINES FOR CANCER IMMUNOTHERAPY

DRUG RESEARCH PROGRAM
DIVISION OF PHARMACEUTICAL CHEMISTRY AND TECHNOLOGY
FACULTY OF PHARMACY
DOCTORAL PROGRAMME IN DRUG RESEARCH
UNIVERSITY OF HELSINKI

Division of Pharmaceutical Chemistry and Technology
Faculty of Pharmacy
University of Helsinki
Finland

Biohybrid Cloaked Nanovaccines for Cancer Immunotherapy

by

Flavia Fontana

ACADEMIC DISSERTATION

To be presented, with the permission of the Faculty of Pharmacy of the University of Helsinki, for public examination in Auditorium 1 at Infocenter Korona (Viikinkaari 11, Helsinki) on June 14th, at 12.00 noon.

Helsinki 2019

Supervisors	Associate Professor Hélder A. Santos Drug Research Program Division of Pharmaceutical Chemistry and Technology Faculty of Pharmacy University of Helsinki Finland
	Professor and Dean Jouni T. Hirvonen Drug Research Program Division of Pharmaceutical Chemistry and Technology Faculty of Pharmacy University of Helsinki Finland
	Professor Vincenzo Cerullo Drug Research Program Division of Pharmaceutical Biosciences Faculty of Pharmacy University of Helsinki Finland
Reviewers	Assistant Professor Joy E. Wolfram Nanomedicine and Extracellular Vesicles Lab Faculty of Medicine Mayo Clinic Florida Jacksonville USA
	Dr. Ciro Chiappini Division of Craniofacial Development and Stem Cell Biology Dental Institute King's College London United Kingdom
Opponent	Professor David Mooney Wyss Institute for Biologically Inspired Engineering School of Engineering and Applied Sciences Harvard University USA

© Flavia Fontana 2019
ISBN 978-951-51-5286-2 (Paperback)
ISBN 978-951-51-5287-9 (PDF)
ISSN 2342-3161

Helsinki University Printing House
Helsinki 2019

The Faculty of Pharmacy uses the Urkund system (plagiarism recognition) to examine all doctoral dissertations.

Abstract

Fontana F., 2019. **Biohybrid Cloaked Nanovaccines for Immunotherapy**

Dissertationes Scholae Doctoralis Ad Sanitatem Investigandam Universitatis Helsinkiensis, 47/2019, pp.78
ISBN 987-951-51-5286-2 (Paperback), ISBN 978-951-51-5287-9 (PDF, http://ethesis.helsinki.fi), ISSN 2342-3161

Immunotherapy is revolutionizing cancer treatment achieving durable and long-term responses in patients. However, only subsets of patients treated experience a positive outcome, due to immunotherapeutic resistance. Combinations of immunotherapeutics can overcome the drug resistance; the administration of a cancer vaccine or an oncolytic virus followed by immune checkpoint inhibitors is under investigation. Thereby, there is an unmet need for powerful, yet safe vaccines. Nanoparticles, in particular porous silicon nanoparticles, present ideal characteristics to formulate nanovaccines, thanks to their size-specific targeting to the lymphoid organs, to their intrinsic adjuvant effect, and to the possibility to simultaneously load adjuvants and antigens. Moreover, biohybrid cell membrane technology has been proposed as an innovative antigenic source. Thus, the aims of the current thesis were to develop a biohybrid multistage nanovaccine formulation and to evaluate its anticancer efficacy in murine tumor models. Firstly, the parameters affecting the formulation of the biohybrid nanosystems were assessed, along with the elucidation of the influence of the cell membrane coating on the colloidal stability in physiological conditions and on the biocompatibility in different cell types. Secondly, the effect of the cell membrane-wrapping on the cellular uptake was evaluated in the presence of inhibitors of selective uptake pathways, to assess the differences between naked and coated nanoparticles. Then, a multistage nanovaccine was engineered by glass capillary microfluidics, followed by the cloaking with the cell membrane. The immunological profile of the nanovaccine was investigated *in vitro*, assessing the expression of co-stimulatory signals and the secretion of proinflammatory cytokines. The efficacy of the biohybrid nanovaccine as a monotherapy and in combination with an immune checkpoint inhibitor was then evaluated in melanoma murine models. Finally, the adjuvant core was changed from synthetic nanoparticles to oncolytic adenoviruses to investigate the translatability of the technique, the influence of the cell membrane-coating on the viral infectivity, and the preventive and therapeutic efficacy of the vaccine in different tumor models. Overall, porous silicon and adenovirus-based biohybrid nanovaccines were developed, providing new insights on the structure and efficacy of these systems as therapeutic cancer nanovaccines.

Acknowledgements

Happenstance is the word summarizing the past 4 years and some months. Happenstance has led to this PhD, to uncountable experiences, friends for life and life for friends. Looking back at that January I realize I had absolutely no idea about the experience I was embarking on. Now, after innumerable failures, problems, long nights, wrinkles, white hair, boosted immune system, I realize the beauty of the journey. All this has been possible thanks to you, yes you, that are reading and also to you, you can skip pages, it is boring, I know. In the next few lines, pages, encyclopedias I will try to briefly acknowledge who walked with me along the road.

I would firstly thank the Faculty of Pharmacy for my current position which allowed me to pursue research without worrying about the hideous world of grant applications. I humbly hope I was able to pay a 0.0000000001% of the investment back.

I am deeply grateful to Mr. Opponent, Professor David Mooney for accepting the invitation and I am looking forward to the discussion.

I am also thankful to my pre-examiners, Dr. Ciro Chiappini and Assistan Professor Joy Wolfram for their insightful comments which improved this thesis.

I was lucky in starting with or collecting along the way supervisors ready to listen and discuss with me, knowing that I already unknowingly had the answer I was looking for (and to correct my contorted sentences).

Jouni, I had the pleasure of your editing on all of my text, including this thesis. I am deeply thankful for your trust in me all along the way and for your support.

Hélder, I am still wondering what you saw in me 6 years ago, during my thesis internship. I felt your support (and a friendly, little, insignificant, pressure) on my shoulders every day since. With your help I discovered that, after all, I still like to spend my days “re-searching”. I am also grateful for all the amazing pictures during these years.

Vincenzo, the creativity boost and the freedom you gave me and Mr. M. had a deep impact on the last two years of my PhD. A good laugh and a metaphor in Napoletan (requiring the presence of a translator) refresh even the worst day. Thank you for being like St. Thomas and not believing in anything without a solid proof.

I am extremely thankful to Professor Jarno Salonen and Ermei for providing me with PSi particles and exceptional editing. Ermei, I am still without words for your “flabbergasted”… I learnt the lesson… after 4 papers.

In the multiverse another me is writing an eulogy at the funeral of her PhD… well not in this universe, so let’s go to the funny part. Each of the people

I crossed path with have thought me something valuable… along with a lot of chitchat and nonsense. Many of them are concentrated on two floors. Seriously, we should have everyone on the same floor, I may have consumed the stairs in between (probably the elevator buttons more often).

First I would like to thank all the present and past members (Dr. Dongfei Liu, Dr. Hongbo Zhang, Dr. Mohammad-Ali Shahbazi, Dr. Barbara Herranz, Dr. Neha Shrestha, Mr. Eloy Ginestar) of Santos' lab for their help. Each of you has contributed in this journey whether in giving 10 minutes extra time in cell lab or baking yet another cake.

One of them, I will not name her, otherwise she will kick me after the dinner (yes, Alexandra is you) was an accomplice in routinely defenestrate two professors from the coffee room and their early morning coffee. I still think Professor T. hates us.

Now, image a spring school, Sicily, warm weather, and the discovery that there is never enough pasta for Monica. Jokes aside, you have been my guiding light in these last months and I cannot thank you enough for everything (one day I may spell the word biohybdrid correctly… or is it biohybrid?).

Giulia and Patricia, it seems that indeed all shops and museums in Basel are closed on Sunday, too bad, we have to go back there again. Antti, elämä on… another immunostimulation experiment, Fortessa misses you. At this point, from which pulpit comes João? Luckily Murano Oy closed, I couldn't have listened another time Occidentalis Karma. Ariella, thank you for showing me who a real California girl is.

Finally, Nazanin, Azizam, the assistant director is always available to find you props and actors, and for everything else.

Thanks to Sami, Jukka, Dunja, Tiina, and Jenni for the amazing time in the teaching lab and in the coffee room.

I had several students during this time, little dwarves, smurf, slaves that later became friends. Each stage of this PhD brought along special students, all with special qualities.

I would like to start by thanking the lady of the Zeta Sizer, unbeatable champion with 4000 measurements in 3 months… Miss Silvia Albertini! Your dedication, attitude and hard work made the first publication of this thesis reality.

When I was little I loved Mary Poppins and I never thought I would have met my personal kukkahattutäti able to make us tidy up the whole lab. Cheers to the applegirl and best translator ever Hanna!

Then it is the turn of my personal yoga and meditation teacher, to help me get through the last 4 months. Thank you Daniela, for your patience with an old goldfish forgetting everything.

I haven't had the pleasure of having them as my students, but they have become good friends and long-distance sources of entertainment. Federica and Giusi, you have never met in person but you have so many things in common, including an insane passion for stickers and emoji.

We all have that crazy friend fixed on sweets, craving them, dreaming about them, don't we? Dr. Sara Feola has provided important insights on the formulation development of chocolate salami and on the "Ottoviano's" way of life (no, no angels and songs, please).

At the same there is also that friend, yes that one from Naples city, too cool to say hello in a civilized way. The guy, I forgot the name, Jacopo??, the one that is "supposedly" doing science on the PC? We all know you love Otto (the cat version).

My uncle, Cristian, the Yoda of IVT lab, the harshest critic of ExtraCRAd (we made it) and the talented photographer of my elbow in a lab coat. Thank you for taking some nanoparticles and give them a try on the animals.

Siri, you showed me how to be a scientist and what dedication is. We still believe you can make miracles… or simply amazing science.

Kati, torchbearer of the pains with Accurí (and amazing translator) and Firas, Dracula of the modern days, thank you for lunch, laughs and korvapusti (still waiting for Nutella crepes). Otto for your inspirational talks while we were trying to fix Accuri… and for the dessert!

3 years ago I was an innocent PhD student, I had never experienced jet lag, never went outside my comfort zone. All of that was about to change, please let Mr. M. Fusciello enter together with a crazy, challenging, enticing idea. Will our heroes prove the existence of ExtraCRAd? Prof. Surfiello doesn't believe till he touches, Mr. Capasso wants a series of black and white portraits… so long nights, even longer nights, jet lag without leaving Helsinki, weekend, holidays, cpr to nude mice, miracles, little Lazarus, green cells, red viruses, poor cars. Manlio you are my inspiration as scientist, your emotion and excitement for each "cool" result made me rediscover the passion for research. And besides…. we rock (with the comment from Vince that I am not going to write)!

First they were 5, then they were 3. In these years I haven't learned about time zones yet, forcing Dr. Bea Malacrida to mute the WhatsApp chat (are you still sure Irelend and the U.K. are not in the same time zone as Helsinki?). Aurora, Dr. Grimaudo,… I don't even know what to write anymore… I guess we can say we all survived the PhD… or almost (open a restaurant or going back to farming?).

Sitten, Mikon mummolle, kiitos paljon koska sinä toivotit minut kuin lapsenlapseksi perheeseen.

Well, then I think it's the turn of the dishwasher (with thousands of generations of dishwashers behind him), housekeeper, cook, launderette, personal trainer, cat sitter, driver, biggest threat to any diet.... Mikko, you know what I am going to write... bahf! Such a big effort to bear with you :P

Finally, the triad of giant Amazonian toads, il Sig.ra Bellinetto, Raviola e Banana, you finally had to take a plane and come visit me... if you can find me amongst the trees. Growing is moving forward but never forgetting the foundations (no, non significa cioccolato fondente... non e´ancora ora del dolce).

Helsinki, June 2019

Flavia Fontana

Don't Do Miracles, Do Science

-Siri Tähtinen-

Sikta mot stjärnorna så når du trädtopparna

- Swedish expression-

ὅτι ἃ μὴ οἶδα οὐδὲ οἴομαι εἰδέναι

-Platon, Apology of Socrates-

Table of contents

List of original publications

This thesis is based on the following publications, which are referred to in the text by their respective roman numerals (**I-V**).

I **Fontana, F.**, Albertini, S., Correia, A., Kemell, M., Lindgren, R., Mäkilä, E., Salonen, J., Hirvonen, J. T., Ferrari, F., Santos, H. A., Bioengineered Porous Silicon Nanoparticles@Macrophages Cell Membrane as Composite Platforms for Rheumatoid Arthritis, Advanced Functional Materials, 2018, 28(22), 180355.

II **Fontana, F.**, Lindsted, H., Correia, A., Chiaro, J., Kari, O. K., Sieber, S., Lindgren, R., Mäkilä, E., Salonen, J., Urtti, A., Cerullo, V., Hirvonen, J. T., Santos, H. A., Effect of Cell Membrane Coating on Nanoparticles Uptake and Protein Corona Composition, *submitted*.

III **Fontana, F.,** Shahbazi, M.-A., Liu, D., Zhang, H., Mäkilä, E., Salonen, J., Hirvonen, J. T., Santos, H. A., Multistaged Nanovaccines Based on Porous Silicon@Acetalated Dextran@Cancer Cell Membrane for Cancer Immunotherapy, Advanced Materials, 2017, 29(7), 1603239.

IV **Fontana, F.**[†], Fusciello, M.[†], Groeneveldt, C., Capasso, C., Feola, S., Liu, Z., Mäkilä, E., Salonen, J., Hirvonen, J. T., Cerullo, V., Santos,

H. A., Biohybrid Vaccines for Improved Treatment of Aggressive Melanoma with Checkpoint Inhibitor, ACS Nano, 2019, DOI:10.1021/acsnano.8b09613

V Fusciello, M.[†], **Fontana, F.[†],** Tähtinen, S., Capasso, C., Feola, S., Martins, B., Chiaro, J., Hamdan, F., Peltonen, K., Ylösmäki, L., Ylösmäki, E., Kari, O. K., Ndika, J., Alenius, H., Urtti, A., Hirvonen, J. T., Santos, H. A., Cerullo, V., Artificially Cloaked Viral Nanovaccine, *submitted*.

The publications are referred to in the text by their respective roman numerals (**I-V**). The papers **I** and **III** are reprinted with the kind permission from Wiley, while the paper **IV** is reprinted with the kind permission from American Chemical Society.
In **IV** and **V**, I shared the first authorship with Mr. Fusciello.

Abbreviations and symbols

AcDEX	Acetalated dextran
AIM-2	Absent in melanoma-2
ANOVA	Analysis of variance
APC	Antigen presenting cell
APTS-TCPSi	(3-Aminopropyl)triethoxysilane TCPSi
AR	Aspect ratio
ATP	Adenosine triphosphate
BCR	B cell receptor
CAR	Coxsackievirus and adenovirus receptor
CCM	Cancer cell membrane vesicles
CD	Cluster of differentiation
CpG	Cytosine-phosphate-Guanine
CRAd	Conditionally replicating adenovirus
CTLA-4	Cytotoxic T-lymphocyte antigen 4
DAMP	Damage-associated molecular pattern
DC	Dendritic cell
DLS	Dynamic light scattering
DMEM	Dulbecco's modified Eagle's medium
DNA	Deoxyribonucleic acid
DOX	Doxorubicin
DTX	Docetaxel
ELISA	Enzyme-linked immunosorbent assay
ELS	Electrophoretic light scattering
FCM	Flow cytometry
FFP	Fresh frozen plasma
GM-CSF	Granulocyte macrophage colony stimulating factor
HBSS	Hank's balanced salt solution
HEPES	4-(2-hydroxyethyl)-1-piperazineethanesulfonic acid
HLA-DR	Human leukocyte antigen – DR isotype
ICI	Immune checkpoint inhibitor
IFN	Interferon
IL	Interleukin
imDC	Immature monocyte-derived DC
IMDM	Iscove's modified Dublecco's medium
i.v.	Intravenous administration
LPS	Lipopolysaccharide
MDSC	Myeloid-derived suppressor cell
MEM	Minimum essential medium Eagle

MHC	Major histocompatibility complex
MOI	Multiplicity of infection
MP	Microparticle
MRI	Magnetic resonance imaging
MTS	3-(4,5-dimethylthiazol-2-yl)-5-(3-carboxymethoxyphenyl)-2-(4-sulfophenyl)-2H-tetrazolium, inner salt
NanoCCM	TOPSi@AcDEX@CCM
NEAA	Non-essential amino acids
NK	Natural killer
NOD	Nucleotide-binding oligomerization domain
NP	Nanoparticle
OV	Oncolytic virus
OVA	Chicken ovalbumin
PAMP	Pathogen-associated molecular pattern
PBMC	Peripheral blood mononucleated cell
PBS	Phosphate-buffered saline
PCL	Polycaprolactone
PEG	Polyethylen glycole
PEST	Penicyllin-streptomycin
PLA	Polylactic acid
PRR	Pathogen recognition receptor
PSi	Porous silicon
PTX	Paclitaxel
RANTES	Regulated upon activation, normal T cell expressed, and secreted
RBC	Red blood cell
RES	Reticuloendothelial system
RNA	Ribonucleic acid
ROS	Reactive oxygen species
RPMI	Roswell Park Memorial Institute
SD	Standard deviation
SEM	Standard error of mean
siRNA	Small interfering RNA
STING	Stimulator of interferon genes
TCPSi	Thermally carbonized PSi
THCPSi	Thermally hydrocarbonized PSi
TILs	Tumor-infiltranting lymphocytes
TLR	Toll-like receptor
TME	Tumor microenvironment

TOPSi	Thermally oxidized PSi
tPA	Tissue plasminogen activator
TRAIL	TNF-related apoptosis-inducing ligand
TRITC	Tetramethylrhodamine
TRP-2	Tyrosinase-related protein-2
UnTHCPSi	Undecylenic acid modified THCPSi
VEGF	Vascular endothelial growth factor
Vp	Viral particles
WBC	White blood cell

1 Introduction

Immunotherapy has surged to the honors as a novel concept in cancer therapy with long-term results in subsets of patients treated with monoclonal antibodies or with adoptive cell therapy [1,2]. However, primary and acquired resistance undermines the efficacy of these treatments [3]. Cancer vaccines and oncolytic viruses prime antigen-specific immune responses against tumor associated antigens with potential advantageous combinations with other immunotherapeutics [4-6].

Nanoparticles (NP) represent ideal candidates for vaccine formulation as a result of their properties (*e.g.*, size, shape, and surface characteristics) and of the possibility to simultaneously load and deliver antigens and adjuvants [7,8]. Moreover, nanosystems can present intrinsic adjuvant properties brought along by the material, the responsiveness to intracellular stimuli, and the resemblance to viral and bacterial structures [9-12]. Porous silicon (PSi) represents an innovative material for the development of drug delivery systems, enabling the delivery of poorly soluble drugs [13-18]. Moreover, this material is characterized by a surface-dependent interaction with the cells of the immune system, from immunoneutral to immunostimulatory [11].

Despite the abovementioned advantages, NPs suffer from problems in colloidal stability in physiological-relevant media, formation of a protein corona, and unwanted interactions with cells of the reticuloendothelial system (RES) [19-21]. Recently, biohybrid cloakings have been investigated to improve the colloidal stability, prolong the circulation time in the bloodstream, and reduce the interactions with the RES [22-24]. Furthermore, biohybrid moieties derived from cancer cell membranes constitute an innovative source for the delivery and presentation of antigens [25,26].

This thesis work began with a study on the formulability of PSi NPs characterized by different surface properties and surface charges with cell membrane-derived moieties. The biohybrid nanosystems were then evaluated in terms of improved colloidal stability in human plasma and cytocompatibility in multiple cells. Then, the contribution of the cell membrane wrapping to the cellular uptake of hydrophilic, negatively charged NPs was assessed in the presence of uptake inhibitors, in order to determine the mechanisms employed by naked and coated NPs to enter the cells. Taking into consideration the immunostimulatory properties of PSi NPs, a multistage cancer nanovaccine was prepared by glass capillary microfluidic nanoprecipitation of an acetalated dextran polymeric layer encapsulating PSi, followed by the coating with a cancer cell membrane. The immunological profile of this system was determined *in vitro*, analysing the expression of co-stimulatory signals and the secretion of cytokines. The therapeutic efficacy of

the nanovaccine was then evaluated in murine melanoma models as a monotherapy and in combination with immune checkpoint inhibitors. Finally, the composition of the adjuvant core was changed into an oncolytic adenovirus and the novel nanoplatform, named ExtraCRAd, was assessed for viral infectivity, the pathway followed by ExtraCRAd or naked virus in cellular uptake, and preventive and therapeutic efficacy as a monotherapy *in vivo* in different lung adenocarcinoma and melanoma models.

2 Literature overview

2.1 Immunotherapy and Its Actors

The immune system was considered, for a long time, just the body's army against foreign pathogens, preventing diseases caused by bacteria, viruses, and parasites [27-29]. However, in recent years, the role of the immune system has shifted to include other categories of pathologies. Chronic inflammation and activation of the immune cells of the central nervous system (microglia, astrocytes, and in part, oligodendrocytes) have been associated with development of Alzheimer's disease and other forms of dementia, Parkinson's disease, lateral amyotrophic sclerosis and other neurodegenerative diseases [30-33]. Moreover, immune cells and their soluble mediators play a role in hypertension and cardiovascular diseases, where they are involved in the tissue repairing and remodeling phases [34-36]. A correlation has been established between alterations in the relationship between microbiota and immune system and inflammation-caused metabolic chronic diseases (e.g., obesity and insulin resistance) [37,38]. Sometimes, the immune system itself can cause pathologies, by losing control over the small autoreactive population of cells normally present in the body, overreacting against the body itself, and leading to autoimmune diseases [39]. Finally, a complex relationship has been proved between tumors and the immune system [40].

Immunotherapy is the exploitation of the patient's immune system to treat a disease. Active immunotherapy includes treatments aimed to prime an immune response against antigens (*e.g.*, vaccination and tolerogenic vaccination), while passive immunotherapy is performed by administration of antibodies or adoptively transferred T cells [15,41]. An immunomodulation can be achieved also by the administration of cytokines or immunosuppressant drugs [42]. These therapeutic options interface with different actors playing a role in the immune system. The traditional role of the immune system is mediated by two arms, the innate and adaptive systems [29]. The innate immune system includes cells presenting germline-encoded receptors not subject to rearranging: antigen presenting cells, eosinophils, mast cells, neutrophils, and natural killer (NK) cells, as depicted in **Figure 1** [43].

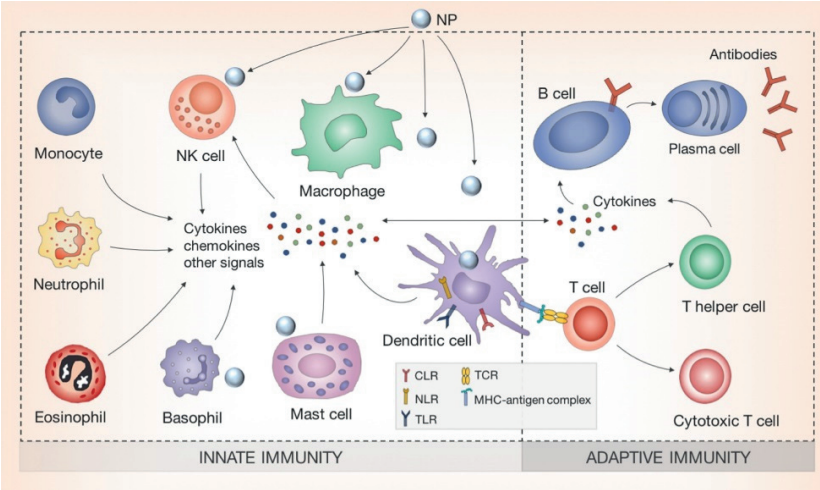

Figure 1. Schematic of the cells and immune mediators belonging to the innate or adaptive immune response. Adapted and reproduced with permission from [44]; copyright © Elsevier B.V. 2017.

These cells use pattern recognition receptors (PRR) to identify pathogen associated molecular patterns, highly conserved features in bacteria and viruses [45,46]. The same receptors are also sensitive to danger associated signals (damage-associated molecular pattern, DAMPs) released from necrotic cells (*e.g.*, heat-shock proteins, uric acid, and high-mobility group box 1 protein) [47]. The PRR receptors identified so far are Toll-like receptors (TLR), C-type lectin receptors, nucleotide-binding oligomerization domain (NOD)-like receptors, inflammasome, retinoic acid inducible gene-I, and absent in melanoma 2 (AIM2)-like receptors [45,46]. These receptors are positioned on the extracellular membrane, in the endosomal compartments, and in the cytoplasm [48-51]. The receptor mediates the activation of innate cells either into effector cells that eliminate the pathogen, or in the case of antigen presenting cells (APCs), they mature and prime cells of the adaptive arm [43]. The adaptive immune response is constituted by lymphocytes, T and B cells, whose receptors recognize the antigens presented by the APCs [52]. The traditionally proposed mechanism of APCs-mediated activation of naïve T cells focuses on 3 signals: (1) antigen presentation on the major histocompatibility complex (MHC; class I for cytosolic or cross presented antigens, class II for endosomal and extracellular ones); (2) presentation of co-stimulatory signals (*e.g.*, cluster of differentiation CD80); and (3) secretion of proinflammatory cytokines [53]. Naïve T cell can differentiate into CD4 helper T cells, CD8 cytotoxic lymphocytes, and regulatory T cells based on the position of the antigen and the state of activation of the APCs [54-57]. However, recently the type of PRR

activation has been shown to influence the downstream differentiation of the lymphocytes [57]. B cells can be activated by the presence of B cell receptor (BCR)-specific antigens, co-stimulation provided by T-helper cells (CD40), together with a specific cytokine environment, leading to the production of specific antibodies isotypes. However, these cells can also be activated T cell-independently, by a combination of signals provided by TLRs and antigens on BCRs, leading to the production of immunoglobulin M [52].

These players represent the target for cancer immunotherapy and nanotechnology in particular, as discussed in the next section.

Cancer immunotherapy is based on the theory that the interaction between the tumor and immune cells is a three stage immunoediting process, as shown in **Figure 2**.

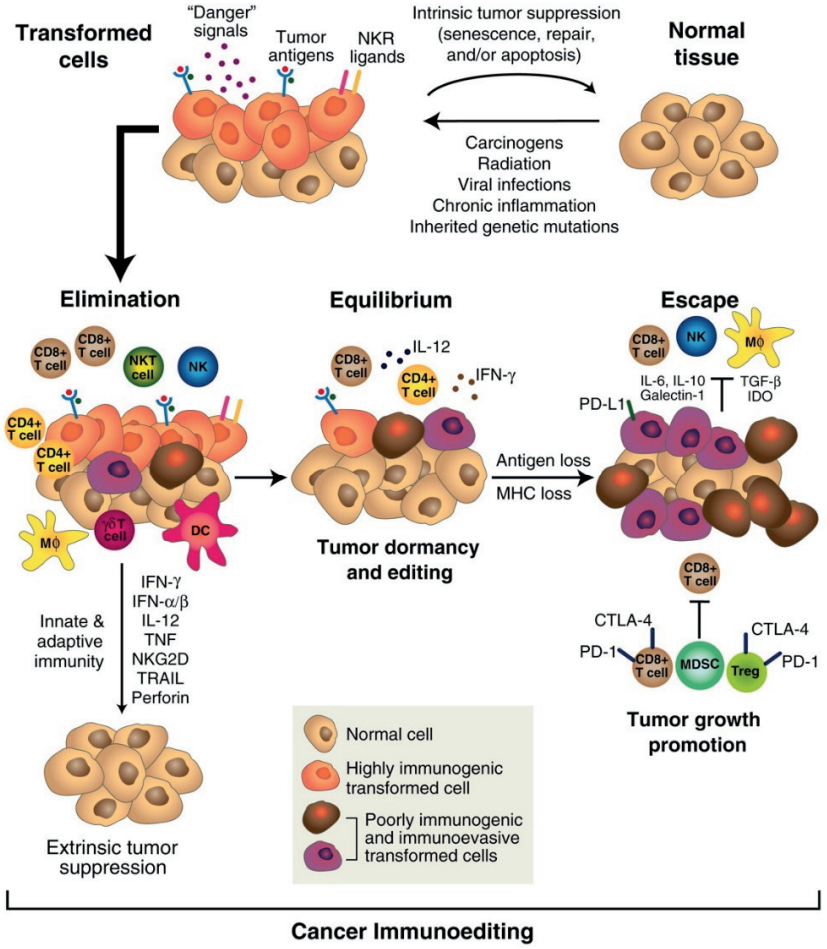

Figure 2. Cancer immunoediting as a three stage process: a cancer tissue presents danger signals and tumor antigens, which are recognized by a

variety of immune cells in the elimination phase. This phase can evolve into a dynamic equilibrium, which is eventually broken, with changes in the tumor microenvironment promoting the tumor growth. Reproduced with permission from [58]; copyright © 2011, American Association for the Advancement of Science.

The first phase, elimination, involves cells of the immune system scavenging the body for mutated cells and killing them. In the second stage, cancer cells that fortuitously escaped from the first stage start growing and organizing into a tumor; however, this growth is controlled in a dynamic equilibrium by the immune system. Finally in the third phase, tumor escape, due to the array of mutations acquired and the selective clonal antigen downregulation caused by the immune system, the tumor growth is uncontrolled [59]. Thereby, several therapeutic options aim to restore the balance between immune cells and tumor (second phase), or in the best cases to result in eradication of all the cancer cells (first phase).

Monoclonal antibodies interfering with the mechanisms of regulation of the immune system (immune checkpoint inhibitors, ICI) currently represent the gold standard in the treatment of hot tumors (cancer tissues characterized by a high infiltration of immune cells) [2,60]. However, the therapeutic efficacy of ICI is limited in patients with cold tumors [3]. Cancer nanovaccines and oncolytic viral vaccines constitute promising platforms for the priming of a cancer-specific immune response, to be supported by the following administration of ICIs, in cold tumors [61-65].

2.2 Nanotechnology for Cancer Immunotherapy

Nanotechnology has played a role in biomedical applications since the first investigations on liposomes and polymeric nanosystems [66,67]. NPs owe their popularity to the advantages they bring when compared to conventional drug formulations [68,69]. In particular, nanosized systems can modify the dissolution rate of poorly water-soluble compounds, increasing their efficacy and allowing a reduction in the dose, or rekindle the research into potent small drug molecules discarded into the discovery process because of their suboptimal physicochemical properties for their formulation [70,71]. Moreover, the delivery of a therapeutic compound with NPs modifies the pharmacokinetics of the drug, resulting in different sites of accumulation, lower or less dangerous side effects (*e.g.*, the delivery of doxorubicin —DOX— into liposomal platforms reduces dose-dependent cardiotoxicity, but induces palmar-plantar erythrodysesthesia) [72-74]. Nanosized drug delivery systems constitute versatile platforms for the simultaneous delivery of multiple drugs

(also with different physicochemical properties), of drugs and RNAs (with different targets and kinetics for the release), and of drugs and imaging moieties (theranostic particles allowing the simultaneous treatment and diagnosis)[75-80]. In spite of all the abovementioned advantages, targeted NPs struggle to reach the tissue of interest: *e.g.*, a meta-analysis of the data reported in literature revealed that, on an average, only 0.7% of the injected dose of particles reaches the tumor in animal models [81]. Moreover, upon administration, the foreign platforms become cloaked by tissue-specific proteins, leading to the formation of a protein corona [19,82]. The modification of the particles' surface is patient-specific and the formation of a protein corona may have undesired effects on the performance of the NP (*e.g.*, loss of efficacy of targeting moieties, undesired flagging by the complement, unspecific uptake by immune cells, immunotoxicity). These factors lead to differences in the pharmacokinetics and interfere with the particles uptake by the target cells [20,83-86]. Thereby, the engineering of NPs needs further development, in concert with deeper research into the interactions between such NPs and the human body [87].

Nevertheless, NPs serve as exquisite tools in immunotherapy, both for immunostimulation and immunosuppression [7,88,89]. Different parameters influence the interactions between the immune system and NPs, as summarized in **Figure 3** and in **Table I**.

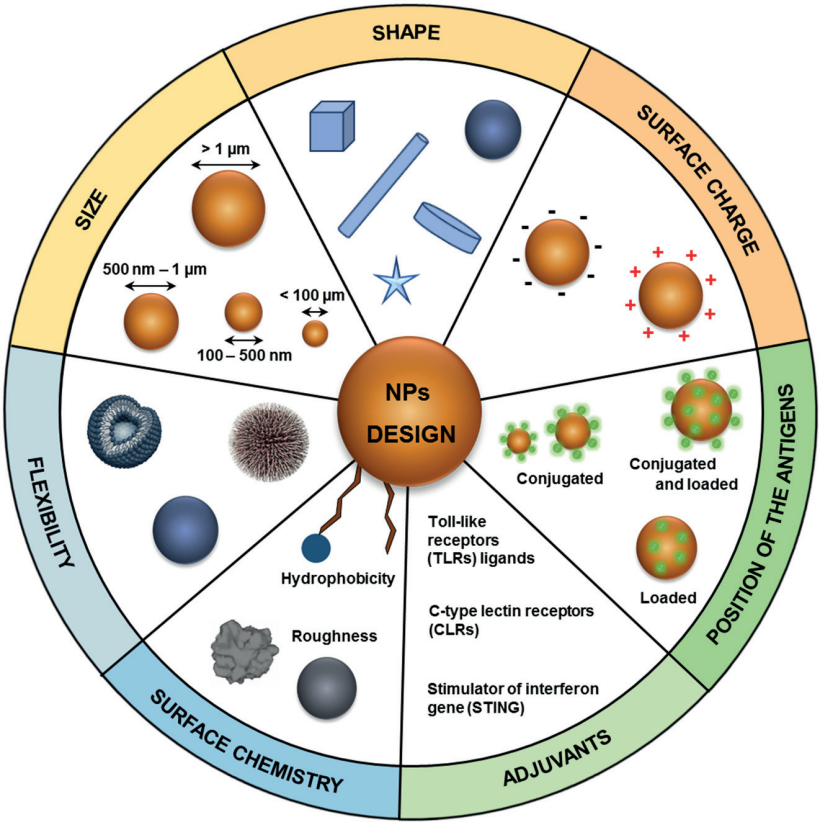

Figure 3. NPs parameters influencing the interaction with the immune system. A careful development of the NPs precisely tailors the effect of the biomaterial on the immune cells. Reproduced with permission from [90], copyright © 2019, Elsevier B.V.

The size of a nanoplatform influences its distribution and draining to the lymph nodes, together with the type of immune response induced, whether it is an antibody or a cell-mediated one [91-93]. The shape exerts an effect mainly due to the effect on the cellular uptake; particles presenting different aspect-ratio (AR), from spherical to filaments, are characterized by different uptake efficiencies [94-96]. The surface charge of a NP is responsible for enhanced interaction with the cell membrane, leading to increased uptake [97]. In addition, a surface presenting different charges will interact with different proteins, ultimately presenting a different protein corona [98,99]. Moreover, other properties of the NPs impacting the interaction with immune cells are the surface chemistry (mainly the hydrophobicity of the system) and the elastic module of the particle. An increase in the hydrophobicity of the surface increases the immunogenicity of the particle due to the danger signal

delivered to the dendritic cells (DCs), together with the delivery of complement fragments that adsorb non-specifically to the particles' surface [11,86,100-102]. As for the elasticity/rigidity, rigid particles are internalized faster by APCs, resulting in increased activation of the cell [103-105]. Finally, the loading of adjuvants in the particles increases the immunogenicity of the formulation, while the position of the antigen on the particles influences both the immunogenicity and type of immune response [106].

Table I. Parameters influencing the immunogenicity of NPs.

Parameter	NPs	Effect	In Vitro	In Vivo	Ref
Size	Polypropylen sulfide spheres	Size-dependent translocation to lymph nodes	-	Interstitial injection of fluorescent NPs. 20 nm NPs faster lymphatic drainage; 20 and 40 nm NPs longer residence time in lymph node	107
	Lecithin/glyceryl monostearate oil-in-water emulsions	Size dependent adjuvant effect	-	Subcutaneous injection of smaller NPs (230 nm) induced higher antibody titer and cellular activation	108
	Carboxylated polystyrene spheres	Size dependent immune activation	-	40 nm particles induced higher titer of antibodies, together with higher priming of CD4 and CD8 T cells	91
	Silica NPs	Size dependent enhanced cross presentation	70 and 100 nm particles enhanced the antigen cross presentation	-	109
Shape	Polystyrene particles modified to obtain different AR	Shape dependent uptake by APCs	Elongated particles adhere more than spheres, but they are less uptaken	-	94
	Mesoporous silica rods with different AR	Shape dependent biodistribution	-	Spherical particles are retained in the liver, while long rods are sequestrated in the spleen	110,111

Table I. Cont.

Parameters	NPs	Effect	In vitro	In Vivo	Ref
Shape	Polystyrene particles modified to obtain different AR	Shape dependent activation of APCs	APCs are activated by spherical particles more than by elongated ones	-	[112]
	Spherical or rod-like particles	Shape dependent type of immune activation	-	Spherical particles induced Th1-mediated response, while rod particles promoted Th2-mediated activation	[95]
Surface Charge	Hyaluronic acid-modified chitosan NPs	Charge dependent composition of the protein corona	Hyaluronic acid-modified NPs bind anti-inflammatory proteins and do not bind clusterin	-	[113]
	Gold NPs with different surface modifications and charges	Charge dependent biodistribution of the NPs	-	Neutral charged particles interact the most with immune cells (Kupffer cells in liver, white and marginal pulp in spleen)	[114]
Hydrophobicity	Gold NPs with different hydrophobicity	Hydrophobicity dependent immunostimulation	Higher hydrophobicity leads to higher cytokine and immune stimulation	-	[115]
	PSi NPs with different surface chemistry	Surface chemistry dependent immmunostimulation	Increased presentation of co-stimulatory signals and T cell proliferation	-	[11]

Table I. cont.

Parameters	NPs	Effect	In Vitro	In Vivo	Ref
Elasticity/Rigidity	PEG-based nano hydrogels	Flexibility dependent biodistribution	Softer particles have reduced uptake by macrophages	Softer particles have prolonged blood circulation	[116]
	Rigid liposomes	Flexibility dependent activation of APCs	-	Intramuscular injection resulted in increased activation of APCs and increased priming of naïve T cells	[117]
Position of the Antigen	PLGA NPs	Antigen position on activation of the immune system	-	Enhanced production of antibodies and memory cells for the formulation with antigen encapsulated and adsorbed	[90]

APCs, antigen presenting cells; AR, aspect:ratio; DCs, dendritic cells; NPs, nanoparticles; PEG, polyethylene glycol; PLGA, poly(lactic-co-glycolic acid); PSi, porous silicon.

The new wave of interest in research about cancer immunotherapy culminated in the choice of immunotherapy as the breakthrough of the year in 2013 by Science, resulting into a shift from the development of NPs for the delivery of chemotherapeutics to nanosystems for immunotherapy [1]. Cancer immunotherapy focuses on three main approaches to modify the immune balance in the tumor microenvironment (TME) and to restore the functional tumor-specific T cells: (1) adoptive T cells therapy, with cells primed *ex vivo*; (2) modification of the TME, with the use of ICI; and (3) cancer vaccination for the priming of novel tumor antigen-specific T cells [118].

Materials engineering plays a role in all the three different therapeutic approaches, as shown in **Figure 4**. Biomaterials scaffolds can influence the immune environment *in vivo*, by slowing down the release of modulators from the matrix or microparticles (MPs) embedded in the scaffold; engineered particles are used in the *ex vivo* manipulation of immune cells, and nanomaterials serve also as drug delivery systems or vaccines targeted to the lymphoid organs or to the tumor microenvironment [119-121].

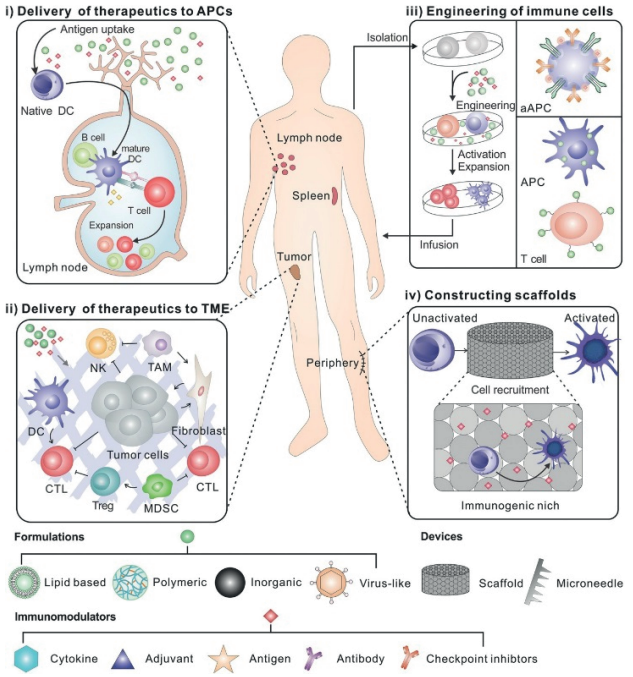

Figure 4. Different areas of research for biomaterials in cancer immunotherapy: as delivery systems to the lymphatic organs or the tumor microenvironment, for *ex vivo* engineering of the immune cells (adaptive therapy), or as scaffolds for the *in vivo* recruitment, activation, and priming of cells. Reproduced with permission from [119]; copyright © 2017 WILEY-VCH Verlag GmbH & Co. KGaA, Weinheim.

Different types of materials have been explored for the creation of immunomodulatory niches for the activation and priming of immune cells *in vivo* [122,123]. In particular, polymers and inorganic mesoporous silica have been loaded with chemoattractants (*e.g.*, granulocyte-macrophage colony stimulating factor, GM-CSF), adjuvants and antigens to attract and prime APCs against the tumor [124-126]. Alternatively, the priming of APCs can be mediated by DNA and siRNA loaded into MPs incorporated into the synthetic niche [127,128].

Micro/nanoparticles can also function as artificial APCs. For example, in adoptive T cell therapy, cancer specific T cells are isolated from the patient before being purified and expanded *ex vivo* [129]. The NPs are decorated with antigen-specific MHC together with immunostimulatory signals (*e.g.*, CD28), or with CD3 and loaded with interleukin (IL)-2, to bind with T cells and stimulate them [130,131]. In this application, the shape of the system is

fundamental. For example, non-spherical particles are more effective in the proliferation of the lymphocytes [132].

The two main areas of investigation for the role of NPs in cancer immunotherapy concern the delivery of therapeutics to the tumor microenvironment and their use as cancer vaccines [118]. Traditional nanosized delivery systems for chemotherapeutics have been repurposed to interfere with the TME, by acting on the vasculature and the remodeling of the immune cells [133,134]. The TME contains immunsuppressive cells like M2 macrophages and myeloid-derived suppressor cells (MDSC); such cells can be repolarized to proinflammatory, anti-tumoral ones or directly depleted, to allow for the action of anti-tumoral T cells [135]. The administration of TLR agonists by NPs repolarizes the macrophages to M1 [136], while different nanoformulations have been investigated for the delivery of bisphosphonates, RNAi, cytokines and growth factors to facilitate the repolarization or killing of the M2 population [137-140]. Finally, the co-administration of traditional chemotherapeutics induces immunogenic cell death, with the release of DAMPs and tumor antigens. The simultaneous loading of chemotherapeutics and immunostimulating molecules into a single particle allows the exploitation of the antigens released by the dying cells as vaccines [134,141,142].

Nanovaccines have been developed according to two different approaches (**Figure 5**): (1) NPs can serve as a delivery system for antigens and adjuvants, targeted to the lymph node and to specific types of APCs, and (2) the biomaterials constituting the NPs can act as adjuvants, delivering the antigens to APCs [143]. Polymeric MPs and NPs have been prepared for the loading and delivery of model cancer antigens (usually melanoma-associated model antigens like chicken ovalbumin, OVA, or tyrosinase related protein 2, TRP-2) and a variety of TLR-agonists and other adjuvants [144,145]. The treatment with these formulations induced antigen-specific immune response, with the priming of CD8 T cells [146-149]. Other nanoplatforms like micelles, liposomes, gold NPs, protein NPs, can efficiently deliver antigens and adjuvants, and promote an immune response [150-157].

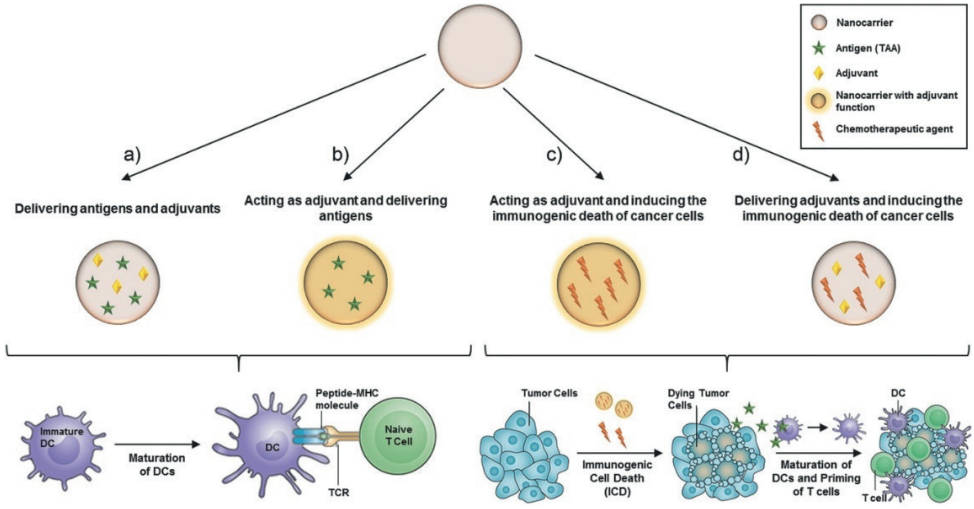

Figure 5. Strategies for the development of cancer vaccines. a) nanovaccines for the co-delivery of antigens and adjuvants; b) immunogenic nanoplatforms for the delivery of antigens; c) immunogenic nanoplatforms inducing immunogenic cell death of cancer cells; and d) NPs delivery adjuvants and chemotherapeutic agents to induce immunogenic cell death. Reproduced with permission from[143]; copyright © 2018 WILEY-VCH Verlag GmbH & Co. KGaA, Weinheim.

Furthermore, nanovaccines may have intrinsic adjuvant properties due to the biomaterial itself, which induces activation of PRRs (*e.g.*, by polymers activating TLRs or stimulator of interferon genes, STING) [158-163]. The immunostimulative properties of the NPs have been associated with different mechanisms, as detailed in Table I. In the case of polymeric NPs, increasing the molecular weight of polymers increases their immunogenicity [10], while higher degradation rates are correlated with the activation of APCs [9]. Nanovaccines assembled from or containing pH-responsive polymers enable the endosomal escape of the loaded antigens, while the rupture of the endosome delivers an activation signal to the APCs [158,164,165]. Alternatively, cues from nature (specifically viral structures) are recognized by APCs as pathogen-associated molecular patterns (PAMPs), leading to immunostimulation, and have been exploited as cancer vaccines.[166] Nanovaccine platforms have also been evaluated in combination with ICI to achieve a "prime and boost" effect [163,167,168]. However, NPs developed according to the traditional perspective as carriers for antigens and adjuvants may result in the induction of an unbalanced immune response in the clonal selection of cells not presenting the antigen, resulting in an inefficient antigen presentation [3,15,143]. Thereby, alternative sources of antigens and core adjuvant nanoplatforms are currently

being developed and are discussed in the following sections, starting from the development of biohybrid coatings as an innovative source of antigens for the investigation of novel materials like PSi and for the re-evaluation of oncolytic viruses as natural vaccine adjuvants.

2.3 Biohybrid Nanosystems–Cell Membrane

Some of the most critical limitations of the abovementioned nanosystems are limited circulation time and interactions with the cells of the immune system. To solve these challenges and taking inspiration from nature, two different approaches have been proposed so far: (1) the bottom-up one focuses on the functionalization of nanomaterials with biological stealth molecules (*e.g.*, surface functionalization with CD47 markers that transmit a "do-not-eat-me" signal to macrophages and other cells of the RES [169,170], hitch-hiking particles onto cells [171-174]); and (2) a top-down approach aiming to decorate the surface of micro/nano-carriers with moieties derived from the cell membrane, resulting in the development of biohybrid systems carrying all the advantages of biological camouflage [21]. Alternatively, NPs can be directly bound to the surface of cells (*e.g.*, by red blood cells, RBCs) to increase their circulation time in the bloodstream [171,175].

To date, several different sources of membranes have been explored to coat different types of micro/nano-platforms with different type of applications, from drug delivery to artificial intracellular bioreactors, as shown in **Figure 6** and listed in **Table II** [21,176].

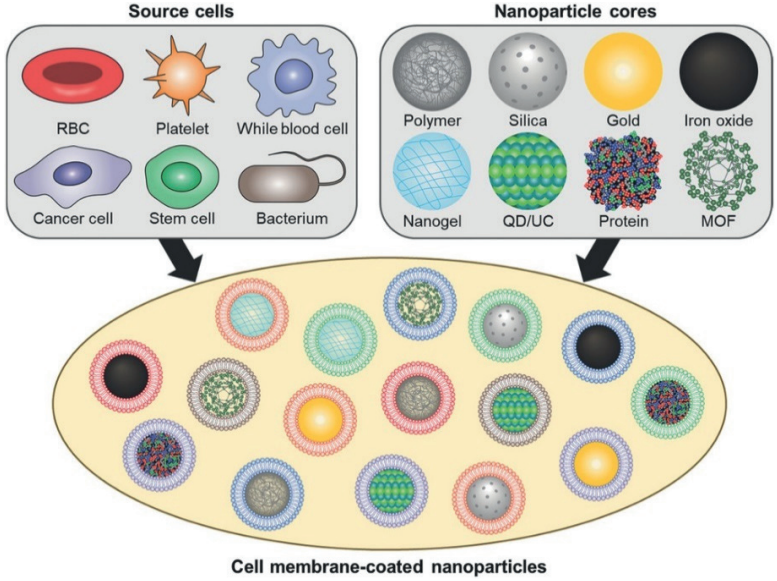

Figure 6. Summary of the different cells used as sources of cell membranes and examples of the cores coated so far. Modified and reproduced with permission from [21]; copyright © 2018 WILEY-VCH Verlag GmbH & Co. KGaA, Weinheim.

The membrane of RBCs is regarded as an optimal biocamouflage source due to the prolonged circulation of such cells, with limited interactions and uptake by the RES [177-180]. The prolonged circulation time leads to enhanced accumulation into tumor or inflamed tissues by passive accumulation due to enhanced permeability and retention effect [181-186]. Moreover, RBCs can be collected in high amounts from the patient or acquired from blood donors, with good possibility for a blood type standardized formulation for scale-up [21,171]. The attractive feature of prolonged circulation is particularly sought after in the case of drug delivery systems [21]. Moreover, the coating with membrane moieties is useful also to improve the biocompatibility and circulation time of imaging and photothermal probes. A further use of RBC membrane-coated nanoplatform is for immune modulation, both for cancer immunotherapy and as a vaccine against viral pathogens [187-189]. Concerning these applications, RBCs membranes need a further modification with the introduction of targeting moieties or antigens by lipid insertion, to allow for a targeting to the tissue of interest or for the priming of an antigen-specific immune response [190]. Finally, RBC-nanosponges have been developed to detect new viral antigens and remove hemolytic animal and bacterial toxins, small toxic molecules (*e.g.*, pesticides) or to adsorb excessive chemotherapeutic drugs, and as a decoy target for anti-RBC antibodies in autoimmune hemolytic anemia [191-195].

Platelets have recently gained prominence as membrane sources due to their wide availability, and their natural targeting to the sites of inflammation (in wounds, cancer, and vasculature) [196,197]. The applications of these platforms range from drug and growth factor delivery for the treatment of infections, cancer, restenosis, and wound healing, to photothermal cancer therapy and detoxification of autoantibodies [21,198,199].

The development of platforms coated with the cell membrane of immune cells exploits the intrinsic targeting of such cells to the sites of inflammation (*e.g.*, cancer and autoimmune diseases like rheumatoid arthritis) [200-202]. Leuko-like vectors represent the first examples of biohybrid PSi platforms coated with macrophage cell membrane for targeting of inflamed endothelium [203]. Other core particles (mainly polymeric, mesoporous silica, liposomes, iron oxide, gold nanoshells and upconversion particles) were evaluated for drug delivery of chemotherapeutics, for photothermal therapy,

for detoxification from bacterial toxins in sepsis, and for antibody-based detection of circulating cancer cells [204-209].

The rationale behind the investigation of platforms cloaked with a cell membrane derived from stem cells is the striking resemblance between stem cells and cancer cells, in particular for the ability of stems cells to target the tumors [210,211]. Stem cells are also employed towards organ regeneration [212].

Finally, a clever approach to induce immunity against bacterial infection is to coat the NPs with membrane fragments derived from the outer membrane of bacteria [213].

Table II. Examples of biohybrid platforms presented according to the source of cell membrane.

Type of Membrane	Type of Core Particle	Application	Drug / Imaging Agent	Ref
RBC	Gold NPs and nanocages Iron oxide NPs Upconversion NPs Bismuth NPs Melanin NPs Perfluorocarbon-loaded HSA NPs/PLGA NPs	Prolonged circulation, photothermal therapy, photoacoustic therapy, photodynamic therapy, ROS generation, MRI contrast agents	/	23,181,182,184,214-219
	PLGA NPs	Prolonged circulation	Targeting peptides inserted in cell membrane DOX	22,190,220
	PLA NPs PLGA NPs	Delivery of chemotherapeutic and prolonged circulation	DOX	24,183
	PLGA NPs	Targeted delivery of chemotherapeutic, prolonged circulation	PTX	221
	PLGA NPs PEG nanohydrogels Gold nanowire motors	Nanosponge for toxins, autoantibodies, small molecules purification	/	191,192,194,222-226
	PLGA NPs	Bacterial antigens inserted in the membrane vaccination	/	188,226
	PLGA NPs	Tumor antigens cancer vaccine	/	189
	Iron oxide-loaded PLGA NPs	Detection of viral pathogens	/	195,227

Table II. Cont.

Type of Membrane	Type of Core Particle	Application	Drug / Imaging Agent	Ref
RBC	Chitosan magnetically guided NPs	Prolonged circulation	DOX/PTX/Iron Oxide	228
	PCL core coated with thermosensitive polymer and cell membrane functionalized with dye	Prolonged circulation, on-demand release	PTX	229
	Silica core coated with a layer of titanium oxide	Prolonged circulation, on demand release	DTX	230
	Poly(L- γ -glutamylcarbocistein) NPs Chitosan-based nanogels	Prolonged circulation, pH-dependent release	PTX PTX/IL-2	231,232
	Gelatin NPs nanogels	Prolonged circulation, detoxification	Vancomycin	233,234
	Intrabody NPs	Prolonged circulation, intracellular delivery	Intrabodies (anti-human telomerase reverse transcriptase)	235
	Ace-DEX NPs	Glucose-sensitive delivery of insulin, prolonged circulation	Insulin, glucose oxidase, catalase	236
Cholesterol-reinforced RBC		Remote loading, prolonged circulation, pH-dependent release	DOX	237
Platelets	PLGA NPs	Binding to inflamed tissues, binding to infected tissues	DOX/vancomycin	238
		Decoys for autoantibodies	/	239
	Nanogels	Enhanced tumor targeting	DOX/TRAIL	238
	Silica NPs	Targeting to circulating tumor cells	TRAIL	240
	Polymeric NPs	Sequential targeting to bone and myeloma	Bortezomib, tPA	241
WBC	PSi MPs	Avoiding immune clearance, prolonged circulation, transport through inflamed endothelium, enhanced accumulation in tumor	DOX	203
	Iron oxide magnetic nanoclusters	Binding to circulating cancer cell, enrichment of circulating cancer cells	/	208
Monocytes/ Macrophages/Neutrophiles	PLGA NPs, mesoporous silica NPs, liposomes	Enhanced stability in serum, increased uptake in tumor cells, prolonged circulation, augmented accumulation in tumor, targeting and treatment of metastases	DOX, emtansine, carfilzomib	204,205,242,243

Table II. Cont.

Type of Membrane	Type of Core Particle	Application	Drug / Imaging Agent	Ref
Macrophages	Gold NPs, upconversion NPs	Prolonged circulation, enhanced uptake, increased photothermal activity	/	206,244
	PLGA NPs	Detoxification from endotoxins	/	207
Neutrophils	PLGA NPs	Targeting to the inflamed joints, reduction of the inflammation	/	245
Bacteria-activated Macrophages	Gold/silver nanocages	Prolonged circulation, retention at the site of infection, irradiation-dependent antibacteric effect	/	246
T Cells	PLGA NPs	Avoiding immune clearance, improved efficacy together with low dose irradiation	PTX	247
	Gelatin nanogels	Enhanced *in vitro* efficacy, higher accumulation in the tumor	DOX	248
Stem Cells	PLGA MPs and NPs	Stem-cell mimicking, preservation of cardiac functions, similar effect to cardiac stem cells, retention in site of ischemia	Cardiac stem cells medium (with GF), VEGF	212,249
	Iron oxide NPs, upconversion NPs	Enhanced stability in physiological fluids, magnetic hyperthermia applications, photodynamic therapy	/	250,251
Endothelial Cells	Various NPs	Cell-mediated encapsulation in the membrane, MRI, magnetic hyperthermia	/	252
β Cells	Electrospun nanofibers	Proliferation of β cells cultured over the scaffold, maturation of the cells	/	253
Hybrid Membranes	RBC+Platelets, PLGA NPs	Prolonged circulation, detoxification, targeting to atherosclerotic plaque	/	254
	Platelets+WBC, magnetic beads	Isolation and enrichment of circulating tumor cells	/	255
	Leutosomes (WBC+cancer cell), liposomal NPs	Prolonged circulation, enhancement of dose delivered to tumor	PTX	256
	Mesenchymal stem cell+RBC, PLGA NPs	Cell proliferation *in vitro*, targeting to liver, attenuation of acute liver toxicity	/	257

Table II. Cont.

Type of Membrane	Type of Core Particle	Application	Drug/Imaging agent	Ref
Bacterial Outer Vesicles	Gold NPs	Enhanced stability in physiological buffer, increased priming of APCs	/	[213]

Ace-DEX, acetal-functionalized dextran; APCs, antigen presenting cells; DOX, doxorubicin; DTX, docetaxel; GF, growth factor; HAS, human serum albumin; IL-2, interleukin 2; MPs, microparticles; MRI, magnetic resonance imaging; NPs, nanoparticles; PEG, polyethylene glycol; PLGA, poly(lactic-co-glycolic acid); PTX, paclitaxel; RBC, red blood cell; tPA, tissue plasminogen activator; TRAIL, TNF-related apoptosis-inducing ligand; VEGF, vascular endothelial GF; WBC, white blood cell.

2.3.1 Cancer Cell Membrane Coated Platforms

In the treatment of cancer, and particularly in the case of metastatic stage, it is of paramount importance to be able to deliver the therapeutic agent at the site of action. Coating nanosized drug delivery systems or theranostics with membranes derived from cancer cells increases the targeting efficiency of the system due to a homotypic effect demonstrated in several experiments with different source cells [26,258-262]. Thereby, the coating with cancer cell membrane conjugates leads to enhanced stability of the nanosystems in biological environment and to targeting and preferred uptake in the target tissue [263-267]. Moreover, the membranes of cancer cells are rich in tumor antigens or neoantigens, allowing for more effective cancer vaccines [26,167,268,269]. Such vaccines will prime the immune system towards a wider range of antigens compared to traditional NPs carrying only a limited amount of known antigens [25,270]. This will prevent the mechanisms of immune evasion adapted by the cancer cells by downregulating the antigen presentation on the MHC [271,272].

In the first proof of concept, Fang *et al.* demonstrated the maturation of APCs after incubation with polymeric NPs loaded with an adjuvant and coated with a cell membrane derived from cancer cells [26]. The APCs activated by this nanoplatform primed T cells, with the secretion of interferon (IFN)-γ and *in vitro* T cell-mediated killing assay [26]. The following *in vivo* evaluation was performed on murine melanoma models swapping the core particle from PLGA to CpG adjuvant NPs [25]. The prophylactic vaccination with the NPs induced a multi-antigen immune response, which effectively prevented the

tumor growth when the animals were rechallenged [25]. Moreover, biohybrid nanovaccines represent the ideal priming phase in prime and boost immune therapeutic schemes, with the subsequent administration of ICI to support and potentiate the immune response elicited by the vaccine [273-276]. Kroll *et al.* evaluated the therapeutic efficacy of this combination therapy in a poorly immunogenic melanoma model, increasing the number of animals with prolonged survival when compared to the monotherapy with ICI [25].

In conclusion, the use of cell membranes derived from cancer cells represents an innovative and attractive technique to deliver multiple antigens, while improving the total stability of the system.

2.4 Porous Silicon (PSi)

During the last decades, innovative materials have been explored as potential NPs for drug delivery, including PSi. This material was initially reported by the Uhlirs [277], but the first to theorize possible biomedical applications of the porous substrate, given its biocompatibility and biodegradability, was Professor Leigh Canham in 1995 [278]. Usually, PSi is produced by anodization of a silicon wafer in an ethanolic fluoridic acid solution, followed by micronization, milling, or high-pressure homogenization to MPs or NPs [279-283]. Alternatively, microfabrication techniques can produce PSi MPs with discoidal shape or microneedles [284-286], or bottom-up processes can lead to the production of microcrystalline PSi NPs with homogenous size distribution between 3 and 20 nm [287]. PSi was firstly investigated due to its photoluminescent properties, which render it a suitable platform for biosensors and for theranostics [288,289].

Additionally, this material is very versatile for the type of chemistry that can be introduced on the surface [13]. The surface of "as-anodized" particles (hydrides) is not stable to oxidative processes from the atmospheric O_2; moreover, this reactivity may interfere and degrade payloads and is fundamental in the formation of reactive oxygen species (ROS), decreasing the biocompatibility of the material [290-292]. Different surface modifications have been proposed to stabilize the surface, and one of the most commonly employed is the thermal oxidation of the particles, which occurs from temperatures higher than 400°C and is complete (full removal of hydrides) for temperatures higher than 600°C with the introduction of O_2 atoms on the surface and in the Si backbone [293,294]. Salonen *et al.* developed the thermal carbonization and hydrocarbonization processes, allowing the transformation of the hydride groups into hydrocarbon and carbons [295-298]. After regeneration of the surface with hydrofluoric acid, silanolic groups form on the external

layer for further functionalization with acidic and basic moieties, and then with coating, imaging, and targeting moieties [299].

Other advantages of PSi NPs for drug delivery applications include tunable pore size with large pore volume, and high surface area [13], enabling also a control over the degradation speed to orthosilicic acid in biological conditions [300-303]. Amongst the factors controlling the degradation rate, surface functionalization has a prominent role and a common surface functionalization to enhance the circulation time, PEGylation has shown a dramatic increase in the degradation time of PSi particles with the extension of the PEG chain [304]. Moreover, the degradation of PSi particles is dependent on the concentration of ROS, where the particles in tissues presenting higher ROS levels (*e.g.*, tumors) exhibited faster degradation compared to particles in healthy tissues [305].

The high pore volume and surface area allow a high loading degree for drugs, biologics or second-stage nanovectors [284,306,307]. However, one of the downsides of PSi concerns the control over the release of the payload, where the conformation of the large pores cannot prevent the leakage of the drug, inducing premature release [13]. This problem spurred the search for possible solutions from surface modifications to different physical entrapment techniques [13]. Payloads can be entrapped within the pores after loading by sealing of the pores. The sealing happens after the oxidation process or by formation of a silicate shell by reaction between the degradation product of PSi and reagents in solution [308-310]. Moreover, polymers can be chemically conjugated on the surface of the particles, effectively preventing the premature release of the drug [311]. Amongst the physical entrapment methods, PSi NPs were encapsulated into polymeric or lipidic matrix by conventional emulsion [312-314], by microfluidics [315-318], by aerosol flow reactor [319], and by biopolymers and thermosensitive polymers adsorbed onto the PSi particles' surface [320-322].

PSi particles have been developed and evaluated for the diagnosis, treatment, and theranostics in different pathologies. For example, PSi composites were investigated as drug delivery systems in cancer, in cardiovascular diseases, and in the treatment of metabolic disorders (mainly diabetes) [13,323,324].

PSi vectors have also been extensively investigated in cancer therapy. For example, NPs have been modified with targeting ligands and encapsulated into pH-sensitive matrices to produce a punctual drug delivery at the site of interest [316,325-334]. As for bigger particles, discoidal MPs constitute the first stage in a multistadius vector, and are designed to marginate in the blood vessels, allowing a more intimate contact with the endothelial cells for an

easier delivery of the second stage into the cancer tissue [306,335-339]. Recently, PSi was investigated as a platform for the delivery of small molecules to treat the injury in myocardial infarction [333,340,341]. PSi MPs and NPs serve as optimal carriers for oral delivery of small molecules [307], to improve their dissolution rate and bioavailability, and of insulin and other therapeutic peptides like GLP-1 [342-344]. PSi NPs were also investigated for the delivery of growth factors analogues to the brain [345]. Finally, PSi NPs have also applications for the treatment of acute liver failure [346].

2.4.1 Immunological Profile of PSi

Like other engineered biomaterials, PSi interacts with the immune system. In particular, the silicon nanostructured surfaces increase the total level of cytokines secreted by the peripheral blood mononuclear cells (PBMC), without significant differences when compared to standard polystyrene [347]. However, when PSi is processed into MPs and NPs, it exhibits surface dependent activation of APCs. The highest levels of immunostimulation are achieved by particles with hydrophobic surfaces (thermally hydrocarbonized PSi, THCPSi) or by fast-degrading hydrophilic particles (**Figure 7**) [11].

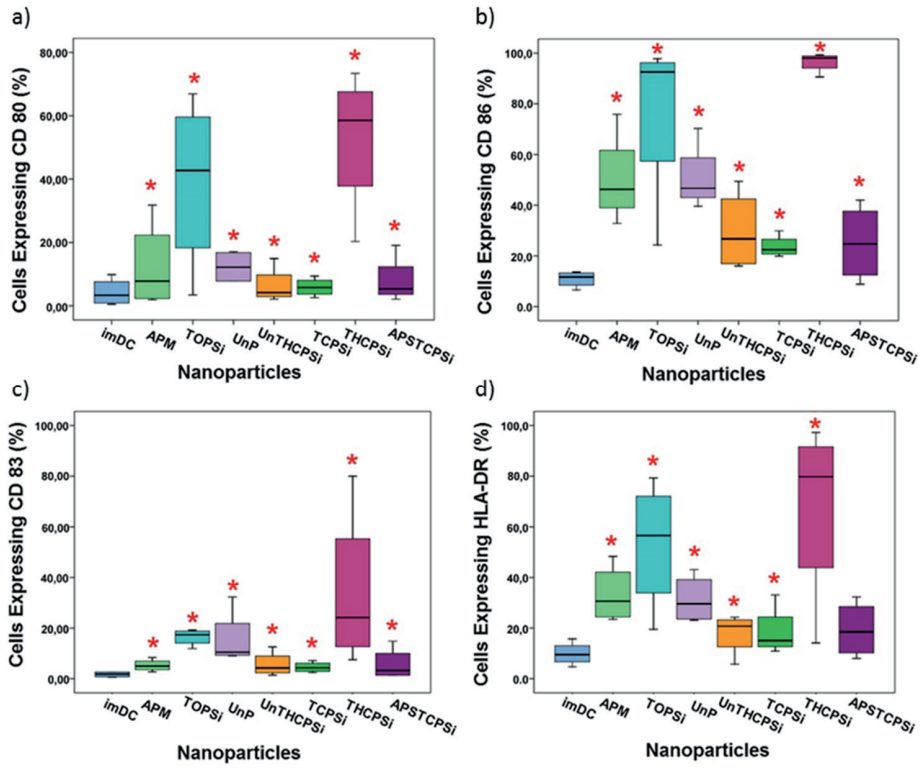

Figure 7. PSi surface-mediated activation of APCs. a) Percentage of immature monocyte derived dendritic cells (imDC) expressing CD80 after incubation with the particles; b) percentage of imDC expressing CD86; c) percentage of imDC expressing CD83; and d) percentage of imDC presenting human leucocyte antigen DR isotype (HLA-DR). Reproduced with permission from [11]; copyright © 2014 Elsevier B.V.

The high immunogenicity of THCPSi can be explained by the adsorption of protein fragments and by the activation of DAMP, while for the hydrophilic particles, the rapid degradation leads to the production of (ortho)silicic acid, an immunostimulant molecule, and to the precipitation of silica crystals with the activation of DAMPs [11,348]. In the case of PSi MPs, the immunostimulatory effect is mainly mediated by the activation of IFN-type I genes in a MyD88 and STING independent way. This leads to an increase in the production of IFN-β and regulated upon activation, normal T cell expressed, and secreted (RANTES) [349]. Moreover, PSi MP-mediated delivery of antigens to APCs enhances the cross presentation, probably due to an early localization in the early endosomes, followed by a translocation to the endoplasmic reticulum [349]. PSi MPs surfaces are suitable for further modification with other adjuvants.

For example, lipopolysaccharide (LPS) and monophosphoryl lipid A (MPL) were successfully adsorbed on the particles' surface, and promoted inflammasome-mediated activation of the APCs, enhancing the secretion of IL-1β, IL-6 and TNF-α [350]. The mature APCs activate CD8 T cells with increased secretion of IFN-γ. Finally, the treatment with adjuvant-adsorbed MPs enhanced the efficacy of a combinatory therapy with liposomal doxorubicin [351].

PSi has also been applied in particle-mediated antibody dependent cell cytotoxicity (ADCC) and in immunostimulant antibodies [13]. The binding of CD40 monoclonal antibody increased the activation of B cells when compared to the antibody in solution [352]. PSi particles can also be loaded with chemotherapeutic drugs and targeted via monoclonal antibody to CD326, promoting ADCC and immunostimulation with the secretion of IL-12 by T cells [353].

Thereby, given its immunologically attractive properties, PSi constitutes an attractive choice as the core material in a cancer nanovaccines.

2.5 Oncolytic Viruses (Adenovirus)

The interest toward the use of pathogenic viruses as a treatment for tumors was sparked already in the 1950's, by observations of spontaneous regression of established tumors concomitantly with or after a viral infection [354]. These treatments, despite the initial reduction in the tumor, did not present long term efficacy and were associated with possible severe side effects, due to the inoculation of pathogenic viruses (*e.g.*, West Nile virus), thus they were dismissed in favour of the more promising chemotherapy [354]. The return of viruses for therapeutic use started with their molecular biology modification into transfection vectors for gene therapy [355]. Moreover, the elucidation of the pathways of interferon mediated signalling pointed to the lack or diminished activity of viral defences in tumoral cells, making oncolytic viruses (OVs) an ideal agent for cancer therapy [356,357]. The first OV, Imlygic (T-Vec), was approved in 2015 by the Food and Drug Administration and the European Medicinal Agency for the treatment of melanoma [358,359].

The mechanisms of action of oncolytic viruses are multiple and diverse [6]. The traditionally proposed action is based on selective lysis in cells defective for interferon and apoptosis pathways [360]. Lately, a second mode of action for OVs has been investigated, as shown in **Figure 8**. OVs in their cell lytic action serve also as cancer vaccines, inducing the release of tumor associated antigens and neoantigens together with DAMPs, while acting themselves as adjuvants [361]. The viral nucleic acid present in an infected cancer cell phagocytized by APCs activates TLR, inducing the maturation of the APCs [362].

Moreover, studies on viral vectors for gene transfer revealed an immunogenic role of the capsid with the activation of proinflammatory pathways in different cell types [355]. The immunological action of OVs in the tumor microenvironment transforms immunologically cold tumors into hot tumors, with a synergistic effect when combined with immune checkpoint inhibitors [363,364]. OVs can also modify and disrupt tumor vasculature by targeting to the vascular endothelial growth factor (VEGF) [365-367].

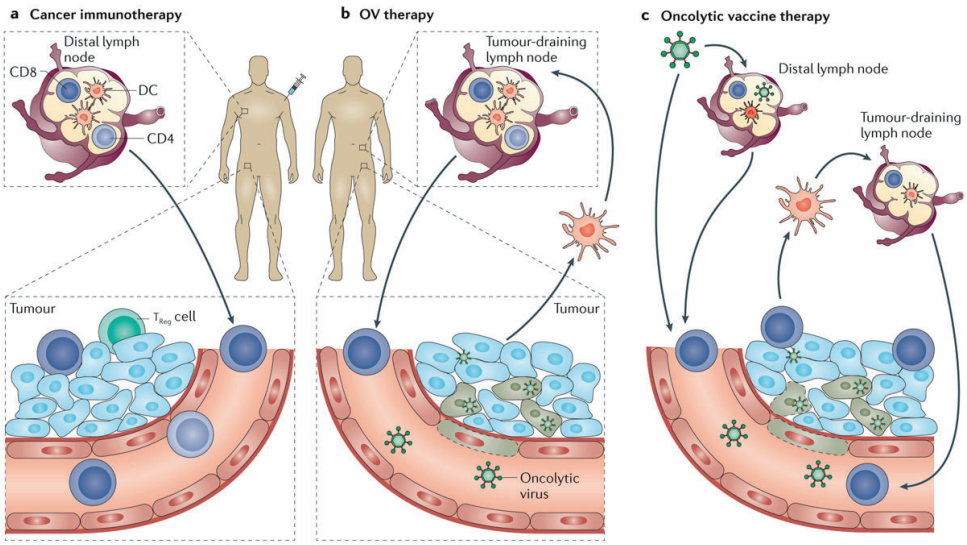

Figure 8. Comparison between the mode of action of a) traditional cancer immunotherapy and b) oncolytic viral therapy in the tumor microenvironment; c) OVs act also as vaccines, priming distal lymph nodes and turning the tumor microenvironment less immunosuppressive. Reproduced with permission from [368]; copyright © 2014 Macmillan Publishers Limited.

The OVs designed so far have been engineered for intratumoral local administration to maximize the lytic effect. However, given the variability among solid tumors, the not always easy access to lesions, and the presence of metastases, intravenous (i.v.) administration of the viruses is currently being investigated [369,370]. One major obstacle is represented by neutralizing the antibodies and pre-existing immunity to the specific OVs, which cause the inactivation of the majority of the virus administered i.v.[6]. Possible solutions include the use of different serotypes, the coating and cloaking of the virus with PEG and other polymers, or a vaccination scheme with the priming phase with OVs and the boost phase mediated by a completely different virus [360,371-375]. The modifications sought in the development of OVs aim to achieve

enhanced targeting to cancer cells, attenuating the pathogenicity, increase the antitumor immunity, control and limit the effect of the antiviral immune response, and improve the bioavailability [360]. Moreover, the approval of an OV in the clinic requires also the establishment of procedures to obtain clinical-scale and -grade production of the viral vector, suitable purification complying with the requirements set by regulatory authorities and an online quality control system [376].

Adenovirus is an attractive candidate for oncolytic viral therapy, because it is easily produced with high titer into immortalized cell lines with protocols for the purification, either by centrifugation with cesium chloride gradients or by chromatographic methods, which are widely available [376]. Moreover, its genome is easy to modify with deletions of early genes, which usually prevent viral spreading, and the insertion of transgenes with the engineering of conditionally replicating adenoviruses (CRAd) [360]. In particular, two widely described modifications involve a 24 base pairs deletion in the gene coding for EA1, allowing the viral replication only in cells defective in the Rb mechanism (*i.e.*, cancer cells) and the insertion of genes coding for immunostimulatory factors (*e.g.*, GM-CSF) [354]. Human adenoviruses are present in roughly 50 different serotypes, all characterized by linear double stranded DNA, enclosed within a non-enveloped icosahedric capsid, as shown in **Figure 9** [377].

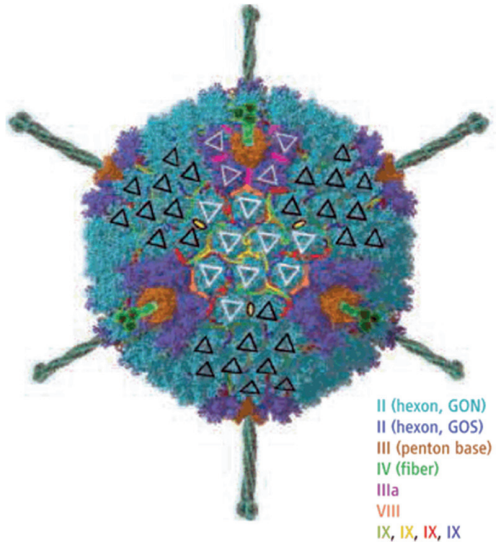

Figure 9. Structure of a human adenovirus, showing the fibers, hexons and pentons. The average size of the core is 90 nm. Reproduced with permission from [378]; copyright © 2010, American Association for the Advancement of Science.

There are three types of proteins forming the capsid: (1) hexons, with a structural role; (2) pentons, for the secondary binding to $\alpha_v\beta_{3,5}$ integrins for internalization; and (3) fibers for the interaction and recognition with coxsackie and adenovirus receptor (CAR) [377,379,380]. The therapeutic efficacy of this virus is partially mined by the diffuse pre-existing immunity and by the need of the CAR receptor on the target cells to promote viral internalization. In an effort to address these issues, less common or hybrid, chimeric, serotypes have been developed, together with engineering of the fibers to modify biodistribution, reactions with the neutralizing antibodies, and interactions with and internalization into the tumor cells [379,380].

One first generation oncolytic adenovirus is currently approved in China, in combinatorial treatments with chemotherapeutics in the treatment of head and neck cancer [381]. Other viruses, encoding for the expression of immunostimulatory cytokines are in clinical trials [354,382]. Moreover, CRAd modified to increase the CpG adjuvant sequences was coated with antigenic peptides with the formulation of a complete cancer vaccine, PeptiCRAd [383]. The vaccine is easily assembled by simply mixing the oncolytic adenovirus with peptides modified to increase their positive charge, where by electrostatic interaction the antigens adsorb on the surface of the capsid, tilting the balance between the relative viral and anti-tumoral immune response. Recently, a similar modification was developed also for an enveloped virus like vaccinia, resulting in a complete vaccine platform delivering tumor-specific antigens [63].

Thereby, adenoviruses can be considered as biological NPs, exhibiting a complexity still not achievable with synthetic NPs, which provide immunostimulatory cues to APCs, serving *de facto* as adjuvant cores for cancer nanovaccines.

2.6 Glass Capillary Microfluidics and Nanoprecipitation

Microfluidics is the technique involving fluids at the micro/nano-scale for analytical and synthetic purposes [384-386]. However, one of the major applications of microfluidics resides in the preparation of MPs and NPs [387-390]. This technique presents several advantages when compared to the bulk preparation methods. For example, given the size of the channels, small volumes of reagents are needed, which is important in the case of expensive reagents/drugs, and at the same time, obtaining libraries of particles with different properties [391,392]. Moreover, the high degree of control over the process parameters leads to the production of homogenous micro/nano-systems, characterized by high drug loading degree [393]. The most important feature of microfluidics is the possibility to achieve a laminar flow in the channel, defined by the following parameters, such as the Reynold number (a

dimensional number indicating the ratio between inertial to viscous forces in the channel), capillary number (ratio between the viscous forces and the surface tensions between the liquids), and the flow ratio (indicating the ratio between the flow rate of the different phases) [391,394]. Other advantages of microfluidics are the short diffusion distance between the molecules in the fluids, enhancing the mixing efficiency and reducing the mixing time, as well as the possibility to continuously produce the particles [395]. Furthermore, the yield of production can be as high as 700 g of particles per day, with an easy scaling-up mediated by the connection in series or parallel of multiple chips [396]. Microfluidics platforms are designed and produced by a variety of materials (*e.g.*, polydimethylsiloxane, glass capillaries, and polycarbonate) [391].

Glass capillary microfluidics provides the possibility to use organic solvents without compromising the integrity of the chip, and they are quite robust platforms, durable, with a wide range of channel geometries, as shown in **Figure 10** [391,393,396,397].

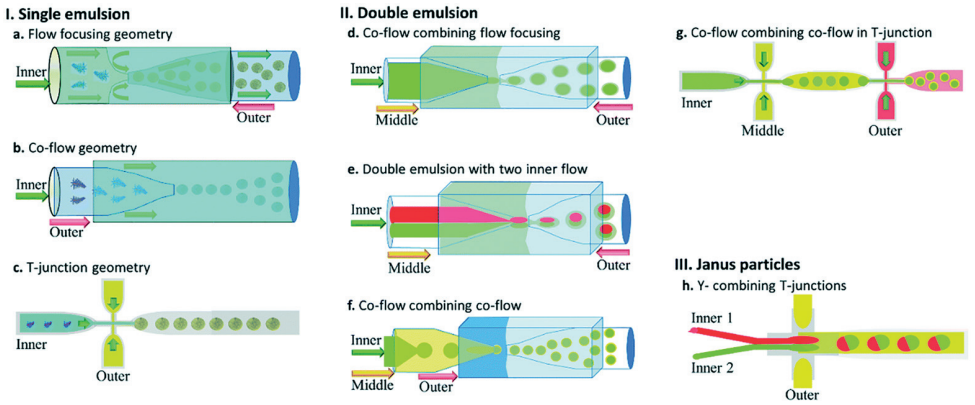

Figure 10. Configurations achievable in microfluidics platforms for the preparation of micro- and nano-drug delivery systems. a, b, d ,e, and f are the geometries available in glass capillary microfluidics. Reprinted with permission from [396]; copyright © 2017, The Royal Society of Chemistry.

MPs are usually obtained through droplet-based microfluidics, employing geometries shown in **Figure 10** (a, d, e, and f). The emulsion droplets generated present homogenous dimension, high encapsulation efficiency, and the possibility to co-encapsulate different drugs [391]. MPs produced by single and double emulsion have been investigated in the delivery of chemotherapeutics for colon cancer and oral delivery of model drugs, and proteins [315,317,329,398-403].

NPs can be successfully produced by nanoprecipitation from two miscible solvents in a 3D-hydrodynamic focused geometry [396]. The fast mixing

time inside the fluidics channel is smaller than the nucleation time for the polymer, thereby both the nucleation and nuclei growth occur in the same conditions, resulting in NPs with homogenous size [393,404]. NPs with different applications, ranging from delivery of chemotherapeutics in cancer to receptor-mediated oral delivery of insulin and analogues have been engineered by microfluidics nanoprecipitation in glass capillaries [316,318,342]. Lately, ultra-high loading degree particles are being investigated to increase the drug delivery efficiency [405].

3 Aims of the study

The main goal of this thesis was to develop nanovaccines made of a biohybrid nanosystem containing inorganic nanoparticles or OVs cloaked into cancer cell membranes for cancer immunotherapy applications.

More specifically, the aims of the present work were:

- To evaluate the influence of PSi nanoparticles' surface chemistry on the membrane extrusion process, on the stability in biologically relevant media, and on the cytocompatibility in different cells.

- To investigate the effect of the cell membrane source and coating, on the uptake of hydrophilic, negatively-charged particles in different cell lines.

- To develop a multistage biohybrid system as a nanovaccine for cancer immunotherapy and evaluating the immunological profile of the system *in vitro*.

- To assess the *in vivo* therapeutic efficacy of the nanoplatform in two murine melanoma models and assay the potential of a combination therapy with immune check-point inhibitors.

- To explore the translatability of the cancer cell membranes coating to OVs both *in vitro* and in murine tumor models, checking the masking effect of the cell membrane towards neutralizing antibodies, as well as the efficiency and immunostimulation of the biohybrid nanovaccine as preventive and therapeutic treatment.

4 Experimental

The methods employed in the experiments of the studies described in this thesis are presented in this section. The details of the methods herein described can be found in the original publications (**I**-**V**). The PSi nanomaterials employed in some of the works here presented (publications **I**, **II**, **III**, and **IV**) were fabricated by the collaborators at the Laboratory of Industrial Physics, Department of Physics and Astronomy, University of Turku, Finland. The *in vivo* work presented in publication **IV** and the work presented in publication **V** have been performed in collaboration with the ImmunoViroTherapy Lab, Drug Research Program, Division of Pharmaceutical Biosciences, University of Helsinki, Finland.

4.1 Materials (I-V)

The detailed description of the materials employed in this thesis can be found from the materials and methods sections of original publications **I**-**V**.

4.2 Methods

4.2.1 Cell Membrane Extraction and Membrane Extrusion Technique

The following protocol applies to all the cell lines employed as a source of cell membrane (**I**-**V**). The concentration of a cell suspension was determined and the cells were then washed 3 times with cold phosphate buffer saline (PBS; 1X). The pellet of the cells was resuspended in lysing buffer (20 mM of TrisHCl pH 7.5, 10 mM of KCl, 2 mM of $MgCl_2$, all from Sigma Aldrich, USA; 1 mini tablet of proteases inhibitors/10 mL, Thermo Fisher, USA; Milli-Q water), and the separation of the cell membranes was performed by ultracentrifugation, as previously described[26]. The lysing buffer was then discarded and replaced with the medium chosen for the extrusion process (see details in the materials and methods section of the original publications **I**-**V**).

The final systems were produced through a membrane extrusion, adopting an extruder (Avanti Polar Lipids, USA) and polycarbonate membranes (pore sizes reported in publications **I**-**V**, Whatman, UK). The samples and cell membrane vesicles were suspended into the buffer of choice and passed through the extruder 21 times, before being collected into a new Eppendorf for the following studies.

4.2.2 Nanoparticles Production

4.2.2.1 PSi Nanoparticles

The PSi forming the core of the systems described in this thesis has been prepared as follows: silicon wafers (p+ -type, ⟨100⟩ and resistivity of 0.01-0.02 Ω cm) were anodized into aqueous hydrofluoric acid (38%):EtOH (1:1) solution by applying electrical current (50 mA/cm^2)[301]. The porous layer was detached by the wafer substrate through a rapid increase in the current to the region used for electropolishing[322]. Generally, free-standing films were first modified, then reduced to nanoparticles by wet milling and the particles were separated into different size fractions by centrifugation[318]. The particles were then washed and stored in 99.5% of EtOH.

In the works presented herein, we employed particles with different surface modifications for further studies. The list of the type of modification, abbreviation, chemicals used in the modification, procedure and resulting size and surface charge of the batches employed is presented in **Table III**, alongside with references describing the preparation methods in detail.[13]

Table III. Surface modification of the PSi NPs employed in publications **I**-**IV**.

Surface Modification	Abbr	Chemical	Procedure	Size [nm]	Surface Charge [mV]	Ref
Thermally Carbonized	TCPSi	Acetylene	Performed on THCPSi films. Additional 10 min of acetylene flow (1 L/min), followed by annealing for 10 min, under N_2 flow, at 820°C. The films were then cooled back to RT under N_2 flow.	159,8	-26,5	406
3-aminopropyltriethoxysilane TCPSi	APTS-TCPSi	3-aminopropyltriethoxysilane-toluene solution (10%)	Performed on TCPSi films. Immersion in HF, followed by immersion in APTS-toluene solution. The medium employed in the wet milling is 5% APTS-toluene solution	187.0	+35.1	299,318
Undecylenic acid-modified thermally hydrocarbonized	UnTHCPSi	Acetylene, followed by undecylenic acid	Exposure of the films to a flow of N_2 (1L/min) for the O_2 and moisture removal. Thermal hydrocarbonization in a flow 1:1 of N_2:acetylene for 15 min at 500°C, followed by cooling to room temperature under N_2 flow. Undecylenic modification: dipping films into acid solution for 16 h at 120°C.	140.5	-21.9	407,408
Thermally Oxidized	TOPSi	-	Thermal oxidation at 300°C for 2 h with ambient air	179.5	-23.7	409

HF, hydrofluoric acid; N_2, nitrogen; O_2, oxygen; RT, room temperature.

4.2.2.2 Synthesis of Acetalated Dextran (AcDEX) (III-IV)

The detailed protocol for the synthesis of AcDEX polymer has been reported in the literature [318]. Briefly, dextran (1 g, MW 9 000-11 000 kDa, Sigma Aldrich, USA) was put into a two-neck round bottom flask, previously dried, and purged with N_2. About 10 mL of dimethyl sulfoxide (DMSO, Sigma Aldrich, USA) were employed to dissolve dextran. Then, 15.6 mg of pyridinium-ptoluenesulfate (Sigma Aldrich, USA) and 3.4 mL of 2-methoxypropene (Sigma Aldrich, USA) were added to the flask. The reaction was performed for 1 h, before being quenched with trimethylamine (1 mL, Sigma Aldrich, USA). The obtained polymer was precipitated in water (200 mL) and washed twice with 0.01% v/v trimethylamine solution (pH 8.0), yielding acetalated dextran.

4.2.2.3 Glass Capillary Microfluidics and Nanoprecipitation (III-IV)

Co-flow microfluidics configuration was employed in the nanoprecipitation fabrication of the NPs presented in the original publications **III** and **IV**. The microchip in publication **III** was assembled, as previously described, using borosilicate glass capillaries mounted on a glass slide[316]. The inner capillary (580 μm and 1000 μm, internal and external diameter, World Precision Instruments, USA) was tapered to ca. 20 μm in a pipette puller (P-97, Sutter Instruments Co, USA) before being carefully sanded to a diameter of approximately 80 μm. This capillary was inserted and coaxially aligned within a bigger capillary (internal diameter 1000 μm). The capillaries and the connections were sealed, where needed, with transparent epoxy resin (5 min Epoxy, Devcon). The microchip was connected with polyethylene tubes attached to syringes controlled by automatic injection pumps (PHD 2000, Harvard Apparatus, USA). The microchip employed in the original publication **IV** was modified from the literature and the two capillaries were assembled within the structure for an easier setup of the system[410].

The NPs were prepared by nanoprecipitation in glass capillary microfluidics device. In detail, a solution of the polymers (10 mg/mL) in 95% of EtOH was prepared and used to resuspend 1 mg of TOPSi NPs. A layer of AcDEX was deposited on the surface of TOPSi particles, encapsulating them. The parameters chosen for the encapsulation were inner solution (particles and polymer), at a flow rate of 2 mL/h and the outer solution (polyvinyl alcohol, 1% w/v, Sigma Aldrich, USA), at a flow rate of 40 mL/h. The preparation procedure of the final system is described in detail in the experimental section of the original publications **III** and **IV**.

4.2.3 ExtraCRAd (V)

The OVs constituting the core of ExtraCRAd were prepared in the facilities of the IVT Lab, according to standard protocols described elsewhere[383,411,412]. Briefly, the viruses employed in publication **V** were: Ad5Δ24, developed by creating a 24 base-pair deletion (Δ24) in the E1A gene to allow for the replication only in cancer cells with mutated Rb/p16 pathway; Ad5Δ24-CpG is an OVs (24 bp deletion) equipped with a CpG-enriched genome in the E3 gene; Adeno5-luc is an adenovirus carrying a luciferase transgene.

The viruses were selected by colony formation and propagated in A549 cells or HEK 293 cells before being purified using cesium chloride gradients. The viral particle concentration was determined by analyzing the optical density at 260 nm, while the standard infectivity assay (ICC) on A549 were performed to determine the infectious titer.

All the viruses produced were aliquoted and kept at -80°C in A195 buffer (10 mM of Trizma Base, 75 mM of NaCl, 5% (w/v) Sucrose, 0.02% w/v of Tween 80, 1 mM of $MgCl_2$, 100 μM of EDTA, 0.5 % of EtOH 99.5%, and 10 mM of L-hystidine) until further use.

4.2.4 Physicochemical Characterization (I-V)

All the biohybrid systems presented in this thesis have been extensively characterized.

4.2.4.1 Dynamic and Electrophoretic Light Scattering (DLS and ELS)

DLS and ELS were employed to determine the hydrodynamic diameter (*Z*-average), the polydispersity index, and the surface charge of the developed nanosystems (**I**-**V**), using a Zetasizer Nano ZS instrument (Malvern Ltd, UK). The measurements were performed either in Milli-Q water, 5.4% of glucose, 0.9% of NaCl physiological solution or PBS (1X). Further details on the dispersing media can be found from the original publications.

4.2.4.2 Stability Studies in Physiologically Relevant Media

The behavior of the nanosystems in biological conditions in the case of i.v. administration was tested by assessing the stability of the systems in fresh frozen plasma (FFP; provided by Finnish Red Cross), for up to 2 h. FFP was filtered with a 0.2 μm filter (0.2 μm sterile Acrodisc® Syringe Filters with Supor® Membrane, Pall Corporation, USA) before use. About 300 μL of each

sample were pipetted in 1.5 mL of physiological relevant media and stirred at 200 rpm and 37 °C. Aliquots were taken at different times during the incubation period and analyzed by DLS and ELS.

4.2.4.3 Transmission Electron Microscopy (TEM, I-IV) and Cryo-TEM (V)

The morphology of the nanosystems (**I**-**IV**) was investigated by TEM. About 5 μL of sample were deposited on carbon-coated copper grids, followed by overnight drying. The particles were imaged with a Jeol JEM 1400 (Jeol Ltd, Japan) microscope. ExtraCRAd samples from publication **V** were imaged by cryo-TEM on a JEOL JEM-3200FSC microscope. Briefly, about 3 μL of fresh samples were applied to carbon-coated copper grids that were immediately dropped into liquid nitrogen to snap freeze the samples.

4.2.4.4 Scanning Electron Microscopy (SEM, I) with Energy Dispersive X Rays and High Resolution Scanning Electron Microscope (HR-SEM, III)

The surface and elemental composition of the biohybrid nanosystems presented in publication **I** were analyzed by EDX (Oxford INCA 350, Oxford Instruments, UK) connected with an SEM (Hitachi S-4800, Hitachi, Japan) at 30.0 KeV. The samples were applied to carbon-coated copper grids.

In publication **III**, the surface of the nanosystems was imaged with HR-SEM. Briefly, 10 μL of the samples (1 mg/mL) were deposited on fragments of wafers of silicon and dried overnight in open air. The samples were then imaged with a Zeiss Ultra-55 scanning electron microscope (Zeiss, Germany).

4.2.4.5 Light Microscopy (II, III)

An inverted confocal microscope (Leica, TCS SP5 II HCS-A, Leica, Germany) was employed to image cells seeded in Lab-Tek™ 8 chambers slides to evaluate the intracellular uptake of fluorescently labelled NPs in publication **II**. A fluorescent microscope (Leica DM6000, Leica, Germany) was adopted to image the nanosystems developed in publication **III** to confirm the successful conjugation of Trp-2 antigen (FITC-conjugated) onto TOPSi@SpAcDEX particles and further support the presence of the cell membrane on the surface of TOPSi@AcDEX@CCM. TOPSi particles were loaded with tetramethylrhodamine (TRITC, Sigma Aldrich, USA), while the cell membrane was stained with Cell Mask® Deep Red (Thermo Fisher, USA), and the nuclei were stained with DAPI.

4.2.5 In Vitro Evaluation of Biohybrid Systems

4.2.5.1 Continuous Cell Lines and Isolation of Peripheral Blood Monocytes

The following cell lines were utilized in the studies herein presented: human lung carcinoma (A549, American Type Culture Collection (ATCC)® CCL-185™), murine skin melanoma cells (B16F10, ATCC® CRL 6475™), murine skin melanoma cells transfected with ovalbumin (B16.OVA, kindly provided by Prof Richard Vile, Mayo Clinic, Rochester, USA), human B cells with dendritic cell morphology (BDCM, ATCC® CRL2740™), human endothelial somatic hybrids (EA.hy926, ATCC® CRL 2922™), primary human derma fibroblasts (kindly provided by Dr. Jackson, Mitochondrial Medicine group, University of Helsinki, Finland), human embryonic kidney cells (HEK 293, ATCC® CRL-1573™), human liver carcinoma (HepG2, ATCC® HB-8065™), murine dendritic cells (JAWS II, ATCC® CRL-11904™), human macrophages (KG-1, ATCC® CCL-246™), human breast adenocarcinoma cells (MCF-7, ATCC® HTB-22™), epithelial metastatic breast cancer cells (MDA-MB-231, ATCC® HTB-26™), human metastatic prostate cancer cells (PC-3, ATCC® CRL-1435™), human ovarian carcinoma cells (SK-OV-3, ATCC® HTB-77™). BDCM and KG-1 cells were kindly provided by the Institute for Molecular Medicine Finland. All the other cells, when not otherwise specified, were bought from ATCC® (USA).

A549 and SK-OV-3 cells were cultured in Dulbecco's Modified Eagle's Medium (DMEM), low glucose, supplemented with 10% heat inactivated fetal bovine serum (FBS), 1% of penicillin streptomycin (PEST), 1% of L-glutamine, 1% of non-essential amino acids. HEK 293, MCF-7 and PC-3 cells were cultured in 10% of FBS in DMEM high glucose. EA-hy926, fibroblasts, and HepG2 were cultured in 10% of FBS in DMEM high glucose supplemented with 1% of sodium pyruvate. B16F10 and BDCM cells were cultured in Roswell Park Memorial Institute (RPMI) 1640 medium supplemented with 10% of FBS, 1% of PEST, 1% of L-glutamine, and 1% of NEAA. B16.OVA were cultured in 10% of FBS in RPMI, with the supplement of 10% of geneticin (G418, Thermo Fisher, USA) to select the OVA positive cells. KG-1 macrophages were cultured in Iscove's Modified Dulbecco's Medium (IMDM), supplemented with 10% of FBS, 1% of PEST, 1% of L-glutamine, and 1% of NEAA. Finally, JAWS II cells were cultured in 20% of FBS in α-Minimum Essential Medium (MEM) supplemented with 5 ng/mL of murine GM-CSF.

PBMCs (**III**) were isolated from human blood of anonymous blood donors, received by the Finnish Red Cross. PBMCs were obtained from the

whole blood after lysing the erythrocytes with ammonium-chloride-potassium lysing buffer for 5 min, followed by centrifugation and washing with cold PBS. The cells were then cultured in 10% of FBS in RPMI for further use.

All the cells were maintained in an incubator (16 BB gas, Heraeus Instruments GmbH, Germany) at 37°C, 5% CO_2 and 95% relative humidity.

4.2.5.2 Cytocompatibility (I-IV)

The biocompatibility of the nanosystems presented in publications **I-IV** was assessed in several cell lines, both human and murine, by quantifying the adenosine triphosphate (ATP) activity to minimize the interference given by PSi to the assay.[301] Adherent cells (A549, EA.hy926, fibroblasts, HEK-293, HepG2, MCF-7, MDA-MB-231, and PC-3) were seeded at a concentration of 10 000 cells per well in 96-well plates and left attaching overnight before removing the medium and applying the relevant samples. After incubation, the samples were removed and the wells were washed with (4-(2-hydroxyethyl)-1-piperazineethanesulfonic acid) Hank's balanced salt solution (HEPES-HBSS, pH 7.4). Finally, a 1:1 HEPES-HBSS: Cell Titer Glo (Promega, USA) solution was added to each well, the plate was shaken for 2 min and incubated for 15 min before reading the luminescence on a Varioskan Lux (Thermo Fisher, USA) instrument. As for non-adherent cells (BDCM, KG-1, JAWS II, and PBMC), cells were seeded at a concentration of 10 000 cells/well in 50 µL, followed by the addition of 50 µL of the appropriate samples, at double concentration. After incubation, 100 µL of Cell Titer Glo® were added to each well, the plate shaken for 2 min, incubated for 15 min and the luminescence read with Varioskan Lux.

4.2.5.3 Immunological Analyses (I, III, and IV)

The immunological profile of the developed nanosystems was evaluated by quantifying the expression of CD80 and CD86 by antigen presenting cells stimulated with the systems. BDCM, JAWS II, KG-1, and PBMC were seeded at a concentration of 280 000 cells per well in 12-well plates. Then, the samples, at double the concentration were added to the corresponding wells in the 12-well plate wells and the cells incubated for 48 and 72 h. The samples were removed by centrifugation and the cells were incubated with monoclonal antibodies against CD80 and 86 (mouse anti-human CD80-phycoerythrin (PE), mouse anti-human CD86 allophycocyanin, hamster anti-mouse CD80-allophycocyanin, all from BD (BD Biosciences, USA); rat anti-mouse CD86 peridinin chlorophyll protein (PerCP)-Cy 5.5, Biolegends, USA) in the dark at

4 °C. The samples were then washed twice with PBS (1X) and analyzed with the LSR II or Accurí (BD biosciences, USA) flow cytometer (FCM). As for JAWS II cells, the adherent population was detached from the wells with cold PBS-EDTA buffer solution.

The secretion of cytokines was evaluated by enzyme-linked immunosorbent assay (ELISA) assays, as specified in publication **III.**

4.2.5.4 Uptake Studies (II, V)

The uptake pathway of biohybrid nanosystems was evaluated by utilizing selective uptake inhibitors. In particular, the assessment conditions are reported in the materials and methods of the original publication **II**. The cells were preincubated either on ice or with the inhibitor of the uptake for 30 min before adding the samples in order to inhibit the specific pathway of cell uptake. The cell uptake kinetic of naked or membrane-coated fluorescently-labelled PSi NPs was evaluated over 1 and 3 h time points by FCM and confocal microscopy.

As for FCM, the cells were seeded in 12-well plates, pretreated with the inhibitors of the uptake, incubated with the particles, and detached by the wells by cold PBS-EDTA buffer solution. The cells were then analyzed by FCM, evaluating the fraction of particles adsorbed and internalized by fluorescence quenching with trypan blue (0.005%).

Confocal microscopy was utilized for the qualitative imaging of the particles uptake. The cells were seeded in 8-well chambers (LabTek™) and preconditioned with the inhibitors of the cell uptake. Then, the samples were added to the wells and the cells were incubated for 1 or 3 h before staining and fixation.

The cell uptake kinetics of ExtraCRAd was compared to a naked virus over 1, 2, and 3 h by analyzing the luminescence of A549 cells infected with virus carrying luciferase gene. After the incubation period, the wells were washed and the cells were incubated in 5% DMEM for 24 h to allow the expression of the luciferase. Then, the cells were lysed and the luminescence was read in Varioskan.

4.2.5.5 Infectivity Assay (V)

The infectivity was assessed by MTS (3-(4,5-dimethylthiazol-2-yl)-5-(3-carboxymethoxyphenyl)-2-(4-sulfophenyl)-2H-tetrazolium, inner salt) using the CellTiter® 96 Aqueus One Solution Cell Proliferation Assay (Promega,

USA) on A549 and SK-OV-3 cells, at different viral concentrations. The infectivity was evaluated after 3 days of incubation.

4.2.5.6 Neutralizing Antibody Assay (V)

This assay was employed to investigate the ability of ExtraCRAd to shield the virus from neutralizing antibodies. Firstly, ExtraCRAd was assessed against antibodies derived from the serum of immunized mice, then to rule out the interference of other proteins, against monoclonal anti-adeno5 antibody. The serum of the immunized mice was incubated at 56 °C for 90 min to eliminate the complement, and stored at –20°C until further use. Briefly, A549 cells were seeded at a density of 10 000 cells per well in 50 µL of DMEM without FBS and left attaching overnight. Then, the serum was diluted from 1:1 to 1:16384 on $1:4^n$ scale with DMEM without FBS. The luc virus was diluted in 0% DMEM up to a concentration of 3.03×10^9 viral particles per mL and added to the serum dilutions or to the monoclonal antibody (4×10^6 viral particles,vp, for each sample). The samples were then incubated at room temperature for 30 min on a shaker. Finally, 50 µL of each sample were pipetted over the cells into each well. The cells were incubated for 1 h at 37 °C before adding 150 µL of 10% of DMEM to each well and continuing the incubation overnight. Next, lysis of the cells and the addition of the substrate for luciferase (Promega,USA) were performed, and analyses of the luminescence was conducted with a Varioskan Lux instrument.

4.2.6 In Vivo Assessment of Biohybrid Cancer Vaccines (IV-V)

The nanosystems developed in this thesis were assessed *in vivo*, in murine lung adenocarcinoma and melanoma models, as preventive or therapeutic cancer vaccines.

4.2.6.1 B16.F10, B16.OVA, CMT64.OVA, and LL/2 models

The murine strain chosen for the experiments was C57BL/6J, obtained from Scanbur (Denmark) at 4–6 weeks of age. The development of subcutaneous tumor models was achieved by injecting either 1×10^5 of B16F10, 2.5×10^5 of B16.OVA, 7×10^6 CMT64.OVA, or 1.5×10^5 LL/2 tumor cells (when 80% confluent in T175 flasks) on the right flank of each mouse. Details about the treatment schedule are given in the figure legends in the original publications **IV** and **V**. During the experiments, the tumor volume was recorded every two days by using a digital caliper. Maximum (L) and minimum (l) tumor diameters were recorded and tumor volumes were calculated according to the formula: $(L\times l\,2)/2$.

4.2.6.2 Ex-Vivo Immunological Analysis

Tumors and lymphoid organs were collected from the animals after sacrifice. The tissues were smashed into single cell suspensions through strains (70 μm mesh). The cells were preserved at –80°C until use. The samples were pretreated with Fc-blocker for 30 min, before staining for the immunological profile (T cells, CD8, CD4 and CD3) and dendritic cells (CD11b, CD11c, CD86, and CD80). All the anti-mouse antibodies employed were from BD Biosciences (BD). Gallios (Beckman Coulter) or Accuri' (BD Biosciences, USA) FCM was used to acquire data and FlowJo (Threestar) software was used for data analysis.

4.2.7 Ethical Permit (IV-V)

All the experimental protocols presented in publications **IV** and **V** were approved by the Laboratory Animal Center of the University of Helsinki and by the National Animal Experiment Board of Finland, according to the Act (497/2013) and the Decree (564/2013) on Animal experimentation approved by the Finnish Ministry of Agriculture and Forestry and the EU Directive (2010/63/EU), following the EU's Guidelines for Accommodation and Care of Animals.

4.2.8 Statistic Analysis

The results are presented as mean ± standard deviation (SD) or standard error of the mean (SEM). Graphpad Prism versions 5.0 or 7.0 (Graphpad Software, San Diego, California, USA) were used to analyze the data. The statistical analyses employed to analyse the data can be found in the materials and methods sections of the works.

5 Results and Discussion

Biohybrid NPs represent a recent development in the field of nanotechnology and their potential is currently assessed in different applications. In this thesis, cell membrane-wrapped nanosystems were evaluated in terms of formulability, enhancement of colloidal stability in physiological fluids, effect on the biocompatibility and on the immunological profile of multistage nanovaccines. Finally, the innovative antigenic sources represented by the cell membrane with either a synthetic or a viral adjuvant cores were evaluated as preventive or therapeutic cancer vaccines in different tumor models.

5.1 Effect of PSi Surface Chemistry in the Biohybrid System (I)

The first step in the creation of a successful NP is the material development [70]. To ensure the translatability of a nanosystem to the clinics, it is of paramount importance to develop NPs presenting homogenous size distribution with a reproducible manufacturing process [393]. In the case of biohybrid nanovaccines, given the personalized nature of the treatment, the production process needs to be evaluated and optimized for different types of core particles and membrane types. Moreover, one characteristic sought for in the development of NPs is their stability in biological fluids – this is of extreme importance in i.v. injections. Thereby, the focus of this study was to evaluate the formulation parameters for the preparation of reproducible biohybrid nanoplatforms starting from PSi presenting different surface characteristics and to evaluate the stability of those platforms in biological fluids.

5.1.1 Formulation of the Biohybrid NPs

In this preliminary study, three different PSi NPs, namely APTS-TCPSi, UnTHCPSi and TCPSi, were coated with a model cell membrane derived from a human macrophage cell line, KG-1. The PSi particles presented were different in the surface charge (APTS-TCPSi being positively charged, while the other two particles are negatively charged [413]) and in the hydrophilicity/hydrophobicity of the surface (UnTHCPSi are hydrophobic particles, while the other two particles are hydrophilic [11,414]). The formulative parameters assessed were the buffer used for the extrusion (Milli-Q water or Sucrose, 0.3 M) and the influence of the tip sonication associated to the membrane extrusion process. The results of the formulative screenings are presented in **Table IV**.

Table IV. Influence of the extrusion buffer and use of tip sonication on the formulation of PSi characterized by different surface charge and surface hydrophobicity. The nanosystems obtained with different parameters are ranked by desired values of size and zeta potential, where ++ represents the best formulation and - - the worst. Reprinted with permission from publication **I**; copyright © 2018, WILEY-VCH Verlag GmbH & Co. KGaA, Weinheim.

PSi NPs	Buffers	Tip Sonication	Size [nm]	PDI	ζ-potential [mV]	Rank
APTS-TCPSi	Sucrose, 0.3 M	Before	Aggregated		+8.8±1.3	– –
		Before and After	304±100	0.30±0.040	–6.3±1.1	++
	Milli-Q water	Before	334±20	0.30±0.049	+31.2±0.5	+
		Before and After	Aggregated		–5.7±7.1	–
UnTHCPSi	Sucrose, 0.3 M	Before	575±200	0.50±0.07	–21.2±0.3	–
		Before and After	303±200	0.150±0.007	–23.7±0.2	++
	Milli-Q water	Before	649±300	0.24±0.20	–15.1±7.1	+
		Before and after	Aggregated		–8.7±0.9	– –
TCPSi	Milli-Q water	No Sonication	410±180	0.5±0.1	–20.6±6.5	–
		After	Aggregated		–19.8±4.9	– –
		Before	246±100	0.180±0.030	–22.1±5.2	++
	Sucrose, 0.3 M	Before	289±100	0.30±0.07	–23.0±5.9	+

The extrusion of positively charged particles, as previously reported for polymeric NPs [415], resulted in aggregates in both the extrusion buffers due to the electrostatic interactions between the positive charges on the surface of the particle and the negatively charged cell membranes. The use of a double tip sonication (before and after extrusion) partially reduced the size of the aggregates, which presented still inhomogeneous size (as highlighted by the high polydispersity index, PDI). As for the negatively charged PSi NPs, the

effect of the different hydrophobicity of the surface reflected into the need for two different extrusion buffers (Milli-Q water for TCPSi and 0.3 M of sucrose for UnTHCPSi) and for extensive tip sonication in the case of the hydrophobic particles to achieve a stable, homogenous formulation. The successful encapsulation of TCPSi and UnTHCPSi was confirmed also by TEM, while it was possible to observe the aggregates formed by APTS-TCPSi partially coated with the cell membrane (**Figure 11**).

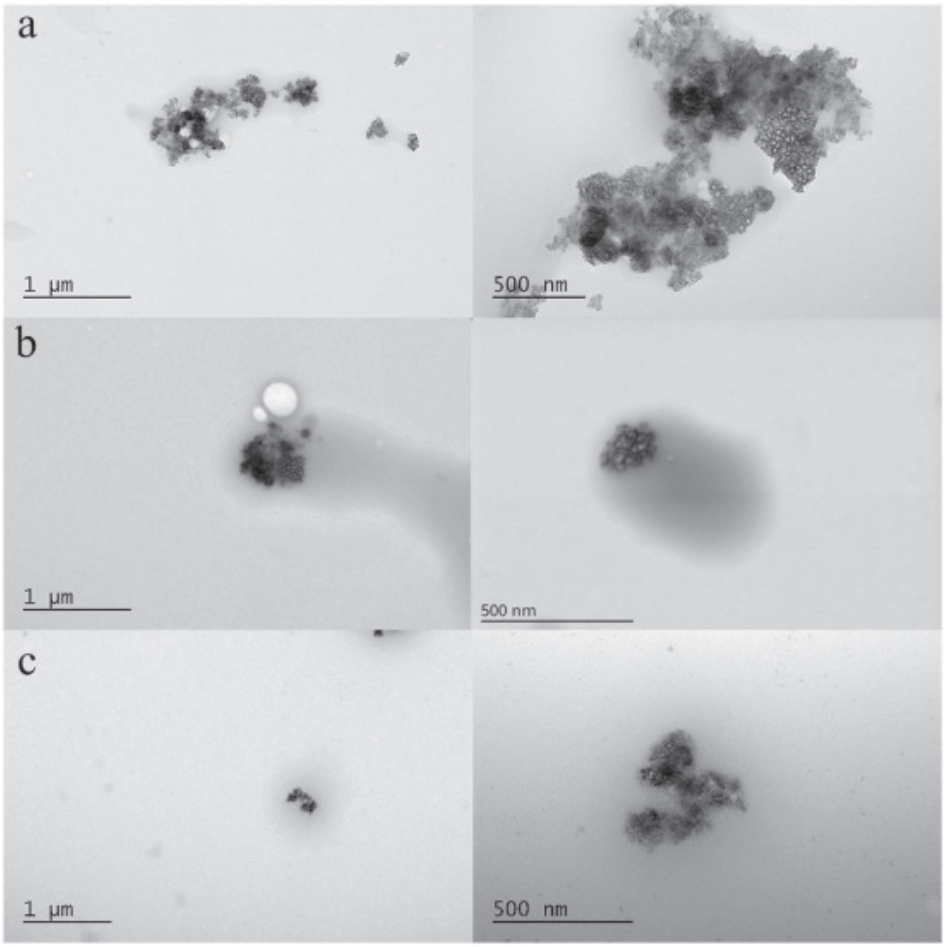

Figure 11. TEM images of a) APTS-TCPSi, b) UnTHCPSi, and c) TCPSi NPs extruded with cancer cell membrane derived from KG-1 macrophages. Reprinted with permission from publication **I**; copyright © 2018, WILEY-VCH Verlag GmbH & Co. KGaA, Weinheim.

Overall, biohybrid platforms constituted of negatively charged PSi NPs presenting different surface properties were developed by adjusting the

formulative parameters (extrusion buffer and tip sonication). However, a limit of this technique resides in the problematic formulation of positively charged NPs.

5.1.2 Stability in Biological Fluids

The engineering of biohybrid NPs coated with cell membrane moieties brings along an innovative concept in the quest for stabilization of NPs in biological fluids. Traditionally, NPs have been modified with PEG to improve their circulation time, by decreasing the aggregation, opsonization, and interaction with immune cells [416]. However, anti-PEG antibodies have been detected both in animal models and in humans with adverse effects on the efficacy of repeated administrations of PEGylated NPs [417]. The coating with cell membranes provides stabilization and masking from the immune cells (mainly by the presence of CD47, "do not eat me", signal on the membrane) [21]. In this study, the stability of hydrophobic UnTHCPSi and hydrophilic TCPSi NPs, as such or after coating with cell membrane, was evaluated to last in human fresh frozen plasma up to 2 h (**Figure 12**).

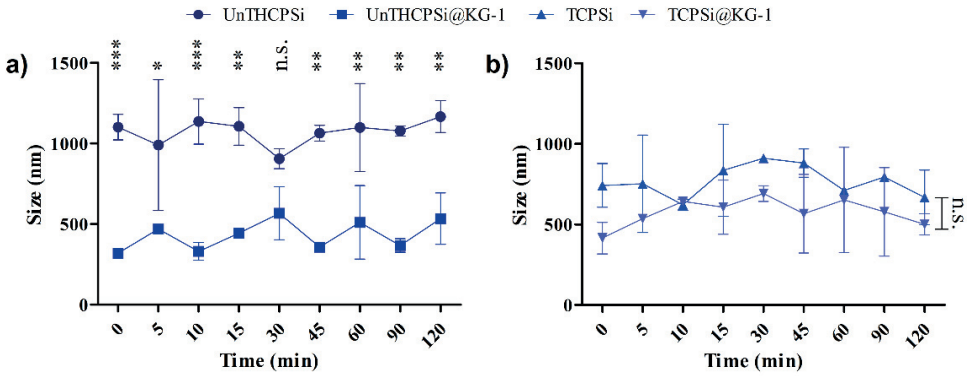

Figure 12. Stability over time of a) UnTHCPSi and UnTHCPSi@KG-1 or b) TCPSi and TCPSi@KG-1 measured by size variation in DLS. The results are presented as mean±s.d. (n=3) and were analyzed by two-way ANOVA, followed by Bonferroni's post-test. The levels of statistical significance were set at $*p<0.05$, $**p<0.01$, and $***p<0.001$. Reprinted with permission from publication I; copyright © 2018, WILEY-VCH Verlag GmbH & Co. KGaA, Weinheim.

The coating with the cell membrane partially improved the stability of the hydrophobic NPs (**Figure 12a**), maintaining the size of the NPs around 500 nm, while the uncoated particles aggregated to 1 μm. In the case of the hydrophilic TCPSi NPs (**Figure 12b**), they displayed a less pronounced

stabilizing effect of the coating with cell membrane, possibly due to their slightly higher hydrophilicity.

In conclusion, the functionalization with cell membrane moieties improved the stability of hydrophobic particles in physiological fluids (human plasma).

5.2 Cytocompatibility of Biohybrid Nanoplatforms (I)

Modifications of PSi NPs' surface influence their interactions with the cells and the mechanisms of their cytotoxicity [413]. Thereby, in this set of experiments, the effect of the surface modification with cell membrane cytocompatibility was evaluated in a panel of primary and immortalized cell lines representative of different human organs, by measuring the intracellular ATP content of the cells after exposure with the NPs (**Figure 13**).

The cytotoxicity of the NPs was cell-type and particle-surface dependent, as previously demonstrated [301,407]. In particular, a dose-dependent toxicity for all the NPs was present in HEK-293 and HepG2 cells, while EA.hy926 cells were sensitive to the hydrophilic TCPSi particles, both coated and uncoated. As for the primary human dermal fibroblasts, all the nanoplatforms were cytocompatible in the lower range of concentrations, with both the coated systems presenting lower compatibility at the highest concentration assessed. In KG-1 macrophages, hydrophilic TCPSi particles, both coated and uncoated, did not exert a toxic effect, while UnTHCPSi and UnTHCPSi@KG-1 were toxic at the highest concentration assessed (500 μg/mL).

An excessive proliferation was noticed, mainly in EA.hy926 cells and partially in KG-1 and HepG2 cells. This might be the result of a locally different concentration of cells or particles amongst the wells, as indicated also by the standard deviation amongst the different replicates. However, an overproliferation of cells when incubated with cell membrane-coated particles has been recorded also in immune cells (Publication **III**, Figure **3**).

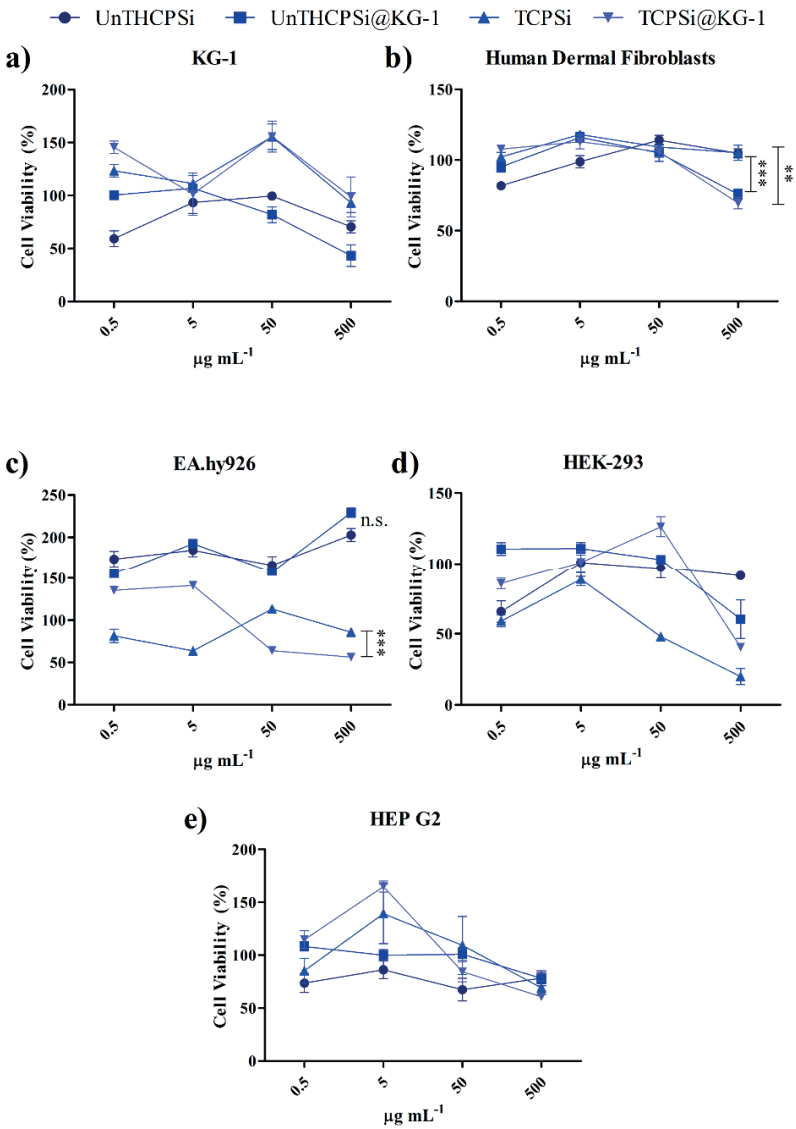

Figure 13. Percentage of viable a) KG-1, b) human dermal fibroblasts, c) endothelial (EA.hy926), d) renal (HEK-293), and e) hepatic (HepG2) cells after 24 h incubation with the particles. UnTHCPSi, UnTHCPSi@KG-1, TCPSi, and TCPSi@KG-1 were assessed at different concentrations (0.5-500 µg/mL). Complete medium and Triton X-100 1% represented the negative and positive controls, respectively. The data are presented as mean±s.d. ($n \geq 3$) and were analyzed by two-way ANOVA, followed by Bonferroni's post-test, to establish comparisons and correlation between naked and membrane-coated particles presenting the same surface chemistry (TCPSi *vs* TCPSi@KG-1, UnTHCPSi *vs*

UnTHCPSi@KG-1). The levels of significance were set at probabilities $^{**}p<0.01$ and $^{***}p<0.001$.

5.3 Influence of the Cell Membrane on the Uptake of PSi NPs (II)

In this set of experiments the effect of the cell membrane coating was evaluated on the cellular uptake in the presence of uptake inhibitors in different cells lines to elucidate the mechanisms of action and any cell-dependent mechanisms [418]. In particular, fluorescently-labelled TOPSi NPs were coated with cell membranes derived from A549, MDA-MB-231, MCF-7, and PC3MM2 cell lines. The uptake was evaluated by assessing autologous samples over each cell line quantitatively by FCM and qualitatively by confocal microscopy.

The variations in the association and uptake of coated and naked NPs in the presence of different uptake inhibitors are presented in **Figure 14**.

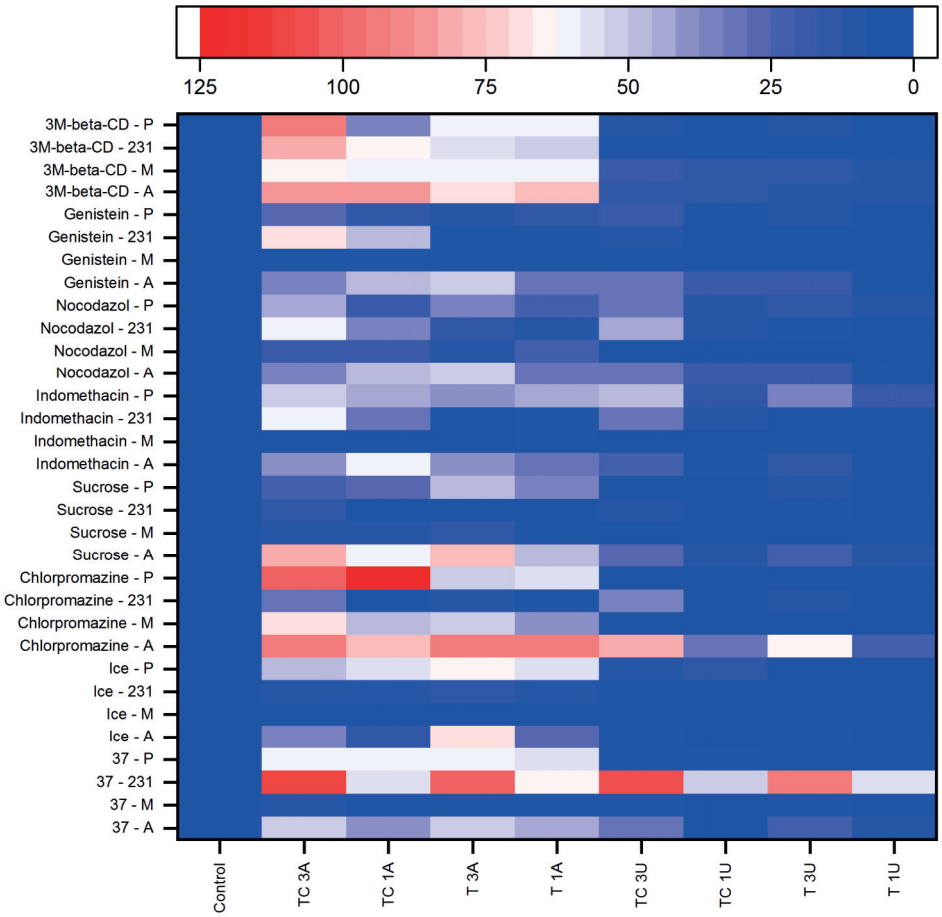

Figure 14. Mechanism of cellular uptake of biohybrid NPs: Cells (A549, A; MCF-7, M; MDA-MB-231, 231; PC3MM2, P) were incubated with different selective inhibitors of specific uptake mechanisms (*i.e.*, ice, chlorpromazine, sucrose, indomethacin, nocodazol, genistein, and 3-methyl-β-cyclodextrin) and with fluorescently modified coated and uncoated particles for 1 and 3 h. The samples were run into FCM to determine the fraction of particles associated before quenching the fluorescence with trypan blue and a second running in FCM. The results are presented as the normalized percentage of positive events recorded in each sample divided by the percentage of a control incubated only with the inhibitors of the uptake to allow for a comparison between different cells and different inhibitors. The data are reported as the mean of 3 samples. TC, TOPSi@cell membrane; T, TOPSi; A, Associated; U, Uptaken.

The effect of the coating with the cell membrane on the uptake of hydrophilic, negatively charged NPs was mostly connected with an increased association with the cell membranes (TC 3A and 1A). The augmented interaction increased the fraction of particles uptaken by the cells. As for the mechanisms, the results suggest that the uptake of both coated and uncoated NPs was mediated by clathrin-dependent (chlorpromazine and sucrose) and caveolin-dependent (genistein) mechanisms, and by interactions with integer and functional cell membranes (3-methyl-β-cyclodextrin). Furthermore, the biohybrid NPs seemed to be less dependent on micropinocytosis (nocodazol) compared to the TOPSi NPs alone.

In conclusion, this set of experiments suggested cell-specific differences in the uptake of biohybrid NPs, according mainly to clathrin and caveolin-dependent mechanisms [419].

5.4 Development and *In Vitro* Assessment of Biohybrid Cancer Nanovaccine (III)

Cancer cell membrane-coated NPs have been proposed as innovative sources of antigens in cancer vaccines, allowing the activation of the immune system and the priming of a cancer-specific immune response [26]. In this study, the intrinsic immunostimulative properties of TOPSi NPs and of a pH-responsive polymer (AcDEX) were combined with cancer cell membrane as the antigenic source [11,420]. The multistage nanovaccine platform was engineered by glass capillary microfluidics, followed by membrane extrusion to coat the cell membrane layer [318,404]. The details concerning the development of the formulation and its cytocompatibility can be found in publication **III**.

The immunological profile of the formulation was evaluated in immortalized human macrophages and B cells with dendritic cell morphology and in PBMCs. The activation profile of the cells was investigated by FCM, analyzing the co-stimulatory markers CD80 and 86 (**Figure 15a-f**). The nanovaccine core enhanced the presentation of both the activation markers in all the cell types. The coating with the cell membrane increased the presence of CD86 in PBMCs, while it decreased the same marker in KG-1. As for CD80, no statistical difference was found between the naked and membrane-coated NPs.

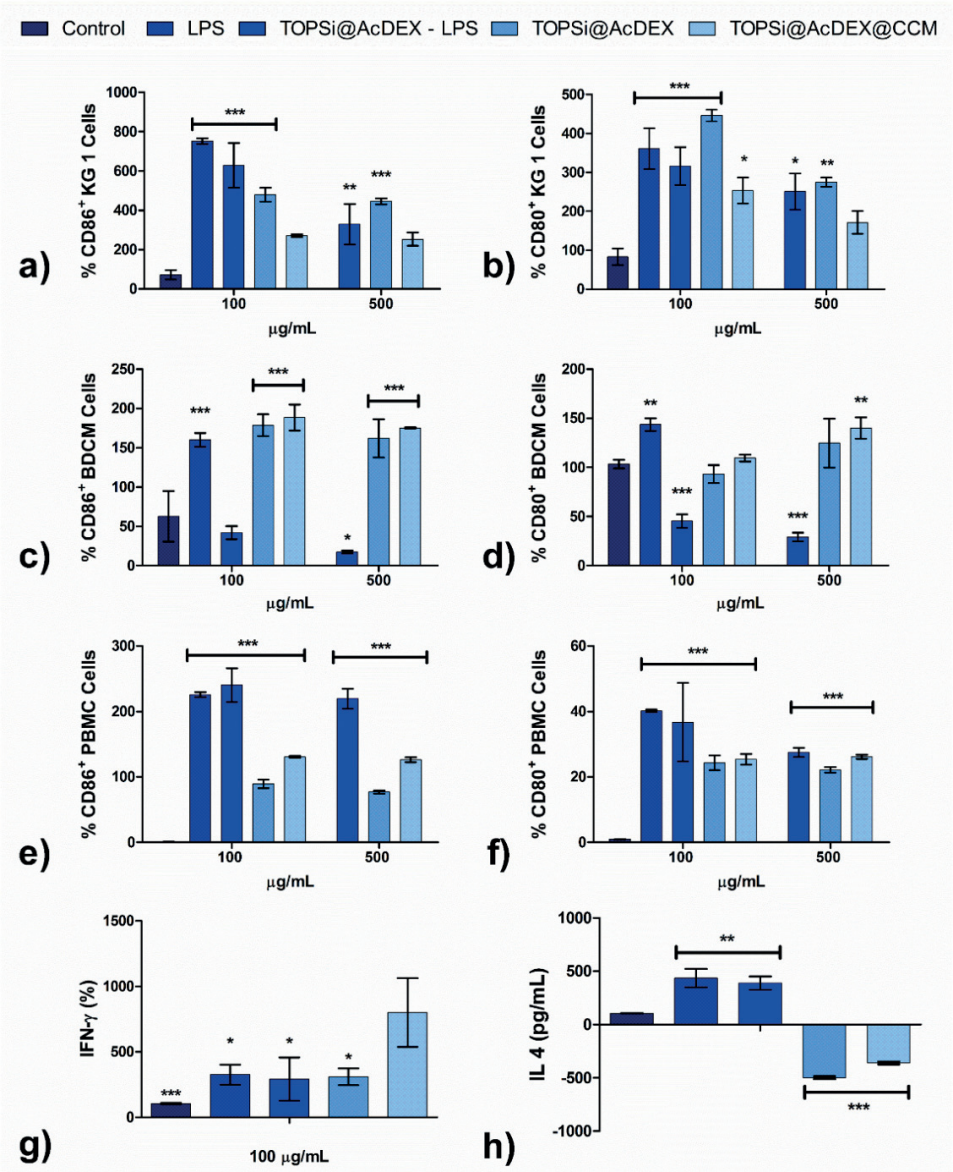

Figure 15. Evaluation of the immunological profile of biohybrid NPs: Percentage of $CD86^+$ a) KG-1, c) BDCM, e) PBMC and percentage of $CD80^+$ b) KG-1, d) BDCM, e) PBMC cells; g) percentage of IFN-γ secreted by PBMC incubated with the particles at 100 µg/mL; h) IL-4 secreted by PBMC incubated with the particles at 100 µg/mL. The results are presented as mean±s.d. ($n \geq 3$). The data were analyzed by one-way ANOVA, followed by Bonferroni's post-test. a)-f) and h) all the samples were compared to the control (cells incubated in medium), g) all the samples were compared to

TOPSi@AcDEX@CCM. The levels of significance were set at $*p<0.05$, $**p<0.01$, and $***p<0.001$. Adapted and reproduced with permission from publication **III**; copyright © 2016 WILEY-VCH Verlag GmbH & Co. KGaA, Weinheim

Given the importance of pro-inflammatory cytokines in the successful priming of naïve T cells to CD8+ cells [53], the cytokine profile produced by the stimulation of PBMCs with the nanovaccine was assessed by ELISA assay. As shown in **Figure 15g** and **15h** and in publication **III**, the biohybrid NPs promoted the secretion of IFN-γ, while no secretion of IL-2 or IL-4 were detected. This type of cytokine profile correlates with a Th-1, cell-mediated, immune response, with the priming of CD8+ T cells and later of antigen-specific cytotoxic T cells [11,422]. Moreover, as reported in publication **III**, PBMCs stimulated with the nanovaccine showed enhanced efficacy in an *in vitro* killing assay against cancer cells of the same cell line as the one used for the membranes.

In conclusion, the *in vitro* assessment of the immunological profile of the nanovaccine highlighted the priming of an immunostimulatory, cell-mediated, immune response suited for a therapeutic cancer vaccine.

5.5 *In Vivo* Therapeutic Efficacy of Biohybrid Nanovaccine in Melanoma (IV)

In this work, the nanovaccine platform developed in publication **III** was assessed in two melanoma models with different immunogenic profiles (one highly immunogenic, B16.OVA, the other B16F10, low) in two therapeutic setups, as a monotherapy and combination therapy with ICI. The therapeutic efficacy of the monotherapy in B16.OVA model can be found in publication **IV**.

5.5.1 Efficacy as Monotherapy in Low Immunogenic Melanoma

In this set of experiments, the therapeutic efficacy of the biohybrid NPs was evaluated on the control over the tumor growth and on the changes in the immunological profile of the tumor microenvironment after two injections. As shown in **Figure 16a**, the nanovaccine controls tumor growth in 44% of the animals, in combination (**Figure 16b** and **16c**) with an increase in the percentage of mature, activated DCs in the tumor, and (**Figure 16d** and **16e**) with an augmented percentage of antigen-experienced $CD8^+$ cells in comparison with the single components of the vaccine. The high aggressivity of the tumor results in an immunosuppressive environment [422]: monotherapy

with a nanovaccine formulation can only partially control the tumor growth [163,189].

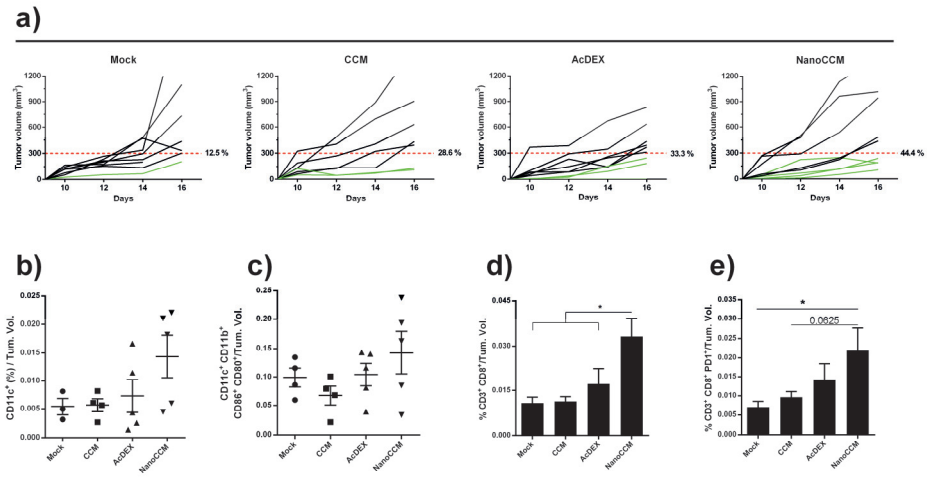

Figure 16. Biohybrid multistage NPs efficacy in B16.F10 models and immunological profile in the tumor microenvironment: a) Single tumor growth curves for each group. A B16.F10 melanoma model was established in female C57BL6/J mice. The mice were treated twice, at day 6 and 13 post tumor establishment. The groups included mock (5.4% isotonic glucose solution), AcDEX (the adjuvant core NPs), CCM (extruded cell membranes), and NanoCCM (cell membrane-coated TOPSi@AcDEX NPs). The value set for the discrimination of responders to the treatment was an absolute tumor volume lower than 300 mm^3. b) Percentage of $CD11c^+$ DCs in the TME. c) Activation profile of DCs in the TME assessed by staining for CD80 and 86 co-stimulatory signals. d) Percentage of $CD8^+$ T cells in the TME. e) Percentage of antigen-experienced tumor infiltrating lymphocytes. The data are presented as mean±SEM. The data were analyzed with unpaired Student's *t*-test or one-way ANOVA. The levels of significance were set at $*p<0.05$ and $**p<0.01$. Reproduced with permission from publication **IV**; copyright © 2019 American Chemical Society.

5.5.2 Correlation Between Immunological Profile of the TME and Efficacy of the Biohybrid NPs

The application of immunotherapy to the treatment of cancers misses a link correlating how changes in the immunological profile of the TME reflect the efficacy of a therapy [423]. In this analysis, the FCM data of the TME were

correlated with the efficacy of the treatment (divided into responders and non-responders), as shown in **Figure 17**.

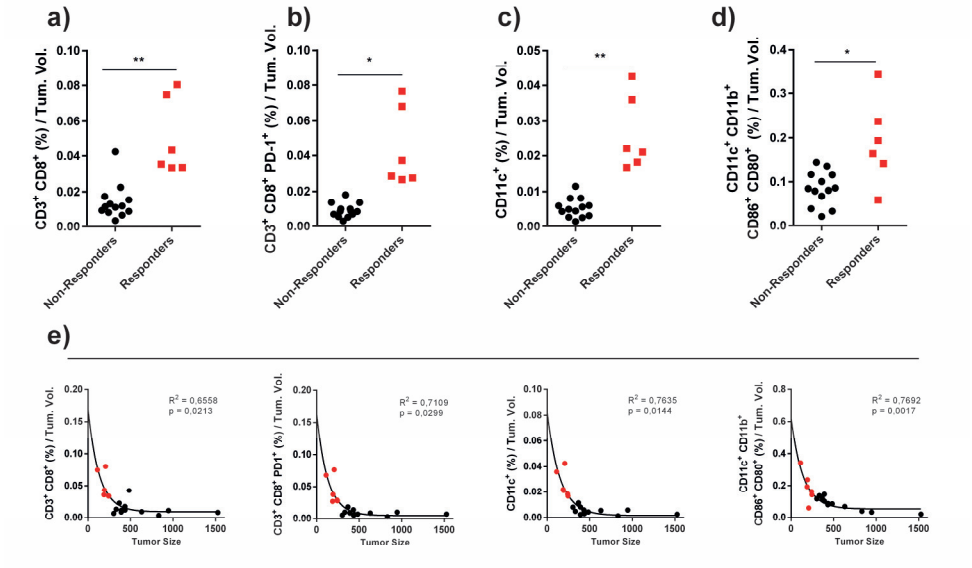

Figure 17. The immunological data shown in **Figure 16** were correlated with the efficacy of the treatment. Mice from all the treatment groups were divided into responders (red) and non-responders (black points) and the immunological profile of the TME was analyzed for changes in a) cytotoxic T cells, b) antigen-experienced cytotoxic T cells, c) activated and mature DCs, and d) DCs. The data were analyzed by unpaired Student's *t*-test and the levels of significance were set at $*p<0.05$ and $**p<0.01$. e) The correlation between immunological changes in the TME and efficacy was tested with Pearson's correlation test (*p*-value is reported in each graph). One phase exponential non-linear models were used for the data fitting and to retrieve the R^2 of each data set. Reproduced with permission from publication **IV**; copyright © 2019 American Chemical Society.

A correlation was established between the small size of the tumors and the increased presence of total and antigen-experienced T cells in the TME (**Figure 17a** and **17b**) and of total and activated DCs (**Figure 17c** and **17d**). Moreover, a fitting was obtained for an exponential model, suggesting the interplay of multiple co-factors in the efficacy of cancer immunotherapy.

5.5.3 Therapeutic Efficacy of a Combination Therapy with ICI

Therapy with ICI has revolutionized the treatment of cancer, achieving long term survival in subsets of patients [60]. However, primary and acquired

immune resistance hinders the global efficacy of these therapeutics [3]. Combination therapies including a priming phase mediated by cancer vaccines, followed by a boost with ICI are currently evaluated in the clinic [4,424].

In these experiments the efficacy of a combination therapy composed of a biohybrid nanovaccine and ICI (anti-cytotoxic T lymphocyte antigen, CTLA-4) was evaluated in a highly immunogenic melanoma model, as shown in **Figure 18**.

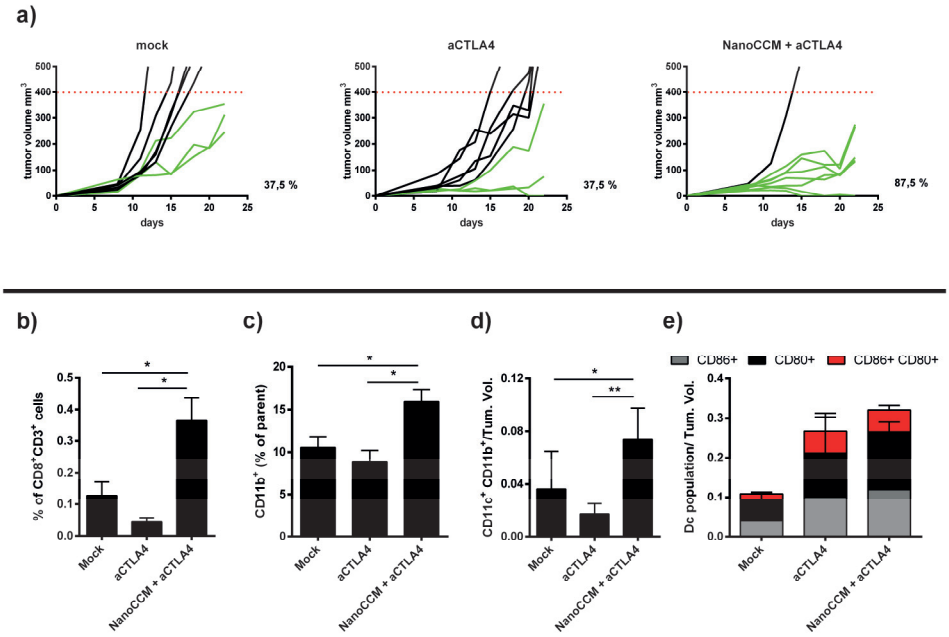

Figure 18. a) Single tumor growth curves for each group. A B16.OVA melanoma model was established in female C57BL6/J mice. The mice were treated three times, at day 6, 13, and 15 post tumor establishment. The groups included mock (5.4% of isotonic glucose solution), aCTLA-4 (intraperitoneal injection of 100 µg of anti-CTLA-4 antibody), and NanoCCM+aCTLA4 (cell membrane-coated TOPSi@AcDEX NPs subcutaneously + aCTLA-4 antibody intraperitoneally). The value set for the discrimination of responders to the treatment was an absolute tumor volume lower than 400 mm^3. b) Percentage of $CD8^+$ tumor infiltrating lymphocytes (TILs) in the TME. c) Percentage of myeloid ($CD11b^+$) cells in the TME. d) Percentage of DCs ($CD11b^+$ and $CD11c^+$) in the TME. e) Percentage of activated and mature DCs, presenting $CD86^+$ (grey), $CD80^+$ (black), or $CD86^+CD80^+$ (red) double positive. The data are presented as mean±SEM. The data were analyzed with unpaired Student's *t*-test. The levels of significance were set at $*p<0.05$ and $**p<0.01$. Reproduced with

permission from publication **IV**; copyright © 2019 American Chemical Society.

The combination therapy of biohybrid nanovaccine and ICI improved the efficacy of the ICI monotherapy, as demonstrated also for oncolytic viruses [64]. As presented in **Figure 18a**, the combination therapy controlled the tumor growth in 87.5% of the animals, including two complete remissions, compared to the 37.5% by the ICI monotherapy. The choice to increase the cut-off value between responders and not responders is motivated by the differences in immunogenicity and tumor growth rate between the two tumor models. Furthermore, the combination treatment modified the immunological profile of the TME, with a significant increase in the percentage of $CD8^+$ TILs and of DCs (**Figure 18b–d**). The monotherapy with ICI promoted the activation of DCs comparably to the combo treatment (**Figure 18e**); however, these activated cells were not able to prime $CD8^+$ cells.

In conclusion, the biohybrid multistage nanovaccine controlled the growth of poorly immunogenic melanoma, modifying the immunological profile of the TME, and increasing the infiltration of both DCs and TILs. Moreover, combination with ICI significantly improved the efficacy of the ICI monotherapy.

5.6 ExtraCRAd–Engineering a Biohybrid Oncolytic Adenovirus (V)

A further step in the development and translatability of biohybrid cancer nanovaccines concerns the modification of the core for a more adjuvant, natural NP, oncolytic adenovirus. ExtraCRAd was engineered by a direct application of the membrane extrusion technique, as shown in **Figure 1** in publication **V**. The viral NPs were then evaluated *in vitro* and *in vivo* for differences in the oncolytic effect, shielding from neutralizing antibodies, and for efficacy in two murine melanoma models.

5.6.1 Engineering of Viral NPs

The new system was developed after screening of the optimal extrusion buffer (**Figure 2d**, publication **V**), identifying both Milli-Q water and PBS (1X) as suitable buffers. The size of the viral NPs increased after extrusion by ca. 10 nm, suggesting the successful coating with the cell membrane. To confirm the coating, naked adenovirus, cell membrane vesicles and ExtraCRAd were imaged in Cryo-TEM (**Figure 2a**, publication **V**).

5.6.2 ExtraCRAd Infectivity and Mode of Action

The encapsulation of an adenovirus within the cell membrane changes the interactions between the cancer cells and the virus. As presented in **Figure 3a** and **3b** in publication **V**, ExtraCRAd displayed enhanced infectivity towards both high and low CAR-expressing cell lines: the incubation with ExtraCRAd resulted in enhanced oncolytic effect in A549 cells (90% reduction in cell viability at 10 and 100 multiplicity of infection —MOI— compared to 10% and 60% reduction achieved when the cells were incubated with 10 and 100 MOI of naked virus, respectively). In SKOV-3 cells, incubation with the viral NPs resulted in a 25% reduction in the cell viability, when compared to the naked virus. Since oncolytic adenoviruses rely on the CAR receptor to infect the cells, the difference between ExtraCRAd and naked virus in SKOV-3 cells suggest the presence of alternative uptake mechanisms for ExtraCRAd [381]. This was confirmed by the *in vivo* efficacy in human lung xenografts in nude mice (**Figure 3c** publication **V**) and by the differences in the uptake kinetics (**Figure 3d** publication **V**), which highlighted a faster intracellular uptake for ExtraCRAd when compared to the naked virus. The following experiments with inhibitors of the uptake (ice, sucrose, and chlorpromazine) suggested the presence of a clathrin-mediated, chlorpromazine inhibited, mechanism of uptake of ExtraCRAd (**Figure S6a-c** in publication **V**). Furthermore, the encapsulation of the virus within the cell membrane shields the viral capsid from the neutralizing antibodies, enhancing the fraction of virus available for infection and priming of the immune response (**Figure 3e** and **3f**, publication **V**).

5.6.3 ExtraCRAd Therapeutic Cancer Vaccine in Lung Adenocarcinoma and Melanoma

In these sets of experiments, the efficacy of ExtraCRAd as a therapeutic cancer vaccine was evaluated in the treatment of lung adenocarcinoma and melanoma. In the highly immunogenic B16.OVA model, four intratumoral injections of ExtraCRAd controlled the tumor growth in all the animals (**Figure 4a**, publication **V**). However, in the less immunogenic and more aggressive model B16.F10, the therapeutic vaccination with ExtraCRAd controlled the growth only in 62.5% of the animals treated (**Figure 4b**, publication **V**). As for the efficacy in a model of solid tumor, lung adenocarcinoma LL/2, the therapeutic vaccination of established tumors with ExtraCRAd wrapped in homologous, tumor-matched, membrane controlled the tumor growth in all the animals treated (**Figures 4c** and **S7** publication

V). These results are correlated with changes in the immunological profile of the TME and the spleen. The vaccination with the viral NPs significantly enhanced the percentage of antigen-specific APCs and of antigen-specific, experienced T cells in the tumor (**Figures 5** and **S8**, publication **V**). Moreover, these changes were not limited to the TME. The intratumoral injections of ExtraCRAd induced the priming of a systemic, antigen-specific immune response against the tumor. **Figures S9** and **S10** in publication **V** present the variations in the immunological profile of the spleens, while **Figure S11** shows the immunological landscape in the tumor draining lymph nodes. The animals vaccinated with the viral NPs showed enhanced percentage of DCs, including the cross-presenting activated ones. This translated into an increase in the percentage of $CD8^+$ T cells and, particularly, in antigen specific $CD8^+$ T cells in a poorly immunogenic tumor model. These results correlate with the ones obtained by adsorbing tumor-specific peptides on the capsid of adenovirus [383], suggesting the potential of adenovirus as an adjuvant in cancer vaccines and the efficacy of cancer cell membrane moieties as antigenic sources.

5.6.4 ExtraCRAd Preventive Cancer Vaccine in Lung Adenocarcinoma and Melanoma

ExtraCRAd's potential in priming an adaptive and memory immune response after a preventive vaccination scheme was evaluated in an immunogenic lung adenocarcinoma model, CMT64.OVA and in B16.F10 melanoma model. As presented in **Figure 6**, publication **V**, the vaccination with tumor-matched ExtraCRAd could control the tumor growth, prolonging the overall survival in both tumor models (more than 50% of animals alive after 40 days in CMT64.OVA cohort and after 28 days in B16.F10 cohort). Furthermore, the efficacy of a treatment with tumor-missmatched membranes was lower in both the tumor models. These results suggest the presence of functional antigens on the cell membrane and the efficacy of the viral NP in inducing an immune response in absence of any oncolytic effect [425].

In conclusion, the membrane extrusion technique was successfully translated and applied to the field of OVs, creating a viral NP, and modifying its mechanism(s) of entry into cells. Moreover, the coating of the virus with elements derived from the cell membrane of cancer cells allowed for the formulation of a powerful cancer vaccine. The treatment of established tumors in monotherapy completely controlled the tumor growth in a highly immunogenic melanoma model and with the majority of the animals in the poorly immunogenic melanoma model. Moreover, this treatment controlled

the tumor growth also in a model of solid lung adenocarcinoma. The changes to the immunological profile of the TME were statistically significant and were mirrored by a systemic cancer-specific immune response. Finally, a pre-immunization with tumor-matched ExtraCRAd could control the tumor growth, prolonging the overall survival in animal challenged with aggressive melanoma or lung adenocarcinoma.

6 Conclusions

Nanoparticles (NPs) have shown great promise in the treatment of cancer and as synthetic nanovaccines. However, these systems face issues concerning stability in physiological media, protein corona composition, and accumulation in the target tissue. The development of biohybrid NPs can help solve some of these challenges by employing materials shaped by evolution. Thereby, in this thesis, the potential of biohybrid coatings of NPs was evaluated with the aim of developing therapeutic cancer vaccines, especially adapting the immunological properties of PSi NPs and OVs.

Firstly, the effect of surface charge and surface hydrophobicity was evaluated in the engineering of biohybrid PSi NPs in terms of size, homogeneity and surface charge. A positive surface charge prevented the successful encapsulation of APTS-TCPSi within the cell membrane, while NPs presenting hydrophobic surfaces required extensive tipsonication before and after extrusion. Membrane-coated hydrophobic PSi NPs exhibited enhanced stability in physiological fluids (human plasma) when compared to the naked particles, while the higher stability of hydrophilic particles cancelled out the contribution of the cell membrane coating. The coating with cell membrane enhanced the biocompatibility of PSi NPs in different cells; however, surface-dependent cytotoxicity was detected in a cell-dependent fashion.

Differences in the cellular uptake between naked and biohybrid NPs were evaluated in different cell lines, in the presence of uptake inhibitors, to elucidate the mechanisms of entry of the biohybrid nanosystems. The uptake was found to be cell-specific and mainly dependent on caveolin and chlatrin mechanisms.

A multistage biohybrid nanovaccine was developed by glass capillary microfluidics by exploiting the immunostimulatory properties of TOPSi NPs and the innovative antigenic source provided from the cancer cell membrane. The nanovaccine induced the activation and maturation of human APCs *in vitro*, as evaluated by the expression of co-stimulatory factors in FCM and cytokine secretion by ELISA.

These observations led to the *in vivo* evaluation of the therapeutic efficacy of the multistage NPs as cancer vaccines for melanoma. Two subcutaneous vaccinations with the formulation controlled the tumor growth in 44.5% of the animals, inducing significant changes in the immunological profiles of the TME. Furthermore, changes in the immunological features of the TME were correlated with the therapy efficacy. Next, the multistage nanovaccine improved the monotherapy efficacy with ICI, increasing the number of animals responding to the treatment, while inducing the priming of a cancer-specific immune response.

Finally, the biohybrid coating technique was translated to OVs, obtaining viral NPs, as confirmed by imaging. The viral encapsulation altered the uptake mechanisms of the virus, enabling enhanced infectivity also in virus-resistant cell lines *in vitro* and *in vivo*. Moreover, the cell membrane layer effectively shielded the virus from neutralizing antibodies. Based on these results, further experiments demonstrated the efficacy of the viral nanovaccine in melanoma and lung adenocarcinoma. In a highly immunogenic melanoma model (B16.OVA) and in a solid lung adenocarcinoma model (LL/2) the intratumoral administration of ExtraCRAd controlled the tumor growth in all the animals, while in B16.F10 the tumors were controlled in 66% of the animals. The vaccination with ExtraCRAd elicited a local and systemic tumor-specific cell-mediated immune response, as determined by the analysis of the immune contexture in the TME and in the spleen. Moreover, the pre-immunization with ExtraCRAd wrapped in tumor-matched membranes controlled the tumor growth and prolonged the overall survival of tumor challenged mice.

Overall, biohybrid nanosystems and nanovaccines were developed in this thesis by engineering PSi NPs, multistage vectors, or adenoviruses with cell membranes derived from tumor cells for improved stability and biocompatibility, as well as to provide an innovative antigenic source in cancer vaccines. The publications focused on PSi NPs and oncolytic adenoviruses, thereby not representing an exhaustive study of the formulation parameters for biohybrid nanovaccines. The *in vivo* studies were focused on a highly immunogenic tumor type (melanoma) and only partially on a solid tumor model (lung adenocarcinoma). Further studies would extend the generalizability and translatability of the techniques and formulations, and would assess preventive and therapeutic efficacy of the two nanovaccine platforms in poorly immunogenic cancer types (*e.g.*, triple negative breast cancer cells). A continuation of this work would also analyze the exact composition of the isolated cell membranes, in order to evaluate which proteins, glycoproteins, and glycans are still present after the process. Further studies are also required to evaluate the influence of heterologous cell membranes on the cellular uptake, together with studies evaluating differences in the composition of the protein corona between the coated and uncoated particles.

The exploitation of biological elements (cell membranes and viruses) as nanosized systems takes advantage of evolution to address some of the current issues related to NPs in cancer therapy. These systems can provide additional features that have not been completely recreated on a lab bench, allowing also for an increased understanding of the properties needed to improve synthetic

particles. In the meantime, biohybrid nanovaccines can already have an effect in the clinical treatment of cancer.

References

1 Couzin-Frankel, J. Cancer immunotherapy. *Science*, 1432-1433, doi:10.1126/science.342.6165.1432 (2013).

2 Sharpe, A. H. Introduction to checkpoint inhibitors and cancer immunotherapy. *Immunol Rev* **276**, 5-8, doi:10.1111/imr.12531 (2017).

3 Sharma, P., *et al.* Primary, adaptive, and acquired resistance to cancer immunotherapy. *Cell* **168**, 707-723, doi:10.1016/j.cell.2017.01.017 (2017).

4 Maeng, H., *et al.* Cancer vaccines: translation from mice to human clinical trials. *Curr Opin Immunol* **51**, 111-122, doi:10.1016/j.coi.2018.03.001 (2018).

5 Vilgelm, A. E., *et al.* Combinatorial approach to cancer immunotherapy: strength in numbers. *J Leukoc Biol* **100**, 275-290, doi:10.1189/jlb.5RI0116-013RR (2016).

6 Breitbach, C. J., *et al.* Oncolytic viruses: therapeutics with an identity crisis. *EBioMedicine* **9**, 31-36, doi:10.1016/j.ebiom.2016.06.046 (2016).

7 Smith, D. M., *et al.* Applications of nanotechnology for immunology. *Nat Rev Immunol* **13**, 592-605, doi:10.1038/nri3488 (2013).

8 Irvine, D. J., *et al.* Synthetic nanoparticles for vaccines and immunotherapy. *Chem Rev* **115**, 11109-11146, doi:10.1021/acs.chemrev.5b00109 (2015).

9 Andorko, J. I., *et al.* Intrinsic immunogenicity of rapidly-degradable polymers evolves during degradation. *Acta Biomater* **32**, 24-34, doi:10.1016/j.actbio.2015.12.026 (2016).

10 Andorko, J. I., *et al.* Impact of molecular weight on the intrinsic immunogenic activity of poly(beta amino esters). *J Biomed Mater Res A* **105**, 1219-1229, doi:10.1002/jbm.a.35970 (2017).

11 Shahbazi, M. A. *et al.* Surface chemistry dependent immunostimulative potential of porous silicon nanoplatforms. *Biomaterials* **35**, 9224-9235, doi:10.1016/j.biomaterials.2014.07.050 (2014).

12 Lou, B. *et al.* Modular core-shell polymeric nanoparticles mimicking viral structures for vaccination. *J Control Release*, doi:10.1016/j.jconrel.2018.11.006 (2018).

13 Li, W. *et al.* Tailoring porous silicon for biomedical applications: from drug delivery to cancer immunotherapy. *Adv Mater* **30**, e1703740, doi:10.1002/adma.201703740 (2018).

14 Santos, H. *et al.* Mesoporous materials as controlled drug delivery formulations. *J Drug Delivery Sci Technol* **21**, 139-155 (2011).

15 Fontana, F., *et al.* Delivery of therapeutics with nanoparticles: what's new in cancer immunotherapy? *Wiley Interdiscip Rev Nanomed Nanobiotechnol* **9**, doi:10.1002/wnan.1421 (2017).

16 Salonen, J., *et al.* Mesoporous silicon in drug delivery applications. *J Pharm Sci* **97**, 632-653, doi:10.1002/jps.20999 (2008).

17 Santos, H. A., *et al.* Porous silicon nanoparticles for nanomedicine: preparation and biomedical applications. *Nanomedicine (Lond)* **9**, 535-554, doi:10.2217/nnm.13.223 (2014).

18 Santos, H. A., *et al.* Mesoporous materials and nanocrystals for enhancing the dissolution behavior of poorly water-soluble drugs. *Curr Pharm Biotechnol* **14**, 926-938 (2013).

19 Corbo, C. *et al.* The impact of nanoparticle protein corona on cytotoxicity, immunotoxicity and target drug delivery. *Nanomedicine (Lond)* **11**, 81-100, doi:10.2217/nnm.15.188 (2016).

20 Corbo, C., *et al.* Personalized protein corona on nanoparticles and its clinical implications. *Biomater Sci* **5**, 378-387, doi:10.1039/c6bm00921b (2017).

21 Fang, R. H., *et al.* Cell membrane coating nanotechnology. *Adv Mater* **30**, e1706759, doi:10.1002/adma.201706759 (2018).

22 Hu, C.-M. J. *et al.* Erythrocyte membrane-camouflaged polymeric nanoparticles as a biomimetic delivery platform. *Proc Natl Acad Sci U S A* **108**, 10980-10985 (2011).

23 Gao, W. *et al.* Surface functionalization of gold nanoparticles with red blood cell membranes. *Adv Mater* **25**, 3549-3553, doi:10.1002/adma.201300638 (2013).

24 Aryal, S. *et al.* Erythrocyte membrane-cloaked polymeric nanoparticles for controlled drug loading and release. *Nanomedicine (Lond)* **8**, 1271-1280, doi:10.2217/nnm.12.153 (2013).

25 Kroll, A. V. *et al.* Nanoparticulate delivery of cancer cell membrane elicits multiantigenic antitumor immunity. *Adv Mater* **29**, doi:10.1002/adma.201703969 (2017).

26 Fang, R. H. *et al.* Cancer cell membrane-coated nanoparticles for anticancer vaccination and drug delivery. *Nano Lett* **14**, 2181-2188, doi:10.1021/nl500618u (2014).

27 Palm, N. W., *et al.* Pattern recognition receptors and control of adaptive immunity. *Immunol Rev* **227**, 221-233, doi:10.1111/j.1600-065X.2008.00731.x (2009).

28 Kimbrell, D. A. *et al.* The evolution and genetics of innate immunity. *Nat Rev Genet* **2**, 256-267, doi:10.1038/35066006 (2001).

29 Murphy, K. *et al. Janeway's immunobiology*. (Garland Science, 2016).

30 Stephenson, J., *et al.* Inflammation in CNS neurodegenerative diseases. *Immunology* **154**, 204-219 (2018).

31 Jevtic, S., *et al.* The role of the immune system in Alzheimer disease: Etiology and treatment. *Ageing Res Rev* **40**, 84-94, doi:10.1016/j.arr.2017.08.005 (2017).

32 Prinz, M. *et al.* The role of peripheral immune cells in the CNS in steady state and disease. *Nat Neurosci* **20**, 136-144, doi:10.1038/nn.4475 (2017).

33 Fung, T. C., *et al.* Interactions between the microbiota, immune and nervous systems in health and disease. *Nat Neurosci* **20**, 145 (2017).

34 Ruparelia, N., *et al.* Inflammatory processes in cardiovascular disease: a route to targeted therapies. *Nat Rev Cardiol* **14**, 314, doi:10.1038/nrcardio.2017.33 (2017).

35 Nosalski, R., *et al.* Novel immune mechanisms in hypertension and cardiovascular risk. *Curr Cardiovasc Risk Rep* **11**, 12, doi:10.1007/s12170-017-0537-6 (2017).

36 Rodriguez-Iturbe, B., *et al.* Role of the immune system in hypertension. *Physiol Rev* **97**, 1127-1164, doi:10.1152/physrev.00031.2016 (2017).

37 Hotamisligil, G. S. Inflammation, metaflammation and immunometabolic disorders. *Nature* **542**, 177-185, doi:10.1038/nature21363 (2017).

38 Saltiel, A. R. *et al.* Inflammatory mechanisms linking obesity and metabolic disease. *J Clin Invest* **127**, 1-4, doi:10.1172/JCI92035 (2017).

39 Davidson, A. *et al.* Autoimmune diseases. *N Engl J Med* **345**, 340-350, doi:10.1056/NEJM200108023450506 (2001).

40 Dunn, G. P., *et al.* Cancer immunoediting: from immunosurveillance to tumor escape. *Nat Immunol* **3**, 991-998, doi:10.1038/ni1102-991 (2002).

41 Kazemi, T., *et al.* Immunotherapeutic approaches for cancer therapy: An updated review. *Artif Cells Nanomed Biotechnol* **44**, 769-779, doi:10.3109/21691401.2015.1019669 (2016).

42 Ophir, E., *et al.* Personalized approaches to active immunotherapy in cancer. *Biochim Biophys Acta* **1865**, 72-82, doi:10.1016/j.bbcan.2015.07.004 (2016).

43 Janeway, C. A., Jr. *et al.* Innate immune recognition. *Annu Rev Immunol* **20**, 197-216, doi:10.1146/annurev.immunol.20.083001.084359 (2002).

44 Silva, A. L., *et al.* Nanoparticle impact on innate immune cell pattern-recognition receptors and inflammasomes activation. *Semin Immunol* (2017).

45 Brubaker, S. W., *et al.* Innate immune pattern recognition: a cell biological perspective. *Annu Rev Immunol* **33**, 257-290, doi:10.1146/annurev-immunol-032414-112240 (2015).

46 Schaefer, L. Complexity of danger: the diverse nature of damage-associated molecular patterns. *J Biol Chem* **289**, 35237-35245, doi:10.1074/jbc.R114.619304 (2014).

47 Kono, H., *et al.* How dying cells alert the immune system to danger. *Nature Reviews Immunology* **8**, 279 (2008).

48 De Nardo, D. Toll-like receptors: Activation, signalling and transcriptional modulation. *Cytokine* **74**, 181-189, doi:10.1016/j.cyto.2015.02.025 (2015).

49 Geijtenbeek, T. B., *et al.* C-type lectin receptors in the control of T helper cell differentiation. *Nat Rev Immunol* **16**, 433-448, doi:10.1038/nri.2016.55 (2016).

50 Chen, G., *et al.* NOD-like receptors: role in innate immunity and inflammatory disease. *Annu Rev Pathol* **4**, 365-398, doi:10.1146/annurev.pathol.4.110807.092239 (2009).

51 Yoneyama, M., *et al.* Viral RNA detection by RIG-I-like receptors. *Curr Opin Immunol* **32**, 48-53, doi:10.1016/j.coi.2014.12.012 (2015).

52 Iwasaki, A., *et al.* Control of adaptive immunity by the innate immune system. *Nat Immunol* **16**, 343-353, doi:10.1038/ni.3123 (2015).

53 Kaliński, P., *et al.* T-cell priming by type-1and type-2 polarized dendritic cells: the concept of a third signal. *Immunol today* **20**, 561-567 (1999).

54 Iwasaki, A., *et al.* Toll-like receptor control of the adaptive immune responses. *Nat Immunol* **5**, 987-995, doi:10.1038/ni1112 (2004).

55 Langenkamp, A., *et al.* Kinetics of dendritic cell activation: impact on priming of TH1, TH2 and nonpolarized T cells. *Nat Immunol* **1**, 311-316, doi:10.1038/79758 (2000).

56 Becattini, S., *et al.* T cell immunity. Functional heterogeneity of human memory CD4(+) T cell clones primed by pathogens or vaccines. *Science* **347**, 400-406, doi:10.1126/science.1260668 (2015).

57 Jain, A., *et al.* Innate control of adaptive immunity: beyond the three-signal paradigm. *J Immunol* **198**, 3791-3800, doi:10.4049/jimmunol.1602000 (2017).

58 Schreiber, R. D., *et al.* Cancer immunoediting: integrating immunity's roles in cancer suppression and promotion. *Science* **331**, 1565-1570 (2011).

59 Dunn, G. P., *et al.* The three Es of cancer immunoediting. *Annu Rev Immunol* **22**, 329-360, doi:10.1146/annurev.immunol.22.012703.104803 (2004).

60 Pardoll, D. M. The blockade of immune checkpoints in cancer immunotherapy. *Nat Rev Cancer* **12**, 252-264, doi:10.1038/nrc3239 (2012).

61 Liu, L., *et al.* Combination immunotherapy of MUC1 mRNA nano-vaccine and CTLA-4 blockade effectively inhibits growth of triple negative breast cancer. *Mol Ther* **26**, 45-55, doi:10.1016/j.ymthe.2017.10.020 (2018).

62 Kang, T., *et al.* Necroptotic cancer cells-mimicry nanovaccine boosts anti-tumor immunity with tailored immune-stimulatory modality. *Biomaterials* **164**, 80-97, doi:10.1016/j.biomaterials.2018.02.033 (2018).

63 Ylosmaki, E., *et al.* Personalized cancer vaccine platform for clinically relevant oncolytic enveloped viruses. *Mol Ther* **26**, 2315-2325, doi:10.1016/j.ymthe.2018.06.008 (2018).

64 Feola, S., *et al.* Oncolytic vaccines increase the response to PD-L1 blockade in immunogenic and poorly immunogenic tumors. *Oncoimmunology* **7**, e1457596, doi:10.1080/2162402X.2018.1457596 (2018).

65 Deng, H., *et al.* The application of nanotechnology in immune checkpoint blockade for cancer treatment. *J Control Release* **290**, 28-45, doi:10.1016/j.jconrel.2018.09.026 (2018).

66 Zylberberg, C., *et al.* Pharmaceutical liposomal drug delivery: a review of new delivery systems and a look at the regulatory landscape. *Drug Deliv* **23**, 3319-3329, doi:10.1080/10717544.2016.1177136 (2016).

67 Petros, R. A., *et al.* Strategies in the design of nanoparticles for therapeutic applications. *Nat Rev Drug Discov* **9**, 615-627, doi:10.1038/nrd2591 (2010).

68 Shi, J., *et al.* Nanotechnology in drug delivery and tissue engineering: from discovery to applications. *Nano Lett* **10**, 3223-3230, doi:10.1021/nl102184c (2010).

69 Kamaly, N., *et al.* Degradable controlled-release polymers and polymeric nanoparticles: mechanisms of controlling drug release. *Chem Rev* **116**, 2602-2663, doi:10.1021/acs.chemrev.5b00346 (2016).

70 Bobo, D., *et al.* Nanoparticle-based medicines: a review of FDA-approved materials and clinical trials to date. *Pharm Res* **33**, 2373-2387, doi:10.1007/s11095-016-1958-5 (2016).

71 Griffin, B. T., *et al.* Pharmacokinetic, pharmacodynamic and biodistribution following oral administration of nanocarriers containing peptide and protein drugs. *Adv Drug Deliv Rev* **106**, 367-380, doi:10.1016/j.addr.2016.06.006 (2016).

72 Petschauer, J. S., *et al.* The effects of nanoparticle drug loading on the pharmacokinetics of anticancer agents. *Nanomedicine* **10**, 447-463 (2015).

73 Kai, M. P., *et al.* Evaluation of drug loading, pharmacokinetic behavior, and toxicity of a cisplatin-containing hydrogel nanoparticle. *J Control Release* **204**, 70-77, doi:10.1016/j.jconrel.2015.03.001 (2015).

74 Barenholz, Y. C. Doxil®—the first FDA-approved nano-drug: lessons learned. *J Control Release* **160**, 117-134 (2012).

75 Wang, A. Z., *et al.* Nanoparticle delivery of cancer drugs. *Annu Rev Med* **63**, 185-198, doi:10.1146/annurev-med-040210-162544 (2012).

76 Spencer, D. S., *et al.* Intelligent nanoparticles for advanced drug delivery in cancer treatment. *Curr Opin Chem Eng* **7**, 84-92, doi:10.1016/j.coche.2014.12.003 (2015).

77 Ball, R. L., *et al.* Lipid nanoparticle formulations for enhanced co-delivery of siRNA and mRNA. *Nano Lett* **18**, 3814-3822, doi:10.1021/acs.nanolett.8b01101 (2018).

78 Kemp, J. A., *et al.* "Combo" nanomedicine: co-delivery of multi-modal therapeutics for efficient, targeted, and safe cancer therapy. *Adv Drug Deliv Rev* **98**, 3-18, doi:10.1016/j.addr.2015.10.019 (2016).

79 Mu, J., *et al.* Development of endogenous enzyme-responsive nanomaterials for theranostics. *Chem Soc Rev* **47**, 5554-5573, doi:10.1039/c7cs00663b (2018).

80 Muthu, M. S., *et al.* Nanotheranostics- application and further development of nanomedicine strategies for advanced theranostics. *Theranostics* **4**, 660 (2014).

81 Wilhelm, S., *et al.* Analysis of nanoparticle delivery to tumours. *Nat Rev Mater* **1**, 16014 (2016).

82 Ke, P. C., *et al.*. A decade of the protein corona. *ACS Nano* **11**, 11773-11776, doi:10.1021/acsnano.7b08008 (2017).

83 Wan, S., *et al.* The "sweet" side of the protein corona: effects of glycosylation on nanoparticle-cell interactions. *ACS Nano* **9**, 2157-2166, doi:10.1021/nn506060q (2015).

84 Ritz, S., *et al.* Protein corona of nanoparticles: distinct proteins regulate the cellular uptake. *Biomacromolecules* **16**, 1311-1321 (2015).

85 Bertoli, F., *et al.* The intracellular destiny of the protein corona: a Study on its cellular internalization and evolution. *ACS Nano* **10**, 10471-10479, doi:10.1021/acsnano.6b06411 (2016).

86 Saha, K., *et al.* Regulation of macrophage recognition through the interplay of nanoparticle surface functionality and protein corona. *ACS nano* **10**, 4421-4430 (2016).

87 Cheng, C. J., *et al.* A holistic approach to targeting disease with polymeric nanoparticles. *Nat Rev Drug Discov* **14**, 239-247, doi:10.1038/nrd4503 (2015).

88 Klippstein, R., *et al.* Nanotechnology-based manipulation of dendritic cells for enhanced immunotherapy strategies. *Nanomedicine* **6**, 523-529, doi:10.1016/j.nano.2010.01.001 (2010).

89 Tran, T. H., *et al.* Nanoparticles for dendritic cell-based immunotherapy. *Int J Pharm* **542**, 253-265, doi:10.1016/j.ijpharm.2018.03.029 (2018).

90 Fontana, F., *et al.* in *Theranostic Biomaterials* (ed Elsevier B.V.) (2019).

91 Fifis, T., *et al.* Size-dependent immunogenicity: therapeutic and protective properties of nano-vaccines against tumors. *J Immunol* **173**, 3148-3154 (2004).

92 Zubris, K. A., *et al.* Ease of synthesis, controllable sizes, and in vivo large-animal-lymph migration of polymeric nanoparticles. *ChemMedChem* **5**, 1435-1438, doi:10.1002/cmdc.201000250 (2010).

93 Hickey, J. W., *et al.* Control of polymeric nanoparticle size to improve therapeutic delivery. *J Control Release* **219**, 536-547, doi:10.1016/j.jconrel.2015.10.006 (2015).

94 Sharma, G., *et al.* Polymer particle shape independently influences binding and internalization by macrophages. *J Control Release* **147**, 408-412, doi:10.1016/j.jconrel.2010.07.116 (2010).

95 Kumar, S., *et al.* Shape and size-dependent immune response to antigen-carrying nanoparticles. *J Control Release* **220**, 141-148, doi:10.1016/j.jconrel.2015.09.069 (2015).

96 Truong, N. P., *et al.* The importance of nanoparticle shape in cancer drug delivery. *Expert Opin Drug Deliv* **12**, 129-142, doi:10.1517/17425247.2014.950564 (2015).

97 Gause, K. T., *et al.* Immunological principles guiding the rational design of particles for vaccine delivery. *ACS Nano* **11**, 54-68, doi:10.1021/acsnano.6b07343 (2017).

98 Dobrovolskaia, M. A., *et al.* Immunological properties of engineered nanomaterials. *Nat Nanotechnol* **2**, 469-478, doi:10.1038/nnano.2007.223 (2007).

99 Albanese, A., *et al.* The effect of nanoparticle size, shape, and surface chemistry on biological systems. *Annu Rev Biomed Eng* **14**, 1-16, doi:10.1146/annurev-bioeng-071811-150124 (2012).

100 Shima, F., *et al.* Manipulating the antigen-specific immune response by the hydrophobicity of amphiphilic poly(gamma-glutamic acid) nanoparticles. *Biomaterials* **34**, 9709-9716, doi:10.1016/j.biomaterials.2013.08.064 (2013).

101 Nel, A. E., *et al.* Understanding biophysicochemical interactions at the nano-bio interface. *Nat Mater* **8**, 543-557, doi:10.1038/nmat2442 (2009).

102 Seong, S. Y., *et al.* Hydrophobicity: an ancient damage-associated molecular pattern that initiates innate immune responses. *Nat Rev Immunol* **4**, 469-478, doi:10.1038/nri1372 (2004).

103 Merkel, T. J., *et al.* Using mechanobiological mimicry of red blood cells to extend circulation times of hydrogel microparticles. *Proc Natl Acad Sci U S A* (2010).

104 Cui, J., *et al.* Mechanically tunable, self-adjuvanting nanoengineered polypeptide particles. *Adv Mater* **25**, 3468-3472, doi:10.1002/adma.201300981 (2013).

105 Benne, N., *et al.* Orchestrating immune responses: How size, shape and rigidity affect the immunogenicity of particulate vaccines. *J Control Release* **234**, 124-134 (2016).

106 Liu, L., *et al.* Immune responses to vaccines delivered by encapsulation into and/or adsorption onto cationic lipid-PLGA hybrid nanoparticles. *J Control Release* **225**, 230-239 (2016).

107 Reddy, S. T., *et al.* In vivo targeting of dendritic cells in lymph nodes with poly(propylene sulfide) nanoparticles. *J Control Release* **112**, 26-34, doi:10.1016/j.jconrel.2006.01.006 (2006).

108 Li, X., *et al.* Relationship between the size of nanoparticles and their adjuvant activity: data from a study with an improved experimental design. *Eur J Pharm Biopharm* **78**, 107-116 (2011).

109 Hirai, T., *et al.* Amorphous silica nanoparticles enhance cross-presentation in murine dendritic cells. *Biochem Biophys Res Commun* **427**, 553-556, doi:10.1016/j.bbrc.2012.09.095 (2012).

110 Shao, D., *et al.* The shape effect of magnetic mesoporous silica nanoparticles on endocytosis, biocompatibility and biodistribution. *Acta Biomater* **49**, 531-540, doi:10.1016/j.actbio.2016.11.007 (2017).

111 Huang, X., *et al.* The shape effect of mesoporous silica nanoparticles on biodistribution, clearance, and biocompatibility in vivo. *ACS Nano* **5**, 5390-5399, doi:10.1021/nn200365a (2011).

112 Mathaes, R., *et al.* Influence of particle size, an elongated particle geometry, and adjuvants on dendritic cell activation. *Eur J Pharm Biopharm* **94**, 542-549, doi:10.1016/j.ejpb.2015.06.015 (2015).

113 Almalik, A., *et al.* Hyaluronic acid coated chitosan nanoparticles reduced the immunogenicity of the formed protein corona. *Sci Rep* **7**, 10542, doi:10.1038/s41598-017-10836-7 (2017).

114 Elci, S. G., *et al.* Surface charge controls the suborgan biodistributions of gold nanoparticles. *ACS Nano* **10**, 5536-5542, doi:10.1021/acsnano.6b02086 (2016).

115 Moyano, D. F., *et al.* Nanoparticle hydrophobicity dictates immune response. *J Am Chem Soc* **134**, 3965-3967, doi:10.1021/ja2108905 (2012).

116 Anselmo, A. C., *et al.* Elasticity of nanoparticles influences their blood circulation, phagocytosis, endocytosis, and targeting. *ACS nano* **9**, 3169-3177 (2015).

117 Christensen, D., *et al.* A cationic vaccine adjuvant based on a saturated quaternary ammonium lipid have different in vivo distribution kinetics and display a distinct CD4 T cell-inducing capacity compared to its unsaturated analog. *J Control Release* **160**, 468-476, doi:10.1016/j.jconrel.2012.03.016 (2012).

118 Lybaert, L.,*et al.* Immunoengineering through cancer vaccines–A personalized and multi-step vaccine approach towards precise cancer immunity. *J Control Release* (2018).

119 Wang, C., *et al.* Tailoring biomaterials for cancer immunotherapy: emerging trends and future outlook. *Adv Mater* **29**, doi:10.1002/adma.201606036 (2017).

120 Goldberg, M. S. Immunoengineering: how nanotechnology can enhance cancer immunotherapy. *Cell* **161**, 201-204 (2015).

121 Cheung, A. S. *et al.* Engineered materials for cancer immunotherapy. *Nano Today* **10**, 511-531, doi:10.1016/j.nantod.2015.06.007 (2015).

122 Ali, O. A., *et al.* Infection-mimicking materials to program dendritic cells in situ. *Nat Mater* **8**, 151-158, doi:10.1038/nmat2357 (2009).

123 Weiden, J., *et al.* Synthetic immune niches for cancer immunotherapy. *Nat Rev Immunol* **18**, 212-219, doi:10.1038/nri.2017.89 (2018).

124 Ali, O. A., *et al.* In situ regulation of DC subsets and T cells mediates tumor regression in mice. *Sci Transl Med* **1**, 8ra19, doi:10.1126/scitranslmed.3000359 (2009).

125 Kim, J., *et al.* Injectable, spontaneously assembling, inorganic scaffolds modulate immune cells in vivo and increase vaccine efficacy. *Nat Biotechnol* **33**, 64-72, doi:10.1038/nbt.3071 (2015).

126 Bencherif, S. A., *et al.* Injectable cryogel-based whole-cell cancer vaccines. *Nat Commun* **6**, 7556, doi:10.1038/ncomms8556 (2015).

127 Singh, A., *et al.* In-situ crosslinking hydrogels for combinatorial delivery of chemokines and siRNA–DNA carrying microparticles to dendritic cells. *Biomaterials* **30**, 5187-5200 (2009).

128 Singh, A., *et al.* An injectable synthetic immune-priming center mediates efficient T-cell class switching and T-helper 1 response against B cell lymphoma. *J Control Release* **155**, 184-192, doi:10.1016/j.jconrel.2011.06.008 (2011).

129 Fesnak, A. D., *et al.* Engineered T cells: the promise and challenges of cancer immunotherapy. *Nat Rev Cancer* **16**, 566-581, doi:10.1038/nrc.2016.97 (2016).

130 Perica, K., *et al.* Enrichment and Expansion with Nanoscale Artificial Antigen Presenting Cells for Adoptive Immunotherapy. *ACS Nano* **9**, 6861-6871, doi:10.1021/acsnano.5b02829 (2015).

131 Oelke, M., *et al.* Ex vivo induction and expansion of antigen-specific cytotoxic T cells by HLA-Ig-coated artificial antigen-presenting cells. *Nat Med* **9**, 619-624, doi:10.1038/nm869 (2003).

132 Meyer, R. A., *et al.* Biodegradable nanoellipsoidal artificial antigen presenting cells for antigen specific T - cell activation. *Small* **11**, 1519-1525 (2015).

133 Kanapathipillai, M., *et al.* Nanoparticle targeting of anti-cancer drugs that alter intracellular signaling or influence the tumor microenvironment. *Adv Drug Delivery Rev* **79**, 107-118 (2014).

134 Bauleth - Ramos, T., *et al.* Nutlin-3a and cytokine co-loaded spermine-modified acetalated dextran nanoparticles for cancer chemo-immunotherapy. *Adv Funct Mater* **27**, 1703303 (2017).

135 Singh, Y., *et al.* Targeting tumor associated macrophages (TAMs) via nanocarriers. *J Control Release* **254**, 92-106, doi:10.1016/j.jconrel.2017.03.395 (2017).

136 Rodell, C. B., *et al.* TLR7/8-agonist-loaded nanoparticles promote the polarization of tumour-associated macrophages to enhance cancer immunotherapy. *Nat Biomed Eng*, 1 (2018).

137 Huang, Z., *et al.* Targeted delivery of oligonucleotides into tumor-associated macrophages for cancer immunotherapy. *J Control Release* **158**, 286-292 (2012).

138 Wang, Y., *et al.* Polymeric nanoparticles promote macrophage reversal from M2 to M1 phenotypes in the tumor microenvironment. *Biomaterials* **112**, 153-163, doi:10.1016/j.biomaterials.2016.09.034 (2017).

139 Zeisberger, S. M., *et al.* Clodronate-liposome-mediated depletion of tumour-associated macrophages: a new and highly effective antiangiogenic therapy approach. *Br J Cancer* **95**, 272-281, doi:10.1038/sj.bjc.6603240 (2006).

140 Conde, J. *et al.,* Dual targeted immunotherapy via in vivo delivery of biohybrid RNAi-peptide nanoparticles to tumor-associated macrophages and cancer cells. *Adv Funct Mater* **25**, 4183-4194 (2015).

141 Roy, A., *et al.* Nanoparticle mediated co-delivery of paclitaxel and a TLR-4 agonist results in tumor regression and enhanced immune response in the tumor microenvironment of a mouse model. *Int J Pharm* **445**, 171-180, doi:10.1016/j.ijpharm.2013.01.045 (2013).

142 Makkouk, A., *et al.* Biodegradable microparticles loaded with doxorubicin and CpG ODN for in situ immunization against cancer. *AAPS J* **17**, 184-193, doi:10.1208/s12248-014-9676-6 (2015).

143 Fontana, F., *et al.* Immunostimulation and immunosuppression: nanotechnology on the brink. *Small Methods* **2**, 1700347 (2018).

144 Hamdy, S., *et al.* Co-delivery of cancer-associated antigen and Toll-like receptor 4 ligand in PLGA nanoparticles induces potent CD8+ T cell-mediated anti-tumor immunity. *Vaccine* **26**, 5046-5057, doi:10.1016/j.vaccine.2008.07.035 (2008).

145 Han, H. D., *et al.* Toll-like receptor 3-induced immune response by poly(d,l-lactide-co-glycolide) nanoparticles for dendritic cell-based cancer immunotherapy. *Int J Nanomedicine* **11**, 5729-5742, doi:10.2147/IJN.S109001 (2016).

146 Ahmed, K. K., *et al.* Development and evaluation of biodegradable particles coloaded with antigen and the Toll-like receptor agonist, pentaerythritol lipid A, as a cancer vaccine. *J Pharm Sci* **105**, 1173-1179, doi:10.1016/j.xphs.2015.11.042 (2016).

147 Heit, A., *et al.* Antigen co-encapsulated with adjuvants efficiently drive protective T cell immunity. *Eur J Immunol* **37**, 2063-2074, doi:10.1002/eji.200737169 (2007).

148 Dolen, Y., *et al.* Co-delivery of PLGA encapsulated invariant NKT cell agonist with antigenic protein induce strong T cell-mediated antitumor immune responses. *Oncoimmunology* **5**, e1068493, doi:10.1080/2162402X.2015.1068493 (2016).

149 Shen, L., *et al.* A trifunctional dextran-based nanovaccine targets and activates murine dendritic cells, and induces potent cellular and humoral immune responses in vivo. *PLoS One* **8**, e80904, doi:10.1371/journal.pone.0080904 (2013).

150 Zeng, Q., *et al.* Tailoring polymeric hybrid micelles with lymph node targeting ability to improve the potency of cancer vaccines. *Biomaterials* **122**, 105-113, doi:10.1016/j.biomaterials.2017.01.010 (2017).

151 Persano, S., *et al.* Lipopolyplex potentiates anti-tumor immunity of mRNA-based vaccination. *Biomaterials* **125**, 81-89, doi:10.1016/j.biomaterials.2017.02.019 (2017).

152 Xu, Z., *et al.* Multifunctional nanoparticles co-delivering Trp2 peptide and CpG adjuvant induce potent cytotoxic T-lymphocyte response against melanoma and its lung metastasis. *J Control Release* **172**, 259-265, doi:10.1016/j.jconrel.2013.08.021 (2013).

153 Hassan, H. A., *et al.* Dual stimulation of antigen presenting cells using carbon nanotube-based vaccine delivery system for cancer immunotherapy. *Biomaterials* **104**, 310-322 (2016).

154 Neumann, S., *et al.* Synthetic TRP2 long-peptide and α-galactosylceramide formulated into cationic liposomes elicit CD8+ T-cell responses and prevent tumour progression. *Vaccine* **33**, 5838-5844 (2015).

155 Molino, N. M., *et al.* Biomimetic protein nanoparticles facilitate enhanced dendritic cell activation and cross-presentation. *ACS Nano* **7**, 9743-9752, doi:10.1021/nn403085w (2013).

156 Zhang, P., *et al.* Polyelectrolyte multilayers assembled entirely from immune signals on gold nanoparticle templates promote antigen-specific T cell response. *ACS Nano* **9**, 6465-6477, doi:10.1021/acsnano.5b02153 (2015).

157 Neek, M., *et al.* Co-delivery of human cancer-testis antigens with adjuvant in protein nanoparticles induces higher cell-mediated immune responses. *Biomaterials* **156**, 194-203, doi:10.1016/j.biomaterials.2017.11.022 (2018).

158 Zhang, C., *et al.* Targeted antigen delivery to dendritic cell via functionalized alginate nanoparticles for cancer immunotherapy. *J Control Release* **256**, 170-181, doi:10.1016/j.jconrel.2017.04.020 (2017).

159 Liu, Q., *et al.* pH-responsive poly(D,L-lactic-co-glycolic acid) nanoparticles with rapid antigen release behavior promote immune response. *ACS Nano* **9**, 4925-4938, doi:10.1021/nn5066793 (2015).

160 Shi, G. N., *et al.* Enhanced antitumor immunity by targeting dendritic cells with tumor cell lysate-loaded chitosan nanoparticles vaccine. *Biomaterials* **113**, 191-202, doi:10.1016/j.biomaterials.2016.10.047 (2017).

161 Yang, Y., *et al.* Multi-shelled dendritic mesoporous organosilica hollow spheres: roles of composition and architecture in cancer immunotherapy. *Angew Chem Int Ed Engl* **56**, 8446-8450, doi:10.1002/anie.201701550 (2017).

162 Wang, C., *et al.* Inflammation-triggered cancer immunotherapy by programmed delivery of CpG and Anti-PD1 antibody. *Adv Mater* **28**, 8912-8920, doi:10.1002/adma.201506312 (2016).

163 Luo, M., *et al.* A STING-activating nanovaccine for cancer immunotherapy. *Nat Nanotechnol* **12**, 648-654, doi:10.1038/nnano.2017.52 (2017).

164 Yoshizaki, Y., *et al.* Potentiation of pH-sensitive polymer-modified liposomes with cationic lipid inclusion as antigen delivery carriers for cancer immunotherapy. *Biomaterials* **35**, 8186-8196, doi:10.1016/j.biomaterials.2014.05.077 (2014).

165 Yuba, E., *et al.* Dextran derivative-based pH-sensitive liposomes for cancer immunotherapy. *Biomaterials* **35**, 3091-3101, doi:10.1016/j.biomaterials.2013.12.024 (2014).

166 Lebel, M.-È., *et al.* Potentiating cancer immunotherapy using papaya mosaic virus-derived nanoparticles. *Nano Lett* **16**, 1826-1832 (2016).

167 Ochyl, L. J., *et al.* PEGylated tumor cell membrane vesicles as a new vaccine platform for cancer immunotherapy. *Biomaterials* **182**, 157-166 (2018).

168 Kuai, R., *et al.* Subcutaneous nanodisc vaccination with neoantigens for combination cancer immunotherapy. *Bioconjug Chem* **29**, 771-775, doi:10.1021/acs.bioconjchem.7b00761 (2018).

169 Rodriguez, P. L ., *et al.* Minimal" Self" peptides that inhibit phagocytic clearance and enhance delivery of nanoparticles. *Science* **339**, 971-975 (2013).

170 Qie, Y., *et al.* Surface modification of nanoparticles enables selective evasion of phagocytic clearance by distinct macrophage phenotypes. *Sci Rep* **6**, 26269, doi:10.1038/srep26269 (2016).

171 Villa, C. H., *et al.* Red blood cells: Supercarriers for drugs, biologicals, and nanoparticles and inspiration for advanced delivery systems. *Adv Drug Delivery Rev* **106**, 88-103 (2016).

172 Brenner, J. S., *et al.* Red blood cell-hitchhiking boosts delivery of nanocarriers to chosen organs by orders of magnitude. *Nat Commun* **9**, 2684, doi:10.1038/s41467-018-05079-7 (2018).

173 Pan, D. C., *et al.* Nanoparticle properties modulate their attachment and effect on carrier red blood cells. *Sci Rep* **8**, 1615 (2018).

174 Wibroe, P. P., *et al.* Bypassing adverse injection reactions to nanoparticles through shape modification and attachment to erythrocytes. *Nat Nanotechnol* **12**, 589 (2017).

175 Chambers, E. *et al.* Long circulating nanoparticles via adhesion on red blood cells: mechanism and extended circulation. *Exp Biol Med (Maywood)* **232**, 958-966 (2007).

176 Balasubramanian, V., *et al.* Biomimetic engineering using cancer cell membranes for designing compartmentalized nanoreactors with organelle‐like functions. *Adv Mater* **29**, 1605375 (2017).

177 Diez-Silva, M., *et al.* Shape and biomechanical characteristics of human red blood cells in health and disease. *MRS Bull* **35**, 382-388 (2010).

178 Huang, Y. X., *et al.* Restoring the youth of aged red blood cells and extending their lifespan in circulation by remodelling membrane sialic acid. *J Cell Mol Med* **20**, 294-301 (2016).

179 Pivkin, I. V., *et al.* Biomechanics of red blood cells in human spleen and consequences for physiology and disease. *Proc Natl Acad Sci U S A* **113**, 7804-7809, doi:10.1073/pnas.1606751113 (2016).

180 de Back, D. Z., *et al.* Of macrophages and red blood cells; a complex love story. *Front Physiol* **5**, 9, doi:10.3389/fphys.2014.00009 (2014).

181 Gao, M., *et al.* Erythrocyte-membrane-enveloped perfluorocarbon as nanoscale artificial red blood cells to relieve tumor hypoxia and enhance cancer radiotherapy. *Adv Mater* **29**, 1701429 (2017).

182 Ren, X., *et al.* Red blood cell membrane camouflaged magnetic nanoclusters for imaging-guided photothermal therapy. *Biomaterials* **92**, 13-24, doi:10.1016/j.biomaterials.2016.03.026 (2016).

183 Luk, B. T., *et al.* Safe and immunocompatible nanocarriers cloaked in RBC membranes for drug delivery to treat solid tumors. *Theranostics* **6**, 1004-1011, doi:10.7150/thno.14471 (2016).

184 Piao, J.-G., *et al.* Erythrocyte membrane is an alternative coating to polyethylene glycol for prolonging the circulation lifetime of gold nanocages for photothermal therapy. *ACS Nano* **8**, 10414-10425 (2014).

185 Su, J. *et al.,* Enhanced blood suspensibility and laser-activated tumor-specific drug release of theranostic mesoporous silica nanoparticles by functionalizing with erythrocyte membranes. *Theranostics* **7**, 523-537, doi:10.7150/thno.17259 (2017).

186 Peng, J., *et al.* Erythrocyte-membrane-coated prussian blue/manganese dioxide nanoparticles as H2O2-responsive oxygen generators to enhance cancer chemotherapy/photothermal therapy. *ACS Appl Mater Interfaces* **9**, 44410-44422, doi:10.1021/acsami.7b17022 (2017).

187 Wang, F., *et al.* Nanoparticle-based antivirulence vaccine for the management of methicillin-resistant staphylococcus aureus skin infection. *Adv Funct Mater* **26**, 1628-1635, doi:10.1002/adfm.201505231 (2016).

188 Wei, X., *et al.* In situ capture of bacterial toxins for antivirulence vaccination. *Adv Mater* **29**, doi:10.1002/adma.201701644 (2017).

189 Guo, Y., *et al.* Erythrocyte membrane-enveloped polymeric nanoparticles as nanovaccine for induction of antitumor immunity against melanoma. *ACS nano* **9**, 6918-6933 (2015).

190 Fang, R. H., *et al.* Lipid-insertion enables targeting functionalization of erythrocyte membrane-cloaked nanoparticles. *Nanoscale* **5**, 8884-8888, doi:10.1039/c3nr03064d (2013).

191 Hu, C.-M. J., *et al.* A biomimetic nanosponge that absorbs pore-forming toxins. *Nat Nanotechnol* **8**, 336 (2013).

192 Pang, Z., *et al.* Detoxification of organophosphate poisoning using nanoparticle bioscavengers. *ACS nano* **9**, 6450-6458 (2015).

193 Nguyen, T. D. T., *et al.* Engineered biomimetic nanoabsorbent for cellular detoxification of chemotherapeutics. *RSC Advances* **6**, 33003-33008 (2016).

194 Copp, J. A., *et al.* Clearance of pathological antibodies using biomimetic nanoparticles. *Proc Natl Acad Sci U S A* **111**, 13481-13486 (2014).

195 Chen, H. W., *et al.* Targeting and enrichment of viral pathogen by cell membrane cloaked magnetic nanoparticles for enhanced detection. *ACS Appl Mater Interfaces* **9**, 39953-39961, doi:10.1021/acsami.7b09931 (2017).

196 Jenne, C. N., *et al.* Platelets in inflammation and infection. *Platelets* **26**, 286-292, doi:10.3109/09537104.2015.1010441 (2015).

197 Walsh, T. G., *et al.* The functional role of platelets in the regulation of angiogenesis. *Platelets* **26**, 199-211, doi:10.3109/09537104.2014.909022 (2015).

198 Fontana, F., *et al.* Platelet lysate-modified porous silicon microparticles for enhanced cell proliferation in wound healing applications. *ACS Appl Mater Interfaces* **8**, 988-996, doi:10.1021/acsami.5b10950 (2016).

199 Hu, C. M., *et al.* Nanoparticle biointerfacing by platelet membrane cloaking. *Nature* **526**, 118-121, doi:10.1038/nature15373 (2015).

200 Frangogiannis, N. G. The inflammatory response in myocardial injury, repair, and remodelling. *Nat Rev Cardiol* **11**, 255-265, doi:10.1038/nrcardio.2014.28 (2014).

201 Kreuger, J., *et al.* Targeting vascular and leukocyte communication in angiogenesis, inflammation and fibrosis. *Nat Rev Drug Discov* **15**, 125-142, doi:10.1038/nrd.2015.2 (2016).

202 Navegantes, K. C., *et al.* Immune modulation of some autoimmune diseases: the critical role of macrophages and neutrophils in the innate and adaptive immunity. *J Transl Med* **15**, 36 (2017).

203 Parodi, A., *et al.* Synthetic nanoparticles functionalized with biomimetic leukocyte membranes possess cell-like functions. *Nat Nanotechnol* **8**, 61-68, doi:10.1038/nnano.2012.212 (2013).

204 Xuan, M., *et al.* Macrophage cell membrane camouflaged mesoporous silica nanocapsules for in vivo cancer therapy. *Adv Healthc Mater* **4**, 1645-1652, doi:10.1002/adhm.201500129 (2015).

205 Cao, H., *et al.* Liposomes coated with isolated macrophage membrane can target lung metastasis of breast cancer. *ACS nano* **10**, 7738-7748 (2016).

206 Xuan, M., *et al.* Macrophage cell membrane camouflaged Au nanoshells for in vivo prolonged circulation life and enhanced cancer photothermal therapy. *ACS Appl Mater Interfaces* **8**, 9610-9618, doi:10.1021/acsami.6b00853 (2016).

207 Thamphiwatana, S., *et al.* Macrophage-like nanoparticles concurrently absorbing endotoxins and proinflammatory cytokines for sepsis management. *Proc Natl Acad Sci U S A* **114**, 11488-11493, doi:10.1073/pnas.1714267114 (2017).

208 Xiong, K. *et al.,* Biomimetic immuno-magnetosomes for high-performance enrichment of circulating tumor cells. *Adv Mater* **28**, 7929-7935, doi:10.1002/adma.201601643 (2016).

209 Gao, C., *et al.* Polymeric capsule-cushioned leukocyte cell membrane vesicles as a biomimetic delivery platform. *Nanoscale* **8**, 3548-3554, doi:10.1039/c5nr08407e (2016).

210 Kidd, S., *et al.* Direct evidence of mesenchymal stem cell tropism for tumor and wounding microenvironments using in vivo bioluminescent imaging. *Stem Cells* **27**, 2614-2623, doi:10.1002/stem.187 (2009).

211 Layek, B., *et al.* Nano-engineered mesenchymal stem cells increase therapeutic efficacy of anticancer drug through true active tumor targeting. *Mol Cancer Ther* **17**, 1196-1206, doi:10.1158/1535-7163.MCT-17-0682 (2018).

212 Tang, J., *et al.* Therapeutic microparticles functionalized with biomimetic cardiac stem cell membranes and secretome. *Nat Commun* **8**, 13724, doi:10.1038/ncomms13724 (2017).

213 Gao, W., *et al.* Modulating antibacterial immunity via bacterial membrane-coated nanoparticles. *Nano Lett* **15**, 1403-1409, doi:10.1021/nl504798g (2015).

214 Rao, L., *et al.* Red blood cell membrane as a biomimetic nanocoating for prolonged circulation time and reduced accelerated blood clearance. *Small* **11**, 6225-6236 (2015).

215 Rao, L., *et al.* Erythrocyte membrane-coated upconversion nanoparticles with minimal protein adsorption for enhanced tumor imaging. *ACS Appl Mater Interfaces* **9**, 2159-2168, doi:10.1021/acsami.6b14450 (2017).

216 Jiang, Q., *et al.* Red blood cell membrane-camouflaged melanin nanoparticles for enhanced photothermal therapy. *Biomaterials* **143**, 29-45, doi:10.1016/j.biomaterials.2017.07.027 (2017).

217 Ding, H., *et al.* Erythrocyte membrane-coated NIR-triggered biomimetic nanovectors with programmed delivery for photodynamic therapy of cancer. *Nanoscale* **7**, 9806-9815 (2015).

218 Deng, J., *et al.* Tumor targeted, stealthy and degradable bismuth nanoparticles for enhanced X-ray radiation therapy of breast cancer. *Biomaterials* **154**, 24-33, doi:10.1016/j.biomaterials.2017.10.048 (2018).

219 Ren, H., *et al.* Oxygen self-enriched nanoparticles functionalized with erythrocyte membranes for long circulation and enhanced phototherapy. *Acta Biomater* **59**, 269-282, doi:10.1016/j.actbio.2017.06.035 (2017).

220 Chai, Z., *et al.* A facile approach to functionalizing cell membrane-coated nanoparticles with neurotoxin-derived peptide for brain-targeted drug delivery. *J Control Release* **264**, 102-111, doi:10.1016/j.jconrel.2017.08.027 (2017).

221 Su, J., *et al.* Long circulation red-blood-cell-mimetic nanoparticles with peptide-enhanced tumor penetration for simultaneously inhibiting growth and lung metastasis of breast cancer. *Adv Funct Mater* **26**, 1243-1252 (2016).

222 Chhabria, V., *et al.* Development of nanosponges from erythrocyte ghosts for removal of streptolysin-O from mammalian blood. *Nanomedicine (Lond)*, doi:10.2217/nnm-2016-0180 (2016).

223 Escajadillo, T., *et al.* A red blood cell membrane-camouflaged nanoparticle counteracts streptolysin O-mediated virulence phenotypes of invasive group A streptococcus. *Front Pharmacol* **8**, 477, doi:10.3389/fphar.2017.00477 (2017).

224 Chen, M. S., *et al.* Fabrication and characterization of a 3D bioprinted nanoparticle-hydrogel hybrid device for biomimetic detoxification. *Nanoscale* **9**, 14506-14511, doi:10.1039/c7nr05322c (2017).

225 Wu, Z., *et al.* Cell-membrane-coated synthetic nanomotors for effective biodetoxification. *Adv Funct Mater* **25**, 3881-3887 (2015).

226 Hu, C. M., *et al.* Nanoparticle-detained toxins for safe and effective vaccination. *Nat Nanotechnol* **8**, 933-938, doi:10.1038/nnano.2013.254 (2013).

227 Lapek, J. D., Jr., *et al.* Biomimetic virulomics for capture and identification of cell-type specific effector proteins. *ACS Nano* **11**, 11831-11838, doi:10.1021/acsnano.7b02650 (2017).

228 Fu, Q., *et al.* Programmed co-delivery of paclitaxel and doxorubicin boosted by camouflaging with erythrocyte membrane. *Nanoscale* **7**, 4020-4030, doi:10.1039/c4nr07027e (2015).

229 Su, J., *et al.* Bioinspired nanoparticles with NIR-controlled drug release for synergetic chemophotothermal therapy of metastatic breast cancer. *Adv Funct Mater* **26**, 7495-7506 (2016).

230 Rao, L., *et al.* Photocatalytic degradation of cell membrane coatings for controlled drug release. *Adv Healthc Mater* **5**, 1420-1427, doi:10.1002/adhm.201600303 (2016).

231 Gao, L., *et al.* Erythrocyte membrane-wrapped pH sensitive polymeric nanoparticles for non-small cell lung cancer therapy. *Bioconjug Chem* **28**, 2591-2598, doi:10.1021/acs.bioconjchem.7b00428 (2017).

232 Song, Q., *et al.* Tumor microenvironment responsive nanogel for the combinatorial antitumor effect of chemotherapy and immunotherapy. *Nano Lett* **17**, 6366-6375, doi:10.1021/acs.nanolett.7b03186 (2017).

233 Li, L. L., *et al.* Core-shell supramolecular gelatin nanoparticles for adaptive and "on-demand" antibiotic delivery. *ACS Nano* **8**, 4975-4983, doi:10.1021/nn501040h (2014).

234 Zhang, Y., *et al.* Erythrocyte membrane-coated nanogel for combinatorial antivirulence and responsive antimicrobial delivery against Staphylococcus aureus infection. *J Control Release* **263**, 185-191, doi:10.1016/j.jconrel.2017.01.016 (2017).

235 Gao, L., *et al.* An effective intracellular delivery system of monoclonal antibody for treatment of tumors: erythrocyte membrane-coated self-associated antibody nanoparticles. *Nanotechnology* **28**, 335101, doi:10.1088/1361-6528/aa7c43 (2017).

236 Fu, Y., *et al.* Erythrocyte-membrane-camouflaged nanoplatform for intravenous glucose-responsive insulin delivery. *Adv Funct Mater* **28**, 1802250 (2018).

237 Zhang, X., *et al.* Remote loading of small-molecule therapeutics into cholesterol-enriched cell-membrane-derived vesicles. *Angew Chem Int Ed Engl* **56**, 14075-14079, doi:10.1002/anie.201707598 (2017).

238 Hu, Q., *et al.* Anticancer platelet-mimicking nanovehicles. *Adv Mater* **27**, 7043-7050, doi:10.1002/adma.201503323 (2015).

239 Wei, X., *et al.* Nanoparticles camouflaged in platelet membrane coating as an antibody decoy for the treatment of immune thrombocytopenia. *Biomaterials* **111**, 116-123 (2016).

240 Li, J., *et al.* Targeted drug delivery to circulating tumor cells via platelet membrane-functionalized particles. *Biomaterials* **76**, 52-65, doi:10.1016/j.biomaterials.2015.10.046 (2016).

241 Hu, Q., *et al.* Engineered nanoplatelets for enhanced treatment of multiple myeloma and thrombus. *Adv Mater* **28**, 9573-9580, doi:10.1002/adma.201603463 (2016).

242 Krishnamurthy, S., *et al.* Monocyte cell membrane-derived nanoghosts for targeted cancer therapy. *Nanoscale* **8**, 6981-6985, doi:10.1039/c5nr07588b (2016).

243 Kang, T., *et al.* Nanoparticles coated with neutrophil membranes can effectively treat cancer metastasis. *ACS Nano* **11**, 1397-1411 (2017).

244 Rao, L., *et al.* Effective cancer targeting and imaging using macrophage membrane - camouflaged upconversion nanoparticles. *J. Biomed. Mater. Res., Part A* **105**, 521-530 (2017).

245 Zhang, Q., *et al.* Neutrophil membrane-coated nanoparticles inhibit synovial inflammation and alleviate joint damage in inflammatory arthritis. *Nat Nanotechnol*, doi:10.1038/s41565-018-0254-4 (2018).

246 Wang, C., *et al.* Pretreated macrophage-membrane-coated gold nanocages for precise drug delivery for treatment of bacterial infections. *Adv Mater*, e1804023, doi:10.1002/adma.201804023 (2018).

247 Zhang, L., *et al.* Human cytotoxic T-lymphocyte membrane-camouflaged nanoparticles combined with low-dose irradiation: a new approach to enhance drug targeting in gastric cancer. *Int J Nanomedicine* **12**, 2129-2142, doi:10.2147/IJN.S126016 (2017).

248 Gao, C., *et al.* Stem cell membrane-coated nanogels for highly efficient in vivo tumor targeted drug delivery. *Small* **12**, 4056-4062, doi:10.1002/smll.201600624 (2016).

249 Bose, R. J., *et al.* Bioengineered stem cell membrane functionalized nanocarriers for therapeutic targeting of severe hindlimb ischemia. *Biomaterials* **185**, 360-370, doi:10.1016/j.biomaterials.2018.08.018 (2018).

250 Lai, P.-Y., *et al.* Biomimetic stem cell membrane-camouflaged iron oxide nanoparticles for theranostic applications. *RSC Adv* **5**, 98222-98230 (2015).

251 Gao, C., *et al.* Stem-cell-membrane camouflaging on near-infrared photoactivated upconversion nanoarchitectures for in vivo remote-controlled photodynamic therapy. *ACS Appl Mater Interfaces* **8**, 34252-34260, doi:10.1021/acsami.6b12865 (2016).

252 Silva, A. K. A., *et al.* Cell-derived vesicles as a bioplatform for the encapsulation of theranostic nanomaterials. *Nanoscale* **5**, 11374-11384 (2013).

253 Chen, W., *et al.* Coating nanofiber scaffolds with beta cell membrane to promote cell proliferation and function. *Nanoscale* **8**, 10364-10370, doi:10.1039/c6nr00535g (2016).

254 Dehaini, D., *et al.* Erythrocyte–platelet hybrid membrane coating for enhanced nanoparticle functionalization. *Adv Mater* **29**, 1606209 (2017).

255 Rao, L., *et al.* Platelet-leukocyte hybrid membrane-coated immunomagnetic beads for highly efficient and highly specific isolation of circulating tumor cells. *Adv Funct Mater* **28**, 1803531 (2018).

256 He, H., *et al.* Leutusome: a biomimetic nanoplatform integrating plasma membrane components of leukocytes and tumor cells for remarkably enhanced solid tumor homing. *Nano Lett* **18**, 6164-6174, doi:10.1021/acs.nanolett.8b01892 (2018).

257 Liang, H., *et al.* Mesenchymal stem cell/red blood cell-inspired nanoparticle therapy in mice with carbon tetrachloride-induced acute liver failure. *ACS Nano* **12**, 6536-6544, doi:10.1021/acsnano.8b00553 (2018).

258 Zhu, J. Y., *et al.* Preferential cancer cell self-recognition and tumor self-targeting by coating nanoparticles with homotypic cancer cell membranes. *Nano Lett* **16**, 5895-5901, doi:10.1021/acs.nanolett.6b02786 (2016).

259 Sun, H., *et al.* Cancer cell membrane-coated gold nanocages with hyperthermia-triggered drug release and homotypic target inhibit growth and metastasis of breast cancer. *Adv Funct Mater* **27**, 1604300 (2017).

260 Rao, L., *et al.* Cancer cell membrane-coated upconversion nanoprobes for highly specific tumor imaging. *Adv Mater* **28**, 3460-3466, doi:10.1002/adma.201506086 (2016).

261 Cheng, H., *et al.* An O2 self-sufficient biomimetic nanoplatform for highly specific and efficient photodynamic therapy. *Adv Funct Mater* **26**, 7847-7860 (2016).

262 Li, S. Y., *et al.* Cancer cell membrane-coated biomimetic platform for tumor targeted photodynamic therapy and hypoxia-amplified bioreductive therapy. *Biomaterials* **142**, 149-161, doi:10.1016/j.biomaterials.2017.07.026 (2017).

263 Sun, H., *et al.* Cancer-cell-biomimetic nanoparticles for targeted therapy of homotypic tumors. *Adv Mater* **28**, 9581-9588, doi:10.1002/adma.201602173 (2016).

264 Tian, H., *et al.* Cancer cell membrane-biomimetic oxygen nanocarrier for breaking hypoxia-induced chemoresistance. *Adv Funct Mater* **27**, 1703197 (2017).

265 Chen, Z., *et al.* Cancer cell membrane–biomimetic nanoparticles for homologous-targeting dual-modal imaging and photothermal therapy. *ACS nano* **10**, 10049-10057 (2016).

266 Li, S. Y., *et al.* A biomimetic theranostic O2-meter for cancer targeted photodynamic therapy and phosphorescence imaging. *Biomaterials* **151**, 1-12, doi:10.1016/j.biomaterials.2017.10.021 (2018).

267 Li, S. Y., *et al.* Cancer cell membrane camouflaged cascade bioreactor for cancer targeted starvation and photodynamic therapy. *ACS Nano* **11**, 7006-7018, doi:10.1021/acsnano.7b02533 (2017).

268 Cheung, A. S., *et al.* Adjuvant-loaded subcellular vesicles derived from disrupted cancer cells for cancer vaccination. *Small* **12**, 2321-2333, doi:10.1002/smll.201600061 (2016).

269 Patel, J. M., *et al.* Plasma membrane vesicles decorated with glycolipid-anchored antigens and adjuvants via protein transfer as an antigen delivery platform for inhibition of tumor growth. *Biomaterials* **74**, 231-244, doi:10.1016/j.biomaterials.2015.09.031 (2016).

270 Tian, X., *et al.* A membrane vesicle-based dual vaccine against melanoma and Lewis lung carcinoma. *Biomaterials* **33**, 6147-6154, doi:10.1016/j.biomaterials.2012.05.034 (2012).

271 Vinay, D. S., *et al.* Immune evasion in cancer: Mechanistic basis and therapeutic strategies. *Semin Cancer Biol* **35 Suppl**, S185-S198, doi:10.1016/j.semcancer.2015.03.004 (2015).

272 Mohme, M., *et al.* Circulating and disseminated tumour cells - mechanisms of immune surveillance and escape. *Nat Rev Clin Oncol* **14**, 155-167, doi:10.1038/nrclinonc.2016.144 (2017).

273 van der Burg, S. H., *et al.* Vaccines for established cancer: overcoming the challenges posed by immune evasion. *Nat Rev Cancer* **16**, 219-233, doi:10.1038/nrc.2016.16 (2016).

274 Ali, O. A., *et al.* Vaccines combined with immune checkpoint antibodies promote cytotoxic T-cell activity and tumor eradication. *Cancer Immunol Res* **4**, 95-100, doi:10.1158/2326-6066.CIR-14-0126 (2016).

275 Gotwals, P., *et al.* Prospects for combining targeted and conventional cancer therapy with immunotherapy. *Nat Rev Cancer* **17**, 286-301, doi:10.1038/nrc.2017.17 (2017).

276 Chung, C. K., *et al.* Combinatory therapy adopting nanoparticle-based cancer vaccination with immune checkpoint blockade for treatment of post-surgical tumor recurrences. *J Control Release* **285**, 56-66, doi:10.1016/j.jconrel.2018.07.011 (2018).

277 Uhlir Jr, A. Electrolytic shaping of germanium and silicon. *Bell Syst. Tech. J.* **35**, 333-347 (1956).

278 Canham, L. T. Bioactive silicon structure fabrication through nanoetching techniques. *Adv Mater* **7**, 1033-1037 (1995).

279 Salonen, J., *et al.* Fabrication and chemical surface modification of mesoporous silicon for biomedical applications. *Chem. Eng. J.* **137**, 162-172 (2008).

280 Bley, R. A., *et al.* Characterization of silicon nanoparticles prepared from porous silicon. *Chem. Mater.* **8**, 1881-1888 (1996).

281 Heinrich, J. L., *et al.* Luminescent colloidal silicon suspensions from porous silicon. *Science* **255**, 66-68 (1992).

282 Salonen, J., *et al.* Mesoporous silicon microparticles for oral drug delivery: loading and release of five model drugs. *J Control Release* **108**, 362-374, doi:10.1016/j.jconrel.2005.08.017 (2005).

283 Roberts, D. S., *et al.* Preparation of photoluminescent porous silicon nanoparticles by high-pressure microfluidization. *Part. Part. Syst. Charact.* **34**, 1600326 (2017).

284 Chiappini, C., *et al.* Tailored porous silicon microparticles: fabrication and properties. *Chem Phys Chem* **11**, 1029-1035, doi:10.1002/cphc.200900914 (2010).

285 Alhmoud, H.. *et al.* Porous silicon nanodiscs for targeted drug delivery. *Adv Funct Mater* **25**, 1137-1145 (2015).

286 Elnathan, R.. *et al.* Maximizing transfection efficiency of vertically aligned silicon nanowire arrays. *Adv Funct Mater* **25**, 7215-7225 (2015).

287 Dai, F.. *et al.* Bottom-up synthesis of high surface area mesoporous crystalline silicon and evaluation of its hydrogen evolution performance. *Nat Commun* **5**, 3605, doi:10.1038/ncomms4605 (2014).

288 Fan, D., *et al.* The role of nanostructured mesoporous silicon in discriminating in vitro calcification for electrospun composite tissue engineering scaffolds. *Nanoscale* **3**, 354-361 (2011).

289 Park, J.-H., *et al.* Biodegradable luminescent porous silicon nanoparticles for in vivo applications. *Nat Mater* **8**, 331 (2009).

290 Shabir, Q., *et al.* Quantification and reduction of the residual chemical reactivity of passivated biodegradable porous silicon for drug delivery applications. *Silicon* **10**, 349-359 (2018).

291 Kovalev, D., *et al.* Photodegradation of porous silicon induced by photogenerated singlet oxygen molecules. *Appl Phys Lett* **85**, 3590-3592 (2004).

292 Low, S. P., *et al.* Generation of reactive oxygen species from porous silicon microparticles in cell culture medium. *J. Biomed. Mater. Res., Part A* **93**, 1124-1131 (2010).

293 Pap, A. E., *et al.* Thermal oxidation of porous silicon: study on structure. *Appl Phys Lett* **86**, 041501 (2005).

294 Aggarwal, G., *et al.* Porous silicon surface stability: a comparative study of thermal oxidation techniques. *J Porous Mater* **21**, 23-29 (2014).

295 Bimbo, L. M., *et al.* Cellular interactions of surface modified nanoporous silicon particles. *Nanoscale* **4**, 3184-3192, doi:10.1039/c2nr30397c (2012).

296 Salonen, J., *et al.* Stabilization of porous silicon surface by thermal decomposition of acetylene. *Appl Surf Sci* **225**, 389-394 (2004).

297 Salonen, J., *et al.* Thermal carbonization of porous silicon surface by acetylene. *J Appl Phys* **91**, 456-461 (2002).

298 Salonen, J., *et al.* Studies of thermally - carbonized porous silicon surfaces. *Phys Status Solidi A* **182**, 123-126 (2000).

299 Makila, E., *et al.* Amine modification of thermally carbonized porous silicon with silane coupling chemistry. *Langmuir* **28**, 14045-14054, doi:10.1021/la303091k (2012).

300 Anderson, S., *et al.* Dissolution of different forms of partially porous silicon wafers under simulated physiological conditions. *Phys Status Solidi A* **197**, 331-335 (2003).

301 Santos, H. A., *et al.* In vitro cytotoxicity of porous silicon microparticles: effect of the particle concentration, surface chemistry and size. *Acta Biomater* **6**, 2721-2731, doi:10.1016/j.actbio.2009.12.043 (2010).

302 Martinez, J. O., *et al.* Degradation and biocompatibility of multistage nanovectors in physiological systems. *J Biomed Mater Res A* **102**, 3540-3549, doi:10.1002/jbm.a.35017 (2014).

303 Low, S. P., *et al.* The biocompatibility of porous silicon in tissues of the eye. *Biomaterials* **30**, 2873-2880, doi:10.1016/j.biomaterials.2009.02.008 (2009).

304 Godin, B., *et al.* Tailoring the degradation kinetics of mesoporous silicon structures through PEGylation. *J Biomed Mater Res A* **94**, 1236-1243 (2010).

305 Tzur-Balter, A., *et al.* Mechanism of erosion of nanostructured porous silicon drug carriers in neoplastic tissues. *Nat Commun* **6**, 6208, doi:10.1038/ncomms7208 (2015).

306 Godin, B., *et al.* Discoidal Porous Silicon Particles: Fabrication and Biodistribution in Breast Cancer Bearing Mice. *Adv Funct Mater* **22**, 4225-4235, doi:10.1002/adfm.201200869 (2012).

307 Riikonen, J., *et al.* Systematic in vitro and in vivo study on porous silicon to improve the oral bioavailability of celecoxib. *Biomaterials* **52**, 44-55, doi:10.1016/j.biomaterials.2015.02.014 (2015).

308 Fry, N. L., *et al.* Oxidation-induced trapping of drugs in porous silicon microparticles. *Chem Mater* **26**, 2758-2764 (2014).

309 Kang, J., *et al.* Self-sealing porous silicon-calcium silicate core-shell nanoparticles for targeted siRNA delivery to the injured brain. *Adv Mater* **28**, 7962-7969 (2016).

310 Dorvee, J. R., *et al.* Manipulation of liquid droplets using amphiphilic, magnetic one-dimensional photonic crystal chaperones. *Nat Mater* **3**, 896 (2004).

311 Correia, A., *et al.* Cyclodextrin-modified porous silicon nanoparticles for efficient sustained drug delivery and proliferation inhibition of breast cancer cells. *ACS Appl Mater Interfaces* **7**, 23197-23204 (2015).

312 Fan, D., *et al.* Mesoporous silicon - PLGA composite microspheres for the double controlled release of biomolecules for orthopedic tissue engineering. *Adv Funct Mater* **22**, 282-293 (2012).

313 Liu, D., *et al.* Nanostructured porous silicon-solid lipid nanocomposite: towards enhanced cytocompatibility and stability, reduced cellular association, and prolonged drug release. *Adv Funct Mater* **23**, 1893-1902 (2013).

314 Nan, K., *et al.* Porous silicon oxide–PLGA composite microspheres for sustained ocular delivery of daunorubicin. *Acta Biomater* **10**, 3505-3512 (2014).

315 Zhang, H., *et al.* Fabrication of a multifunctional nano-in-micro drug delivery platform by microfluidic templated encapsulation of porous silicon in polymer matrix. *Adv Mater* **26**, 4497-4503, doi:10.1002/adma.201400953 (2014).

316 Herranz - Blanco, B., *et al.* On-chip self-assembly of a smart hybrid nanocomposite for antitumoral applications. *Adv Funct Mater* **25**, 1488-1497 (2015).

317 Kong, F., *et al.* Gold nanorods, DNA origami, and porous silicon nanoparticle-functionalized biocompatible double emulsion for versatile targeted therapeutics and antibody combination therapy. *Adv Mater* **28**, 10195-10203, doi:10.1002/adma.201602763 (2016).

318 Liu, D., *et al.* Microfluidic assisted one-step fabrication of porous silicon@acetalated dextran nanocomposites for precisely controlled combination chemotherapy. *Biomaterials* **39**, 249-259, doi:10.1016/j.biomaterials.2014.10.079 (2015).

319 Shrestha, N., *et al.* Multistage pH-responsive mucoadhesive nanocarriers prepared by aerosol flow reactor technology: A controlled dual protein-drug delivery system. *Biomaterials* **68**, 9-20, doi:10.1016/j.biomaterials.2015.07.045 (2015).

320 Shrestha, N., *et al.* Thiolation and cell-penetrating peptide surface functionalization of porous silicon nanoparticles for oral delivery of insulin. *Adv Funct Mater* **26**, 3405-3416 (2016).

321 Tamarov, K., *et al.* Temperature responsive porous silicon nanoparticles for cancer therapy - spatiotemporal triggering through infrared and radiofrequency electromagnetic heating. *J Control Release* **241**, 220-228, doi:10.1016/j.jconrel.2016.09.028 (2016).

322 Shrestha, N., *et al.* Chitosan-modified porous silicon microparticles for enhanced permeability of insulin across intestinal cell monolayers. *Biomaterials* **35**, 7172-7179, doi:10.1016/j.biomaterials.2014.04.104 (2014).

323 Zhang, F., *et al.* Sequential antifouling surface for efficient modulation of the nanoparticle–cell interactions in protein-rich environments. *Adv Ther* **1**, 1800013 (2018).

324 Zhang, F., *et al.* Receptor-mediated surface charge inversion platform based on porous silicon nanoparticles for efficient cancer cell recognition and combination therapy. *ACS Appl Mater Interfaces* **9**, 10034-10046, doi:10.1021/acsami.7b02196 (2017).

325 Janoniene, A., *et al.* A versatile carbonic anhydrase IX targeting ligand-functionalized porous silicon nanoplatform for dual hypoxia cancer therapy and imaging. *ACS Appl Mater Interfaces* **9**, 13976-13987, doi:10.1021/acsami.7b04038 (2017).

326 Liu, Z., *et al.* Quercetin-based modified porous silicon nanoparticles for enhanced inhibition of doxorubicin-resistant cancer cells. *Adv Healthc Mater* **6**, 1601009 (2017).

327 Reuter, L. J., *et al.* Coating nanoparticles with plant-produced transferrin–hydrophobin fusion protein enhances their uptake in cancer cells. *Bioconjug Chem* **28**, 1639-1648 (2017).

328 Almeida, P. V., *et al.* A multifunctional nanocomplex for enhanced cell uptake, endosomal escape and improved cancer therapeutic effect. *Nanomedicine (Lond)*, doi:10.2217/nnm-2017-0034 (2017).

329 Kong, F., *et al.* Inhibition of multidrug resistance of cancer cells by co-delivery of DNA nanostructures and drugs using porous silicon nanoparticles@giant liposomes. **25**, 3330-3340 (2015).

330 Wang, C. F., *et al.* Dual-drug delivery by porous silicon nanoparticles for improved cellular uptake, sustained release, and combination therapy. *Acta Biomater* **16**, 206-214, doi:10.1016/j.actbio.2015.01.021 (2015).

331 Wang, C. F., *et al.* Multifunctional porous silicon nanoparticles for cancer theranostics. *Biomaterials* **48**, 108-118, doi:10.1016/j.biomaterials.2015.01.008 (2015).

332 Almeida, P. V., *et al.* Amine-modified hyaluronic acid-functionalized porous silicon nanoparticles for targeting breast cancer tumors. *Nanoscale* **6**, 10377-10387, doi:10.1039/c4nr02187h (2014).

333 Tolli, M. A., *et al.* In vivo biocompatibility of porous silicon biomaterials for drug delivery to the heart. *Biomaterials* **35**, 8394-8405, doi:10.1016/j.biomaterials.2014.05.078 (2014).

334 Kinnari, P. J., *et al.* Tumour homing peptide-functionalized porous silicon nanovectors for cancer therapy. *Biomaterials* **34**, 9134-9141, doi:10.1016/j.biomaterials.2013.08.034 (2013).

335 Scavo, M. P., *et al.* Multistage vector delivery of sulindac and silymarin for prevention of colon cancer. *Colloids Surf B Biointerfaces* **136**, 694-703, doi:10.1016/j.colsurfb.2015.10.005 (2015).

336 Mi, Y. *et al.,* Enzyme-responsive multistage vector for drug delivery to tumor tissue. *Pharmacol Res* **113**, 92-99, doi:10.1016/j.phrs.2016.08.024 (2016).

337 Wolfram, J., *et al.* Multistage vector (MSV) therapeutics. *J Control Release* **219**, 406-415, doi:10.1016/j.jconrel.2015.08.010 (2015).

338 Tanaka, T., *et al.* Sustained small interfering RNA delivery by mesoporous silicon particles. *Cancer Res* **70**, 3687-3696, doi:10.1158/0008-5472.CAN-09-3931 (2010).

339 Tasciotti, E., *et al.* Mesoporous silicon particles as a multistage delivery system for imaging and therapeutic applications. *Nat Nanotechnol* **3**, 151 (2008).

340 Ferreira, M. P. A., *et al.* Drug-loaded multifunctional nanoparticles targeted to the endocardial layer of the injured heart modulate hypertrophic signaling. *Small* **13**, doi:10.1002/smll.201701276 (2017).

341 Ferreira, M. P., *et al.* In vitro and in vivo assessment of heart-homing porous silicon nanoparticles. *Biomaterials* **94**, 93-104, doi:10.1016/j.biomaterials.2016.03.046 (2016).

342 Martins, J. P., *et al.* Engineered multifunctional albumin-decorated porous silicon nanoparticles for FcRn translocation of insulin. *Small* **14**, e1800462, doi:10.1002/smll.201800462 (2018).

343 Araujo, F., *et al.* In vivo dual-delivery of glucagon like peptide-1 (GLP-1) and dipeptidyl peptidase-4 (DPP4) inhibitor through composites prepared by microfluidics for diabetes therapy. *Nanoscale* **8**, 10706-10713, doi:10.1039/c6nr00294c (2016).

344 Shrestha, N., *et al.* Oral hypoglycaemic effect of GLP-1 and DPP4 inhibitor based nanocomposites in a diabetic animal model. *J Control Release* **232**, 113-119, doi:10.1016/j.jconrel.2016.04.024 (2016).

345 Li, W., *et al.* GDNF mimetics delivery by porous silicon nanoparticles for improved Parkinson's disease management. *Nanomedicine: NBM* **14**, 1848 (2018).

346 Liu, Z., *et al.* Multifunctional nanohybrid based on porous silicon nanoparticles, gold nanoparticles, and acetalated dextran for liver regeneration and acute liver failure theranostics. *Adv Mater* **30**, e1703393, doi:10.1002/adma.201703393 (2018).

347 Ainslie, K. M., *et al.* In vitro immunogenicity of silicon-based micro- and nanostructured surfaces. *ACS Nano* **2**, 1076-1084, doi:10.1021/nn800071k (2008).

348 Jurkic, L. M., *et al.* Biological and therapeutic effects of ortho-silicic acid and some ortho-silicic acid-releasing compounds: New perspectives for therapy. *Nutr Metab (Lond)* **10**, 2, doi:10.1186/1743-7075-10-2 (2013).

349 Xia, X., *et al.* Porous silicon microparticle potentiates anti-tumor immunity by enhancing cross-presentation and inducing type I interferon response. *Cell Rep* **11**, 957-966, doi:10.1016/j.celrep.2015.04.009 (2015).

350 Meraz, I. M., *et al.* Activation of the inflammasome and enhanced migration of microparticle-stimulated dendritic cells to the draining lymph node. *Mol Pharm* **9**, 2049-2062, doi:10.1021/mp3001292 (2012).

351 Meraz, I. M., *et al.* Multivalent presentation of MPL by porous silicon microparticles favors T helper 1 polarization enhancing the anti-tumor efficacy of doxorubicin nanoliposomes. *PLoS One* **9**, e94703, doi:10.1371/journal.pone.0094703 (2014).

352 Gu, L., *et al.* Multivalent porous silicon nanoparticles enhance the immune activation potency of agonistic CD40 antibody. *Adv Mater* **24**, 3981-3987, doi:10.1002/adma.201200776 (2012).

353 Shahbazi, M.-A., *et al.* A prospective cancer chemo-immunotherapy approach mediated by synergistic CD326 targeted porous silicon nanovectors. *Nano Res* **8**, 1505-1521 (2015).

354 Larson, C., *et al.* Going viral: a review of replication-selective oncolytic adenoviruses. *Oncotarget* **6**, 19976-19989, doi:10.18632/oncotarget.5116 (2015).

355 Muruve, D. A. The innate immune response to adenovirus vectors. *Hum Gene Ther* **15**, 1157-1166, doi:10.1089/hum.2004.15.1157 (2004).

356 Platanias, L. C. Mechanisms of type-I- and type-II-interferon-mediated signalling. *Nat Rev Immunol* **5**, 375-386, doi:10.1038/nri1604 (2005).

357 Fukuhara, H., *et al.* Oncolytic virus therapy: a new era of cancer treatment at dawn. *Cancer Sci* **107**, 1373-1379 (2016).

358 Coffin, R. Interview with Robert Coffin, inventor of T-VEC: the first oncolytic immunotherapy approved for the treatment of cancer. *Immunotherapy* **8**, 103-106 (2016).

359 Pol, J., *et al.* First oncolytic virus approved for melanoma immunotherapy. *OncoImmunology*, e1115641, doi:10.1080/2162402X.2015.1115641 (2016).

360 Kaufman, H. L., *et al.* Oncolytic viruses: a new class of immunotherapy drugs. *Nat Rev Drug Discov* **14**, 642-662, doi:10.1038/nrd4663 (2015).

361 Lawler, S. E., *et al.* Oncolytic viruses in cancer treatment: a review. *JAMA Oncol* **3**, 841-849, doi:10.1001/jamaoncol.2016.2064 (2017).

362 Russell, S. J., *et al.* Oncolytic viruses as antigen-agnostic cancer vaccines. *Cancer Cell* **33**, 599-605 (2018).

363 Andtbacka, R. *et al.* Talimogene laherparepvec improves durable response rate in patients with advanced melanoma. *J Clin Oncol* **33**, 2780-2788 (2015).

364 Long, G. V., *et al.* Efficacy analysis of MASTERKEY-265 phase 1b study of talimogene laherparepvec (T-VEC) and pembrolizumab (pembro) for unresectable stage IIIB-IV melanoma. *J Clin Oncol*, doi:10.1200/JCO.2016.34.15_suppl.9568 (2016).

365 Hou, W., *et al.* Oncolytic vaccinia virus demonstrates antiangiogenic effects mediated by targeting of VEGF. *Int J Cancer* **135**, 1238-1246 (2014).

366 Breitbach, J. C. J., *et al.* Oncolytic vaccinia virus disrupts tumor-associated vasculature in humans. *Cancer Res* (2013).

367 Liu, T.-C., *et al.* The targeted oncolytic poxvirus JX-594 demonstrates antitumoral, antivascular, and anti-HBV activities in patients with hepatocellular carcinoma. *Mol Ther* **16**, 1637-1642 (2008).

368 Lichty, B. D., *et al.* C. Going viral with cancer immunotherapy. *Nat Rev Cancer* **14**, 559-567, doi:10.1038/nrc3770 (2014).

369 Mell, L. K., *et al.* Phase I trial of intravenous oncolytic vaccinia virus (GL-ONC1) with cisplatin and radiotherapy in patients with locoregionally advanced head and neck carcinoma. *Clin Cancer Res*, clincanres. 3232.2016 (2017).

370 Breitbach, C. J., *et al.* Intravenous delivery of a multi-mechanistic cancer-targeted oncolytic poxvirus in humans. *Nature* **477**, 99 (2011).

371 Tesfay, M. Z., *et al.* PEGylation of vesicular stomatitis virus (VSV) extends virus persistence in blood circulation of passively immunized mice. *J Virol*, JVI. 02832-02812 (2013).

372 O'Riordan, C. R., *et al.* PEGylation of adenovirus with retention of infectivity and protection from neutralizing antibody in vitro and in vivo. *Hum Gene Ther* **10**, 1349-1358 (1999).

373 Morrison, J., *et al.* Virotherapy of ovarian cancer with polymer-cloaked adenovirus retargeted to the epidermal growth factor receptor. *Mol Ther* **16**, 244-251 (2008).

374 Lu, S. Heterologous prime–boost vaccination. *Curr Opin Immunol* **21**, 346-351 (2009).

375 Pol, J. G., *et al.* Maraba virus as a potent oncolytic vaccine vector. *Mol Ther* **22**, 420-429 (2014).

376 Ungerechts, G., *et al.* Moving oncolytic viruses into the clinic: clinical-grade production, purification, and characterization of diverse oncolytic viruses. *Mol Ther Methods Clin Dev* **3**, 16018, doi:10.1038/mtm.2016.18 (2016).

377 Kirn, D. Replication-selective oncolytic adenoviruses: virotherapy aimed at genetic targets in cancer. *Oncogene* **19**, 6660-6669, doi:10.1038/sj.onc.1204094 (2000).

378 Harrison, S. C. Virology. Looking inside adenovirus. *Science* **329**, 1026-1027, doi:10.1126/science.1194922 (2010).

379 Yamamoto, M. *et al.* Current issues and future directions of oncolytic adenoviruses. *Mol Ther* **18**, 243-250 (2010).

380 Mathis, J. M., *et al.* Oncolytic adenoviruses - selective retargeting to tumor cells. *Oncogene* **24**, 7775-7791, doi:10.1038/sj.onc.1209044 (2005).

381 Jiang, H., *et al.* Oncolytic adenovirus research evolution: from cell-cycle checkpoints to immune checkpoints. *Curr Opin Virol* **13**, 33-39 (2015).

382 Pol, J., *et al.* Trial watch: oncolytic viruses for cancer therapy. *Oncoimmunology* **3**, e28694 (2014).

383 Capasso, C., *et al.* Oncolytic adenoviruses coated with MHC-I tumor epitopes increase the antitumor immunity and efficacy against melanoma. *Oncoimmunology* **5**, e1105429 (2016).

384 Bai, Y., *et al.* Applications of microfluidics in quantitative biology. *Biotechnol J* **13**, e1700170, doi:10.1002/biot.201700170 (2018).

385 Sackmann, E. K., *et al.* The present and future role of microfluidics in biomedical research. *Nature* **507**, 181-189, doi:10.1038/nature13118 (2014).

386 Elvira, K. S., *et al.* The past, present and potential for microfluidic reactor technology in chemical synthesis. *Nat Chem* **5**, 905-915, doi:10.1038/nchem.1753 (2013).

387 Ma, J., *et al.* Controllable synthesis of functional nanoparticles by microfluidic platforms for biomedical applications - a review. *Lab Chip* **17**, 209-226, doi:10.1039/c6lc01049k (2017).

388 Riahi, R., *et al.* Microfluidics for advanced drug delivery systems. *Curr Opin Chem Eng* **7**, 101-112 (2015).

389 Marre, S., *et al.* Synthesis of micro and nanostructures in microfluidic systems. *Chem Soc Rev* **39**, 1183-1202, doi:10.1039/b821324k (2010).

390 Rondeau, E. *et al.* Biopolymer microparticle and nanoparticle formation within a microfluidic device. *Langmuir* **24**, 6937-6945 (2008).

391 Fontana, F., *et al.* Microfluidics as a cutting-edge technique for drug delivery applications. *J Drug Delivery Sci Technol* **34**, 76-87 (2016).

392 Valencia, P. M., *et al.* Microfluidic technologies for accelerating the clinical translation of nanoparticles. *Nat Nanotechnol* **7**, 623-629, doi:10.1038/nnano.2012.168 (2012).

393 Liu, D., *et al.* Current developments and applications of microfluidic technology toward clinical translation of nanomedicines. *Adv Drug Deliv Rev* **128**, 54-83, doi:10.1016/j.addr.2017.08.003 (2018).

394 Zhao, C. X. Multiphase flow microfluidics for the production of single or multiple emulsions for drug delivery. *Adv Drug Deliv Rev* **65**, 1420-1446, doi:10.1016/j.addr.2013.05.009 (2013).

395 Whitesides, G. M. The origins and the future of microfluidics. *Nature* **442**, 368-373, doi:10.1038/nature05058 (2006).

396 Liu, D., *et al.* Microfluidic-assisted fabrication of carriers for controlled drug delivery. *Lab Chip* **17**, 1856-1883, doi:10.1039/c7lc00242d (2017).

397 Martins, J. P., *et al.* The importance of microfluidics for the preparation of nanoparticles as advanced drug delivery systems. *Expert Opin Drug Delivery* **15**, 469-479 (2018).

398 Pessi, J., *et al.* Microfluidics-assisted engineering of polymeric microcapsules with high encapsulation efficiency for protein drug delivery. *Int J Pharm* **472**, 82-87, doi:10.1016/j.ijpharm.2014.06.012 (2014).

399 Araujo, F., *et al.* Microfluidic assembly of a multifunctional tailorable composite system designed for site specific combined oral delivery of peptide drugs. *ACS Nano* **9**, 8291-8302, doi:10.1021/acsnano.5b02762 (2015).

400 Herranz-Blanco, B., *et al.* Microfluidic assembly of multistage porous silicon–lipid vesicles for controlled drug release. *Lab Chip* **14**, 1083-1086 (2014).

401 Liu, D., *et al.* Microfluidic templated mesoporous silicon–solid lipid microcomposites for sustained drug delivery. *ACS Appl Mater Interfaces* **5**, 12127-12134 (2013).

402 Bertoni, S., *et al.* pH and reactive oxygen species-sequential responsive nano-in-micro omposite for targeted therapy of inflammatory bowel disease. *Adv Funct Mater*, 1806175 (2018).

403 Li, W., *et al.* Hierarchical structured and programmed vehicles deliver drugs locally to inflamed sites of intestine. *Biomaterials* **185**, 322-332, doi:10.1016/j.biomaterials.2018.09.024 (2018).

404 Liu, D., *et al.* A versatile and robust microfluidic platform toward high throughput synthesis of homogeneous nanoparticles with tunable properties. *Adv Mater* **27**, 2298-2304 (2015).

405 Liu, D., *et al.* Core/shell nanocomposites produced by superfast sequential microfluidic nanoprecipitation. *Nano Lett* **17**, 606-614, doi:10.1021/acs.nanolett.6b03251 (2017).

406 Sarparanta, M., *et al.* (1)(8)F-labeled modified porous silicon particles for investigation of drug delivery carrier distribution in vivo with positron emission tomography. *Mol Pharm* **8**, 1799-1806, doi:10.1021/mp2001654 (2011).

407 Bimbo, L. M., *et al.* Biocompatibility of thermally hydrocarbonized porous silicon nanoparticles and their biodistribution in rats. *ACS Nano* **4**, 3023-3032, doi:10.1021/nn901657w (2010).

408 Kovalainen, M., *et al.* Mesoporous silicon (PSi) for sustained peptide delivery: effect of psi microparticle surface chemistry on peptide YY3-36 release. *Pharm Res* **29**, 837-846, doi:10.1007/s11095-011-0611-6 (2012).

409 Bimbo, L. M., *et al.* Drug permeation across intestinal epithelial cells using porous silicon nanoparticles. *Biomaterials* **32**, 2625-2633 (2011).

410 Herranz-Blanco, B., *et al.* Microfluidics platform for glass capillaries and its application in droplet and nanoparticle fabrication. *Int J Pharm* **516**, 100-105, doi:10.1016/j.ijpharm.2016.11.024 (2017).

411 Kanerva, A., *et al.* Targeting adenovirus to the serotype 3 receptor increases gene transfer efficiency to ovarian cancer cells. *Clin Cancer Res* **8**, 275-280 (2002).

412 Kanerva, A,. *et al.* Enhanced therapeutic efficacy for ovarian cancer with a serotype 3 receptor-targeted oncolytic adenovirus. *Mol Ther* **8**, 449-458 (2003).

413 Shahbazi, M. A., *et al.* The mechanisms of surface chemistry effects of mesoporous silicon nanoparticles on immunotoxicity and biocompatibility. *Biomaterials* **34**, 7776-7789, doi:10.1016/j.biomaterials.2013.06.052 (2013).

414 Liu, D., *et al.* Impact of pore size and surface chemistry of porous silicon particles and structure of phospholipids on their interactions. *ACS Biomater Sci Eng* **4**, 2308-2313, doi:10.1021/acsbiomaterials.8b00343 (2018).

415 Luk, B. T., *et al.* Interfacial interactions between natural RBC membranes and synthetic polymeric nanoparticles. *Nanoscale* **6**, 2730-2737 (2014).

416 Suk, J. S., *et al.* PEGylation as a strategy for improving nanoparticle-based drug and gene delivery. *Adv Drug Deliv Rev* **99**, 28-51 (2016).

417 Yang, Q. *et al.* Anti-PEG immunity: emergence, characteristics, and unaddressed questions. *Wiley Interdiscip Rev Nanomed Nanobiotechnol* **7**, 655-677, doi:10.1002/wnan.1339 (2015).

418 Behzadi, S., *et al.* Cellular uptake of nanoparticles: journey inside the cell. *Chem Soc Rev* **46**, 4218-4244, doi:10.1039/c6cs00636a (2017).

419 Iversen, T.-G., *et al.* Endocytosis and intracellular transport of nanoparticles: present knowledge and need for future studies. *Nano Today* **6**, 176-185 (2011).

420 Bachelder, E. M., *et al.* Acetalated dextran: a tunable and acid-labile biopolymer with facile synthesis and a range of applications. *Chem Rev* **117**, 1915-1926, doi:10.1021/acs.chemrev.6b00532 (2017).

421 Mailliard, R. B., *et al.* alpha-type-1 polarized dendritic cells: a novel immunization tool with optimized CTL-inducing activity. *Cancer Res* **64**, 5934-5937, doi:10.1158/0008-5472.CAN-04-1261 (2004).

422 Kuzu, O. F., *et al.* Current state of animal (mouse) modeling in melanoma research. *Cancer Growth Metastasis* **8**, 81-94, doi:10.4137/CGM.S21214 (2015).

423 Smyth, M. J., *et al.* Combination cancer immunotherapies tailored to the tumour microenvironment. *Nat Rev Clin Oncol* **13**, 143-158, doi:10.1038/nrclinonc.2015.209 (2016).

424 Sharma, P. *et al.* Immune checkpoint targeting in cancer therapy: toward combination strategies with curative potential. *Cell* **161**, 205-214, doi:10.1016/j.cell.2015.03.030 (2015).

425 Yang, R.. *et al.* Cancer cell membrane-coated adjuvant nanoparticles with mannose modification for effective anticancer vaccination. *ACS Nano* **12**, 5121-5129, doi:10.1021/acsnano.7b09041 (2018).

Recent Publications in this Series

29/2019 Agnes Stenius-Ayoade
Housing, Health and Service Use of the Homeless in Helsinki, Finland
30/2019 Mari Metsäniitty
Forensic Age Assessment in Finland, and Dental Development of Somalis
31/2019 Heli Tolppanen
Prognostication in Acute Heart Failure and Cardiogenic Shock— Focus on Electrocardiography and Biomarkers
32/2019 Olli-Pekka Pulkka
Novel Therapeutic Targets in Gastrointestinal Stromal Tumor
33/2019 Inkeri Spoljaric
GABAergic Signaling and Neuronal Chloride Regulation in the Control of Network Events in the Immature Hippocampus
34/2019 Nina Mars
Healthcare Utilization in Rheumatic Diseases
35/2019 Katrina Albert
Modelling Alpha-Synuclein-Based Parkinson's Disease and Studies with CDNF
36/2019 Felix Siebenhühner
The Role of Multi-Scale Phase Synchronization and Cross-Frequency Interactions in Cognitive Integration
37/2019 Elisa Saarnio
Associations among Vitamin D Binding Protein Gene Polymorphisms, Total, Free and Bioavailable 25-Hydroxyvitamin D, and Skeletal Outcomes — Studies in Children, Adolescents, and Middle-Aged Finns
38/2019 Ulrika Julku
Prolyl Oligopeptidase and Alpha-Synuclein in the Regulation of Nigrostriatal Dopaminergic Neurotransmission
39/2019 Reijo Siren
Screening for Cardiovascular Risk Factors in Middle-Aged Men: The Long-Term Effect of Lifestyle Counselling
40/2019 Paula Tiittala
Hepatitis B and C, HIV and Syphilis among Migrants in Finland: Opportunities for Public Health Response
41/2019 Darshan Kumar
Reticulon Homology Domain Containing Protein Families of the Endoplasmic Reticulum
42/2019 Iris Sevilem
The Integration of Developmental Signals During Root Procambial Patterning in *Arabidopsis thaliana*
43/2019 Ying Liu
Transcriptional Regulators Involved in Nutrient-Dependent Growth Control
44/2019 Ramón Pérez Tanoira
Race for the Surface — Competition Between Bacteria and Host Cells in Implant Colonization Process
45/2019 Mgbeahuruike Eunice Ego
Evaluation of the Medicinal Uses and Antimicrobial Activity of *Piper guineense* (Schumach & Thonn)
46/2019 Suvi Koskinen
Near-Occlusive Atherosclerotic Carotid Artery Disease: Study with Computed Tomography Angiography

Helsinki 2019 **ISSN 2342-3161** **ISBN 978-951-51-5286-2**